Czech Technical University in Prague

Faculty of Mechanical Engineering

Doctoral thesis

Ing.Ladislav Vesely

May 14, 2018

FACULTY
OF MECHANICAL
ENGINEERING
CTU IN PRAGUE

Czech Technical University in Prague

Doctoral thesis

Study of Power Cycle with Supercritical CO_2

Ing.Ladislav Vesely

supervised by
doc. Ing. Vaclav Dostal, Sc.D.

Doctoral study programme
Mechanical Engineering
Power Engineering Machines and Equipment

May 14, 2018

Annotation Sheet

Author's name:	Ing. Ladislav Veselý
English title:	Study of Power Cycle with Supercritical CO_2
Czech title:	Studie Tepelného Oběhu s Nadkritickým CO_2
Year:	2018
Field of study:	Doctoral study programme: Mechanical Engineering Energy Machines and Equipment / Energetické Stroje a Zařízení
Department:	Department of Energy Engineering / Ústav Energetiky
Supervisor:	doc. Ing. Václav Dostal, Sc.D.
Consultant:	
Bibliographic date:	
Number of Pages:	137
Number of Figures:	105
Number of Tables:	24
Number of Equations:	39
Number of Appendices:	2

Abstrakt

S rostoucím zájmem o solární a geotermální elektrárny a systémy využívající odpadního tepla z mnoha technologií se celý svět více orientuje na využívání plynných cyklů. Tepelné oběhy s nadkritickým CO_2 (S-CO_2) jsou velmi zajímavé tepelné oběhy pro tyto aplikace. S-CO_2 cykly mají mnoho výhod, ale také i nevýhod v porovnání s dalšími tepelnými oběhy, jako je parní nebo Heliový oběh. Výhodou S-CO_2 cyklu je, že je kompaktní a velmi jednoduchý, výkon kompresoru je nižší než pro cyklus využívající helium jako pracovní medium. Jednou z nevýhod je vliv reálných vlastností, které mohou být významně ovlivněny přítomností nečistot v pracovním mediu. Je zřejmé, že nečistoty ovlivňují tepelný oběh, konstrukci komponentů, celkovou účinnost a výkon, z důvodu změn termodynamických a transportních vlastností. Výzkum byl zaměřen na popis vlivu směsí na S-CO_2 cykly. Výzkum je rozdělen do několika oblastí, které jsou vzájemně propojeny pro komplexní přehled a popis účinků směsí na S-CO_2 cykly. Výzkum byl proveden pro binární směsi CO_2 s He, Ar, CO, N_2, O_2, H_2S, H_2, CH_4, Xe, Kr a SO_2. Všechny zkoumané látky, s výjimkou H_2S, Xe a SO_2 mají negativní vliv na cykly a jejich účinnost. Vliv směsí na příkon kompresoru je nepříznivý, nicméně na výkon turbíny je nepatrně pozitivní. Vliv na výměníky tepla je rozdílný pro různé druhy výměníků tepla. Optimální množství sekundární látky je do 1 %. Vliv směsí musí být zohledněn při návrhu S-CO_2 cyklu. Optimalizace je velmi důležitá při návrhu S-CO_2 cyklu pro každou jeho aplikaci a rozvržení cyklu. Je možné dosáhnout minimálního vlivu směsí na S-CO_2 cykly při dobré optimalizaci a návrhu tepelného oběhu. Bez ohledu na čistotu CO_2 může být použito stejné rozložení tepelného oběhu, nicméně pro dosažení maximálního výkonu S-CO_2 cyklu s nečistotami musí být provozní parametry a konstrukce komponentů opakovaně optimalizovány.

Klíčová slova

S-CO_2, Tepelný oběh, Směsi, Nečistoty, Účinnost, Tepelný Výkon, Technicko-Ekonomické hodnocení

Abstract

With the increasing interest in solar and geothermal power plants as well as waste heat recovery systems from many technologies, the whole world is more focused on the gas power cycles. Especially, the supercritical carbon dioxide (S-CO_2) cycles are very interesting for these applications. The S-CO_2 power cycles have a many advantages and disadvantages over the other cycles such as a steam-water cycle or helium Brayton cycle. The advantages are the cycles are compact systems, the compressor power is lower than for helium Brayton cycle, the cycles are very simple. One of the disadvantages is the effect of real properties, which can be significantly altered by the presence of impurities in the working fluid. Because, it is obvious that impurities through the change of thermodynamic and transport properties affect the cycle as they influence cycle component design and thus the overall efficiency of the power cycle and the net power. The research was oriented on the description of the effect of the mixtures on the S-CO_2 power cycle. The research has focused on the several areas, which are connected to each other for the complex overview and description of the effect of the mixtures on the S-CO_2 power cycle. The research was conducted for the binary mixtures of CO_2 with He, Ar, CO, N_2, O_2, H_2S, H_2, CH_4, Xe, Kr and SO_2. The all investigated substances, except for H_2S, Xe and SO_2 have a negative effect on the cycle and the cycle efficiency. The effect of the mixtures on the compressor performance is negative. The effect of the mixtures on the turbine performance is negligibly positive. The effect of mixtures on the heat exchangers is different for different type of the heat exchangers. The optimum amount of the second substance is up to 1 %. The effect of mixtures must be taken into account when designing the S-CO_2 power cycle. The optimization for each application of the S-CO_2 power cycle is very important when designing of the S-CO_2 power cycle. With good optimization and design of the cycle which uses mixtures, marginal negative effect on the cycle efficiency and the net power output can be achieved. Regardless of the CO_2 purity, the same cycle layouts can be used, however in order to achieve good performance with the impurities the cycle operating conditions and components design most be re-optimized.

Keywords

S-CO_2, Power Cycle, Mixtures, Impurities, Efficiency, Net Power, Techno-Economic Evaluation

Čestné prohlášení

Prohlašuji, že jsem tuto Disertační práci vypracoval samostatně a pouze s použitím literatury uvedené v seznamu.

Ing. Ladislav Vesely

V Praze dne 14.05.2018

Poděkování

Rád bych tímto poděkoval panu doc. Ing. Václavu Dostálovi Sc.D. za jeho vedení, pomoc, komentáře a připomínky při tvorbě disertační práce. Dále bych rád poděkoval panu Dr. Geir Skaugen za jeho rady se studovanou problematikou a panu Dr. Subith Vasu Sumathi za jeho rady při řešení problémů s S-CO_2 cykly.

Contents

List of Figures

List of Tables

List of Symbols

Acronyms

S-CO_2	.....	Supercirtitical carbon dioxide
CO_2	.....	Carbon dioxide
He	.....	Helium
Ar	.....	Argon
N_2	.....	Nitrogen
O_2	.....	Oxygen
CO	.....	Carbon monoxide
H_2S	.....	Hydrogen sulfide
CH_4	.....	Methane
SO_2	.....	Sulfur dioxide
Xe	.....	Xenon
Kr	.....	Krypton
H_2O	.....	Water
C_3H_8	.....	Propane
C_2H_6	.....	Ethane
C_4H_{10}	.....	Butane
EOS	.....	Equation of state
RK	.....	Redlich-Kwong equation of state
SRK	.....	Redlich-Kwong-Soave equation of state
PR	.....	Peng-Robinson equation of state
BWRS	.....	Benedict-Webb-Rubin-Starling equation of state
PT	.....	Patel-Teja equation of state
HEX	.....	Heat exchanger
WHR	.....	Waste heat recovery system
CCS	.....	Carbon Capture and Storage
MAGNOX	.....	Gas Cooled Graphite Moderated Reactor
AGR	.....	Advanced Gas-cooled Reactor
SFR	.....	Sodium cooled fast reactor
PCHE	.....	Printed circuit heat exchanger
SNL	.....	Sandia National Laboratories

CFD	.....	Computational Fluid Dynamics
PV	.....	Present value
T	.....	Turbine
C	.....	Compressor
CH	.....	Cooler
H	.....	Heater
RH	.....	Recuperative heat exchanger
LTR	.....	Low recuperative heat exchanger
HTR	.....	High recuperative heat exchanger

Nomenclature

Symbol	Units	Description
$T_{(P_{hs},P_{cs})}$	[°C]	Temperature of the pinch point
N_i	[mol^{-1}]	Number of molecules
m_i	[g/mol]	Mass of molecules
R_u	[J/molK]	Universal gas constant
N_a	[mol^{-1}]	Avogadro constant
k_b	[J/molK]	Boltzmann constant
χi	[-]	Mole fraction of species
Y_i	[-]	Mass fraction of species
Z	[-]	Compressibility factor
P_{net}	[W]	Net power
Q_{in}	[W]	heat input
Q_{out}	[W]	heat output
T_L	[K]	Temperature of low-temperature site
T_H	[K]	Temperature of high-temperature site
η_{th}	[-]	Thermal efficiency
η_{Car}	[-]	Carnot efficiency
P_{tu}	[W]	Turbine power output
P_c	[W]	Compressor input power
Ra	[-]	Pressure ratio
η_{tu}	[-]	Turbine efficiency
η_c	[-]	Compressor efficiency
η_{rec}	[-]	Recuperator effectiveness
$\dot{m}$	[kg/s]	Mass flow
$\Delta\eta$	[%]	Difference of the cycle efficiency
ΔP_{tu}	[W]	Difference of the turbine power output
ΔP_c	[W]	Difference of the compressor input power
P_2	[MPa]	Turbine outlet pressure
ΔT	[°C]	Temperature difference
κ	[-]	Poisson constant
C_p	[kJ/kgK]	Heat capacity at constant pressure
C_v	[kJ/kgK]	Heat capacity at constant volume
U	[W/m^{2}K]	Overall heat transfer coefficient
THT	[-]	Transferred heat fraction
α_t	[m^2/s]	the thermal diffusivity
A	[m^2]	Surface
α	[W/m^{2}K]	Heat transfer coefficient
w_t	[m]	Wall thickness
λ_t	[W/mK]	thermal conductivity
d	[m]	Characteristic dimension

Nu	[-]	Nusselt number
Re	[-]	Reynolds number
Pr	[-]	Prandl number
c	[m/s]	Velocity
ρ	[kg/m^3]	Density
μ	[Pas]	Dynamic viscosity
ν	[m^2/s]	Kinematic viscosity
LCOE	[$/kWhe]	Levelized cost of electricity
IRR	[%]	Internal Rate of Return
NPV	[$]	Net Present Value
PC	[$]	Project cost
PV_{dts}	[$]	PV Depreciation Tax Shield
PV_{lop}	[$]	PV Lifetime Operating Costs
PV_{sc}	[$]	PV Salvage Costs
LEP	[kWhe]	Lifetime Electric Production
FCF	[$]	Cash flow

Chapter 1

Introduction

With the increasing interest in solar and geothermal power plants as well as waste heat recovery systems from many technologies, the whole world is more focused on the gas power cycles. Especially, the supercritical carbon dioxide (S-CO_2) cycles are very interesting for these applications. This is due to many advantages of the S-CO_2 power cycles over the other cycles such as a steam-water cycle or helium Brayton cycle. The advantages are the cycles are compact systems compared to steam-water or helium Brayton cycle, the compressor power is lower than for helium Brayton cycle, the cycles are very simple. However, the S-CO_2 power cycles are quite complex systems. As each power cycle, the S-CO_2 power cycles have also disadvantages. Mainly the compressor which operates near the critical point or the presence of the so called pinch point in the heat exchangers design. However, these issues can be solved. Nevertheless, one of the disadvantages is the effect of real properties, which can be significantly altered by the presence of impurities in the working fluid which can occur as impurities or can be intentionally added to the pure CO_2. The main question is the effect of these substances on each component in the S-CO_2 power cycle.

1.1 Motivation

The effect of impurities on the S-CO_2 power cycle performance is very important. It is obvious that mixtures through the change of thermodynamic and transport properties affect the cycle as they influence cycle component design and thus the overall efficiency of the power cycle and the net power. The impact depends on the type of mixture and the number of substances. An important unknown is the effect of mixtures. It may be positive or negative. Research of this effect is necessary. Since, the design and calculation of the S-CO_2 power cycle is generally performed for pure CO_2 (100 % purity). These results thus may be inaccurate. It is true that medium with 100 % purity can be used as working medium in the S-CO_2 power cycle, but the purity of CO_2 can not be guaranteed throughout the whole operation.

The decrease of purity is possible in various ways and the decrease of purity depends on the impurities. The chemical reaction of CO_2 with the material of the components, from the leakage into the systems (Ar, O_2 or N_2), a special substance for leakage detection (He) or from turbine and compressor lubricants. In some cases working medium from different technologies such as carbon capture and storage (CCS) technologies or other may be used. Several conclusions can be made based on the above remarks.

The basic reasons for investigation of mixtures in the S-CO_2 power cycle are following:

- Most likely 100 % pure CO_2 will not be used.
- Mixtures will appear as a result of impurities or as a specific medium from other systems.

If the above is true, these mixtures will affect:

- Components - heat exchangers, compressors, turbines.
- Pinch point location.
- Cooling of the cycle.
- Techno-Economic Evaluation.

The mixtures clearly have an effect on the power cycle. However, this effect depends on the effect on each of the component in the power cycle. Research of the effect on the components is necessary in order to understand their effect on the power cycle. At the same time, the description of the connection between a compressor and a cooler is necessary. This is important part for the design of the compressor and cooling system. The pinch point is the key issue in the recuperative heat exchanger design. The idea is that mixtures may eliminate this problem. This means that, small amount of the second substance, in the case with binary mixture, may shift the area with the pinch point. The techno-economic evaluation is an important part for the power plant. If the mixtures have an effect on the cycle, this effect will be observed also in the plant economics. A synergy to other technologies working with not pure S-CO_2 is apparent.

1.2 Organization of Thesis

The research is focused on study of power cycle with supercritical CO_2 and the description of the effect of mixtures on the S-CO_2 power cycle performance. The main point of view is thermodynamic with focus on the thermal and physical evaluation and description

for hypothetical substances or new impurities in CO_2. The very important results from this study is the description whether the substance effect on the systems is positive or negative. The research is performed for binary mixtures with high purity of CO_2. Consideration is focused to the low amount of the second component, as potential impurities in the system. The purity of CO_2 is kept between 95% to 99%.

The research is divided into several parts with theoretical description of the effect on the cycle. The parts are connected to each other and give the complex overview and description of the effect of the mixtures on S-CO_2 power cycle.

The parts of the research are following:

- The first part focuses on the description of the effect of mixtures on the S-CO_2 power cycle performance. It evaluates the overall cycle efficiency and the net power.
- The second part is focused on the detail description of the effect on each component in the cycle, especially on the turbine, the compressor and the heat exchangers.
- The third part of the research is focused on the optimization of the S-CO_2 power cycle, mainly the compressor inlet temperature. The results for this part of research are calculation and optimization for the specific cycle layouts for different binary mixtures.
- The fourth part is the techno-economic evaluation for the S-CO_2 power cycle with different binary mixtures for different applications.

Each parts have the theoretical part, where the theoretical background for understanding of the S-CO_2 power cycle and the components is described. The other part is oriented on the description of the calculation, the boundary conditions and the input parameters which are used in the research. The last part is focused on the analysis of the results and conclusions drawn for each part of the research.

The thesis is divided into 9 chapters, where Chapters 2, 3 and 4 present an overall view of current research. The Chapter 2 focuses on a detailed description current research of CO_2 and applications with CO_2. The Chapter 3 focuses on a detailed description current research mixtures with CO_2. The Chapter 4 shows the S-CO_2 cycle layout. The summary of these chapters defines the goals of this research.

The following chapters present my research of the effect of mixtures on the S-CO_2 power cycle. The Chapter 6 is focused on the effect of mixtures on the S-CO_2 power cycle performance. The Chapter 7 shows the effect of mixtures on the cycle components, especially the effect on the heat exchangers, the compressors and the turbines. The Chapter 8 is focused on the optimization of the power cycles, where the effect of mixtures on the compressor inlet temperature is presented. The Chapter 9 is focused on the techno-economic evaluation of

the S-CO2 power cycle. The last chapters (Chapter 10) summarizes the main conclusions of the research and evaluate the overall problem of the effect of the mixtures on the S-CO_2 power cycle.

1.3 Hypothesis of Thesis

The hypothesis of this research is the detail description of the effect of mixtures on the S-CO_2 power cycle. Other hypothesis is description of substances which have negative or positive effect on the cycle and the components. The maximum amount of the second substance in CO_2, with still acceptable impact on the cycle is necessary to define. At the same time, the techno-economic evaluation is important for future design of the S-CO_2 power cycle.

This work will give an overall insight on the issue of impurities on S-CO_2 power cycle. It is an initial research of the effect of mixtures on the S-CO_2 power cycle. The results will be used as the input information for the future applications of the S-CO_2 power cycle. Especially, the S-CO_2 power cycle with working medium from different application, which produces CO_2 or from the direct-fired S-CO_2 power cycles.

Chapter 2

Overall View of Current Research of CO_2 and Applications with CO_2

Carbon dioxide (CO_2) is very interesting substance, with many benefits compare to different working medium. These benefits maybe used for high efficiency energy systems due to the operation of the power cycle in the critical region. The supercritical area of CO_2 for operation of the power cycle is very much considered for future applications. This is due to the low temperature and pressure of the critical point. Many applications for the S-CO_2 power cycles exists and use the benefits of CO_2. Nevertheless, the S-CO_2 power cycles have also disadvantages. This chapter provides the basic information on the CO_2 and the applications of pure CO_2, to the S-CO_2 power cycles, advantages and disadvantages and presentation of previous research.

2.1 Description of Properties

CO_2 is a three atomic molecule. CO_2 occurs in gas phase at ambient conditions. The sublimation temperature is -78.5 °C. The melting point and boiling points are -78 °C, -56.6 °C respectively. The critical point of CO_2 occurs at the temperature of 30.98 °C and pressure of 7.32 MPa. The critical point and phases of CO_2 are shown in Figure 2.1.

The ideal area for operation of the S-CO_2 power cycle is in the supercritical region entirely. However, in certain cases and applications, the S-CO_2 cycles are operated under the critical pressure or temperature. For example, the condensing S-CO_2 cycle [1] or the direct fired S-CO_2 cycle [2]. In such cases operating parameters of power cycle are in supecritical region, but partly the cycle operates below the critical point. The operation near the critical point is the main benefit of the S-CO_2 power cycle, because work of compressor is significantly reduced, see Figure 2.2. The reason for this decrease is caused by large property changes of CO_2 near the critical point. The variation of specific heat is shown in Figure 2.3. The

enthalpy an density variation are shown in Figure 2.4 and Figure 2.5.

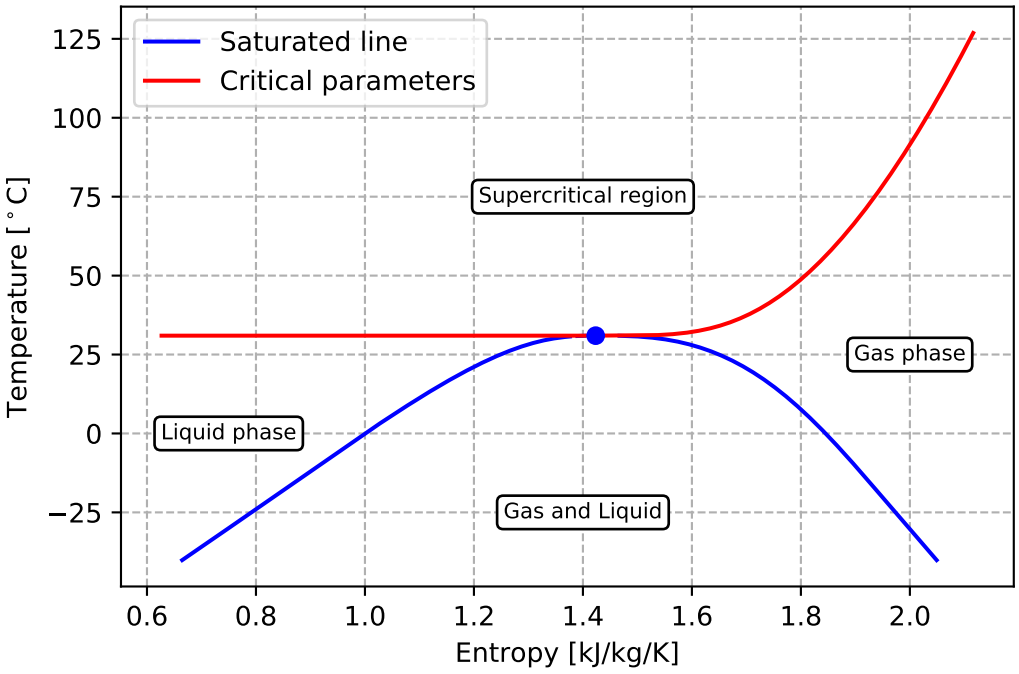

Figure 2.1: The phase diagram of CO_2

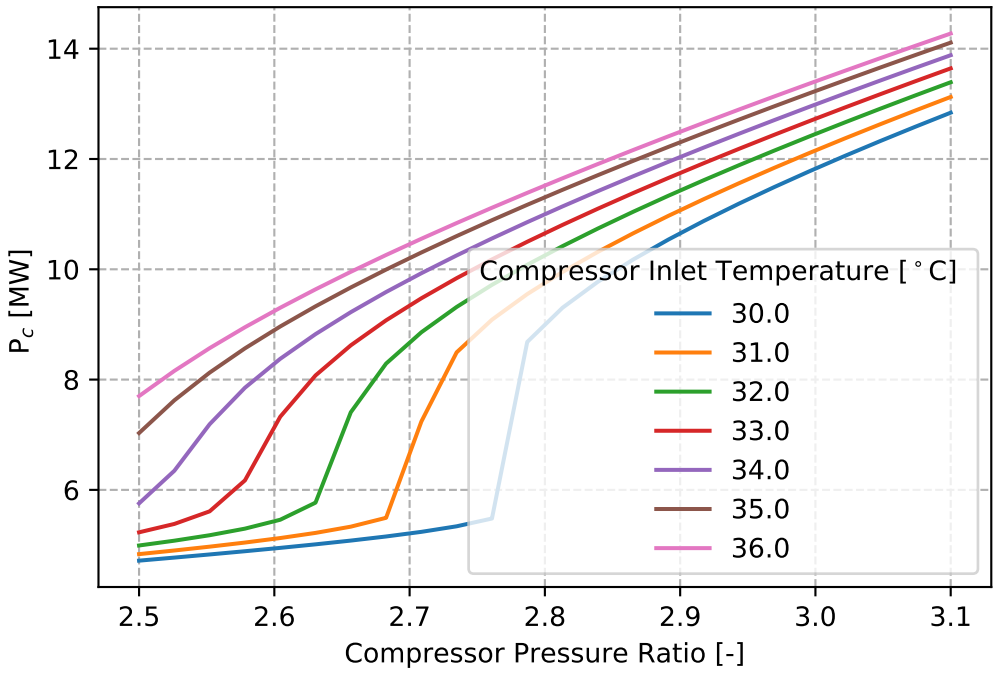

Figure 2.2: Reduction of $\mathbf{P}_c$ for certain operating conditions.

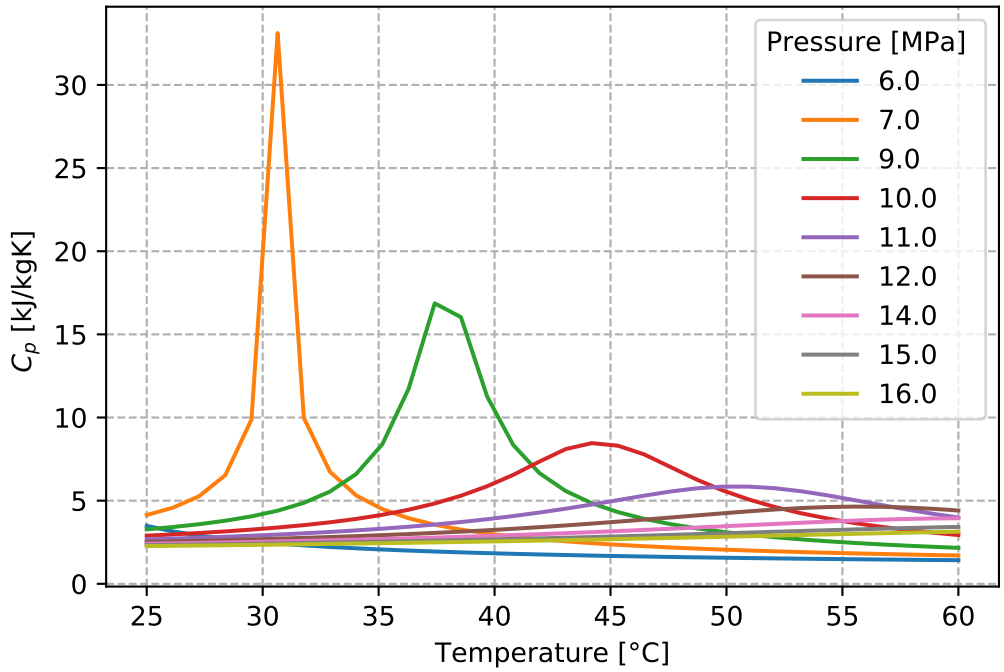

Figure 2.3: Specific heat capacity on temperature and pressure.

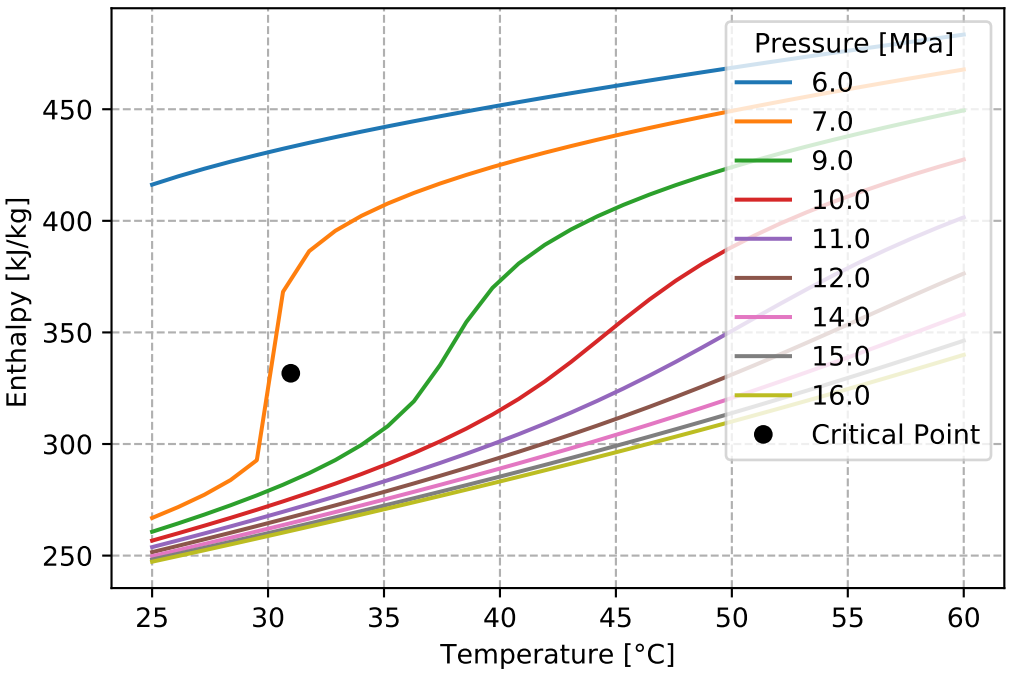

Figure 2.4: Enthalpy of CO_2 in the critical region.

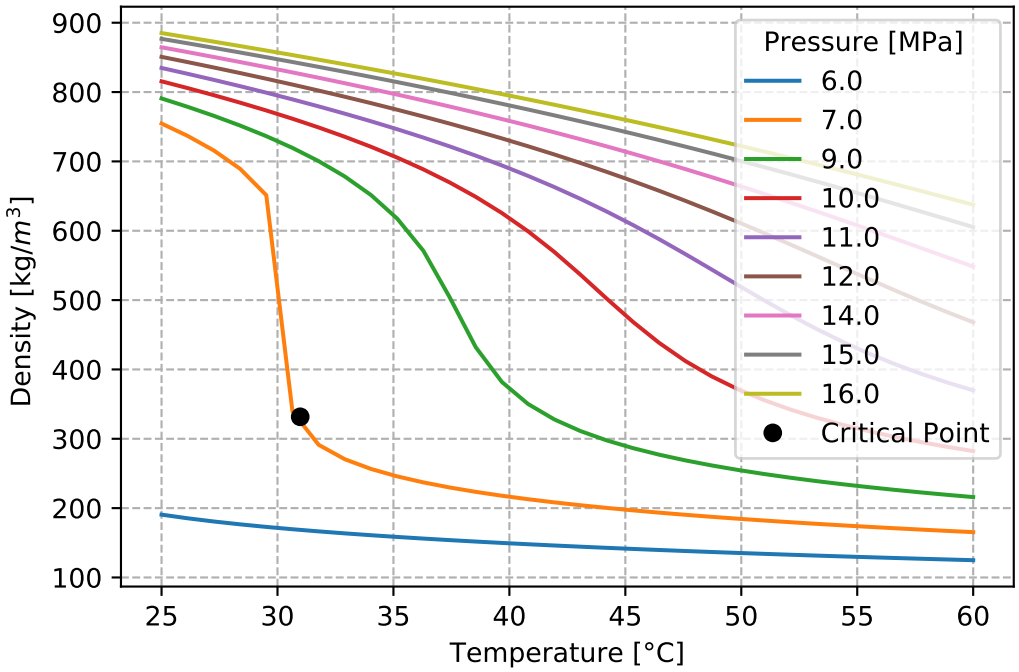

Figure 2.5: Density of CO_2 in the critical region.

According to these figures, it is obvious that properties of CO_2 are changing significantly. Property changes contribute to lower S-CO_2 compressor work. Especially, the density of CO_2 is a very important property, which significantly affects compression. The properties of CO_2 correspond more to the ideal gas when moving further away from the critical point.

2.2 S-CO_2 Power Cycles

The S-CO_2 power cycle is an alternative to other power cycles such as the Rankine cycle or the Ericsson-Brayton cycle. [3] The advantage of the S-CO_2 power cycles is in high efficiency at relatively low operating temperatures, which makes the power cycle a very attractive system [4,5]. However, the S-CO_2 power cycles have also several disadvantages and technical issues. The research of these issues and disadvantages is necessary.

2.2.1 Application of S-CO_2 Power Cycles

The use of CO_2 cycles begun in the last century [4]. However, parameters of cycles were under the critical point. With the advent of new technologies and materials, the use of cycles with critical parameters began to be considered. Initially, the use of cycles for nuclear power applications was considered [5]. The S-CO_2 power cycle is considered for new generation of

nuclear reactors, due to previous experience with CO_2 in the field of nuclear power. The development of the S-CO_2 power cycle directed to applications other than nuclear energy started to appear as well. Earlier, the basic cycle layouts were considered. However, with growing interest in S-CO_2 power cycle, the development of new cycle layouts for different application begun.

The new applications of S-CO_2 power cycles includes, the waste heat recovery systems [6], solar power plants [7, 8], geothermal power plants or application to fossil fuel power plants [2]. The typical parameters of the S-CO_2 power cycle applications are shown in Table 2.1.

Table 2.1: Applications of S-CO_2 power cycles. [3]

Application	**Power**	**Operation Temperature**	**Operation Pressure**
	[MWe]	**[°C]**	**[MPa]**
Nuclear	10-300	350-700	20-35
Fossil fuel[1]	300 -600	550 – 1500	15 – 35
Geothermal	1 – 50	100 – 300	15
Solar	10 – 100	500 – 1000	35
Waste heat recovery[2]	1 – 10	200 – 650	15 – 35

From Table 2.1, it is obvious that the range of application is quite large [3]. The S-CO_2 power cycle can be used for majority of heat sources, which are used in energy conversion systems. The S-CO_2 power cycle is being developed for heat source with higher power, approximately 600 MWe, as well as for heat source with low power, approximately from 1 to 50 MWe. Recently, the area of the greatest interest in the S-CO_2 power cycles is for waste heat recovery applications. The S-CO_2 power cycles cycle layout flexibility benefits from multiple heat source application, which is important for waste heat recovery systems. With the development of new cycle layouts, this potential increases. [2, 9, 10]

The new cycle layouts are developed for specific application such as waste heat recovery systems or solar and geothermal power plants. The power range for this application is very similar, approximately from 1 to 50 or 100 MWe (solar power plant), see Table 2.1.

The S-CO_2 power cycle for waste heat recovery system can utilize heat from exhaust (gas turbines) or waste heat from factories as well as from waste heat from existing fossil or nuclear power plants.

Other potential applications are fossil fuel sources, which are considering the highest power, see Table 2.1. [11, 12] The direct S-CO_2 power cycles are a promising application for this area. The syngas or natural gas is considered as a fuel for the direct S-CO_2 power cycle. [A.1]

[1] Syngas, natural gas, ...

[2] Gas turbine, waste heat from factories, ...

Combination of the S-CO_2 power cycle with systems for accumulation of energy are another very interesting topic. The principle is similar as for Compressed Air Energy Storage (CAES) [13], but the working medium is CO_2. Basically, the systems are developed for renewable sources such as solar power plants, or for accumulation of energy from wind. [7]

2.2.2 Advantages and Disadvantages

The main advantage of the S-CO_2 power cycles is that they are more compact than steam or helium Brayton cycles. [4] The compressor and the turbine are significantly smaller due to the high operating pressure. [5] The size of heat exchangers can be optimized by operating parameters and type selection. [A.2] The compression work for each cycle layouts is lower than in the case of helium Brayton cycle. [5] The reduction of compressor work is caused due to the operation near the critical point as shown in Figure 2.2.

Other advantage is the existence of thermodynamic properties data for pure CO_2. The CO_2 is non-toxic and cheap due to its abundance. The low molecular leak due to higher molecular mass. The molecular mass is about 44 g/mol for CO_2. For the Ar is about 38 g/mol and for He is about 4 g/mol. Depending on the operating parameters and thermophysical properties, the components have low cost compared to the other working fluid for Brayton cycle. There is more than twenty years of experience with CO_2 in nuclear power engineering such as MAGNOX or AGR nuclear reactor.

The main disadvantage of the S-CO_2 power cycles is that the S-CO_2 power cycle is not proven technology, many small technical issues may be apparent. One of this issues is the so called "pinch point". The existence of pinch point in heat exchangers significantly affects their design. [5], [A.2] The pinch point may be present for any type of medium, but its influence on the components is especially high when CO_2 is used as a working fluid. The pinch point primarily occurs in the recuperative heat exchangers with identical working fluid and mass flow on the both side (the hot and the cold side) of the heat exchanger.

2.2.3 Pinch Point

The pinch point is caused by change of properties depending on temperature and pressure. The occurrence of the pinch point may be a significant issues in the design of efficient heat exchanger. The pinch point is defined as, the minimum temperature difference in the heat exchanger. [A.2, A.3] This point may be present in all systems and working fluids. The highest impact for the S-CO_2 power cycles is on the recuperative heat exchangers, because, they operate near the critical point in the area where the properly changes are significant.

The pinch point is mainly caused by the variation of the heat capacity of CO_2 and

occurs at the temperature when the heat capacity profiles of the hot and cold streams (each at a different pressure level) intersect. [A.2, A.3] Due to the pinch point, the heat exchangers may have a large size and low efficiency.

The heat capacity changes dramatically near the critical point of CO_2. This large changes, near to the critical point, have a high probability of causing intersection of heat capacity profiles of the hot and cold streams.

The variation of the heat capacity is shown in Figure 2.3. According to Figure 2.3, it is obvious that the peak of heat capacity depends on pressure. The peak is highest near the critical point. The intersections have an effect on the temperature difference. The temperature difference can be theoretically negative, if the calculation is performed using the classical approach based only on mass and energy balance and accounting only for the temperature difference at heat exchanger inlet or outlet. The negative temperature difference is shown in Figure 2.6. This heat exchanger would never work, because the temperature difference is negative.

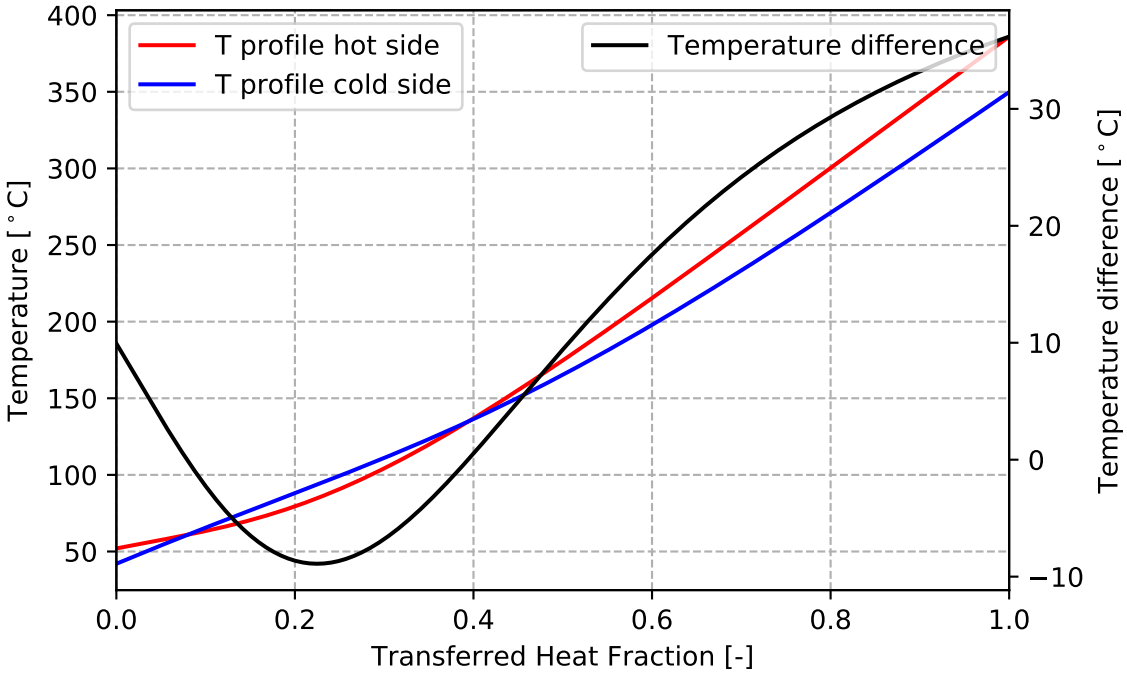

Figure 2.6: Temperature profiles and temperature difference of recuperative heat exchanger. [A.2]

The procedure of calculation has to be changed. One way is to use the temperature of the pinch point. The temperature of the pinch point is the temperature of intersection of the heat capacity. The intersection of the heat capacity can be found, if the thermal-physical properties of CO_2 are known. [A.2, A.3], The calculation of the temperature of the pinch point can be done by Equation 2.1. [A.3]

$$T_{(P_{hs},P_{cs})} = \left(0.0008P_{cs}^2 - 0.0297P_{cs} + 0.0865\right) P_{hs}^2 + \left(0.0291P_{cs}^2 + 1.2782P_{cs} - 3.9973\right) P_{hs} + \left(0.1363P_{cs}^2 - 5.7125P_{cs} + 44.384\right) \tag{2.1}$$

where, $\mathbf{P}_{cs}$ [MPa] is pressure of the cold stream and $\mathbf{P}_{hs}$ [MPa] is pressure of the hot stream. The results are accurate to within approx. ± 2 °C.

The Equation 2.1 was derived from the heat capacity profiles, see Figure 2.3. The dependence of the intersection of the heat capacities has a quadratic profile for each pressure level. The quadratic profiles are described with quadratic equation for each pressure level. The coefficients in quadratic equation from each pressure level have also quadratic profiles. The combination of the quadratic equations give the Equation 2.1. [A.3]

The Equation 2.1 shows the dependence of the intersections of the heat capacity on temperature and pressure. As the heat capacity is already matched to a given temperature, there is no need to determine the heat capacity in the equation, and the result of the Equation 2.1 gives the temperature of the intersection at which the pinch point occurs. The presented function already contains this dependence. The Equation 2.1 enables to verify the occurrence and location of the pinch point before the heat exchanger design is started. Thereby, it is possible to reduce the number of iterations and accelerate the whole calculation process. [A.3]

2.3 Current State of Research

The research on the S-CO_2 power cycles is intensive in the last 20 years. However, a commercial S-CO_2 power systems still does not exist. The research is largely theoretical, focusing on cycle analysis and the design of new cycle layouts for applications from Table 2.1 [2, 9, 10]. However, the research moves to the practical verification of proper functioning of the components in the operating conditions and detailed design of components, especially compressors and heat exchangers.

The research is done for example in the Naval Nuclear Lab [14], Southwest Research Institute [15], Argonne National Laboratory [16], Tokyo Institute of technology [19] or Korea Institute of Energy Research [17] and University of Wisconsin, Madison [18]. The research of a heat exchangers is focused on heat transfer and design of channels for the PCHEs (Printed Circuit Heat Exchangers). [15, 18–20] However, the research also focuses on the shell and tube heat exchangers, plate fin heat exchangers or ceramic heat exchanger (application for direct-fired S-CO_2 cycle) [21] depending on the application and utilization. Because, the gas cycle has at least three different types of heat exchangers, the cooler, the heater and the recuperative heat exchanger, each type of the heat exchanger has a different operating

parameters. Therefore, different types of the heat exchangers can be used.

The important part of the power cycle is the compressor. University of Wisconsin carried out research and developed a compressor and other component of the S-CO_2 cycle. [22] The Sandia National Laboratories (SNL) is conducting research of S-CO_2 power cycle for solar power plants, as well as testing components of the power cycle since 2007. The research is focused on testing of compressor near the critical point of CO_2. The radial compressor with power of 50 kW was used. The compressor speed was 75 000 rpm and mass flow rate was 3.51 kg/s. The compressor efficiency was found to be 66% [23]. The experimental loop was used for testing of turbo compressors, dynamic behaviour of compressors, verification of control elements and dynamic codes. The turbine for 10 kW was developed. The maximal turbine temperature was 600 K. [24]

Other experimental loop is at the Tokyo Institute of Technology and Institute of Applied Energy in Japan. As already mentioned, research on heat exchangers is being carried out there as well as turbine and compressor testing. [25] The power of the experimental loop is 10 kWe, mass flow rate is 1.2 kg/s, the turbine inlet temperature is 550 K and pressure is 12 MPa. The compressor speed is 100000 rpm. The research is focused on the fast nuclear reactors (SFR). The research in Delft University of Technology is focused on CFD simulation of compressor, turbulent flow and study of CO_2 properties. [26] The research of the S-CO_2 power cycle is also carried out in the Czech republic. The Research Center Rez built an experimental loop for testing of components of S-CO_2 power cycle. [A.4]

At the same time, the research of the effect of mixtures on the S-CO_2 power cycle is in progress but, only on a marginal scale [27–29], which is focused on the specific application of the S-CO_2 power cycle, for example direct-fired S-CO_2 power cycle [2, 11, 12]. Another research is being done for CCS. The research is focused on the impact of impurities on compression, liquefaction and transportation [30–33].

2.4 Summary

Research of the S-CO_2 power cycle is done all over the world. As can be seen the research is focused on the behaviour of the cycle layout and components testing. Development of the S-CO_2 power cycle is done from demonstrable benefits, which have been described in this chapter. Research is focused on many application, different cycle layouts and for each component is the system. However, the research is mostly done for pure CO_2. The pure CO_2 will most likely not be used in the real cycle. It is much more likely that the working medium will be a mixture with CO_2. Therefore the research of the effect of mixtures on the cycles and the components of the cycles is necessary.

Chapter 3

Overall View of Current Research of Mixtures with CO_2

As previously described in Chapter 2, the research of the S-CO_2 power cycle is done around the world, but mostly for pure CO_2. However, it is evident that pure CO_2 will most likely not be used in the real cycle. It is much more likely that the working medium will be a mixture of CO_2 as main constitment with other minor gases. This chapter will describe basic properties of potential mixture substances, basic investigated mixtures and description of properties calculations for mixtures. At the same time, equations of state for calculation will be described. The result of this chapter will be detailed description of mixtures that need to be understood for subsequent work.

3.1 Research of Mixtures

The properties of CO_2 are necessary, for the design and the calculation of the S-CO_2 power cycle. The properties of CO_2 are changing rapidly, especially near the critical point of CO_2, as previously described in Chapter 2. The properties of pure CO_2 are described quite well. [34] The problem occurs when the working medium is not pure CO_2, but a mixture with certain high fraction of CO_2. The mixtures with CO_2 are an integral part of gas power cycles. The mixture can occur as an impurity, due to leakage or as a specific working fluid. The mixture can be used to detect leakages [27] or can be used as medium from other systems that produce CO_2, such as carbon capture and storage (CCS) system. [A.5], [35] The mixture can also be a product from combustion in the direct-fired S-CO_2 power cycle. [2] For this reason, the detailed description of thermo-physical properties of mixtures with CO_2 is necessary.

At the same time, the research of the effect of mixtures on the S-CO_2 power cycle is also necessary. This research is in progress but, only on a marginal scale [27–29], which is focused on the specific application of the S-CO_2 power cycle. The most comprehensive

research is being done for CCS, where the research is focused on the impact of impurities on compression, liquefaction and transportation [30–33]. However, this research is focused on the CCS. Although, the problem with compression in CCS is very similar to the problems in S-CO_2 power cycle. Both technologies use the compressor near the critical point or the saturation line of CO_2. The critical point and saturation line are moving when mixtures are used. [A.6] That means, the problem of rapid change of properties of CO_2 near the critical point can be shifted to different temperatures and pressures. The critical point of some substances is shown in Figure 3.1.

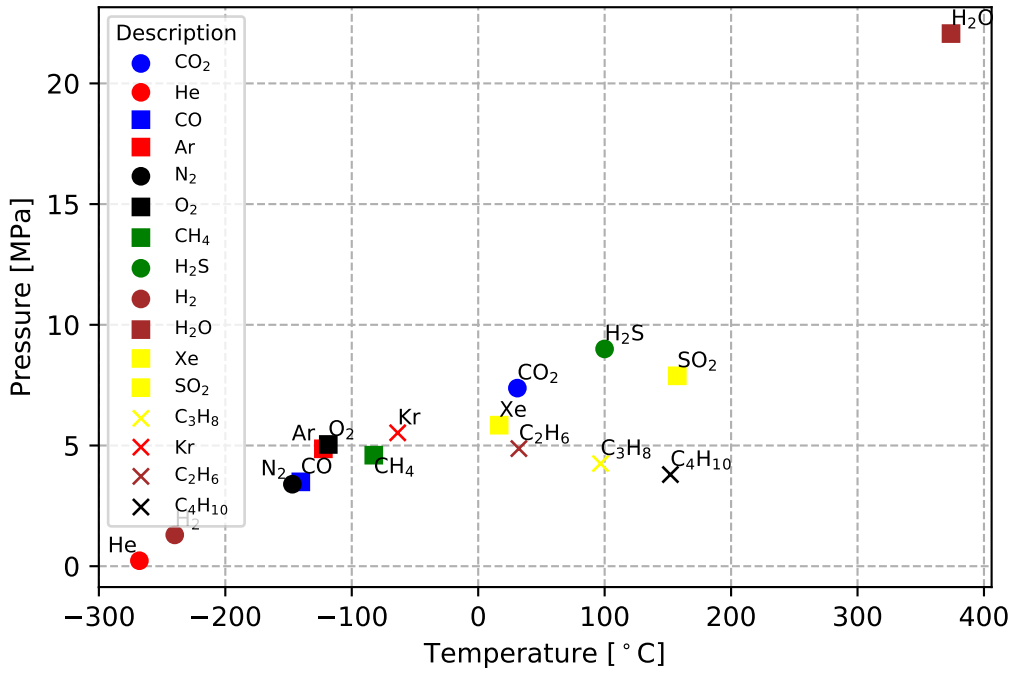

Figure 3.1: The critical point for investigated substances.

The range of the critical temperatures is from -300 to 400 °C and the range of critical pressures is up to 20 MPa, for these specific substances. The critical point for binary mixture with 99 % pure CO_2 is shown in Figure 3.2. The effect on the critical point can be clearly seen. This has an effect on compression and heat transfer, especially for cooler and low temperature recuperative heat exchanger.

The research of the effect of mixtures on the S-CO_2 power cycle is divided in two parts, the research of the direct-fired S-CO_2 power cycle and the in-direct S-CO_2 cycle. For the direct-fired S-CO_2 power cycle the mixture is a product of the combustion process. [11,12], [36] However, the effect of mixtures is the same as for the in-direct S-CO_2 cycles. The difference is that hypothetically we have the same medium in the in-direct S-CO_2 power cycle, when in general we have a different media due to leakages [27] or chemical processes and corrosion that may occur during the cycle operation. [37]

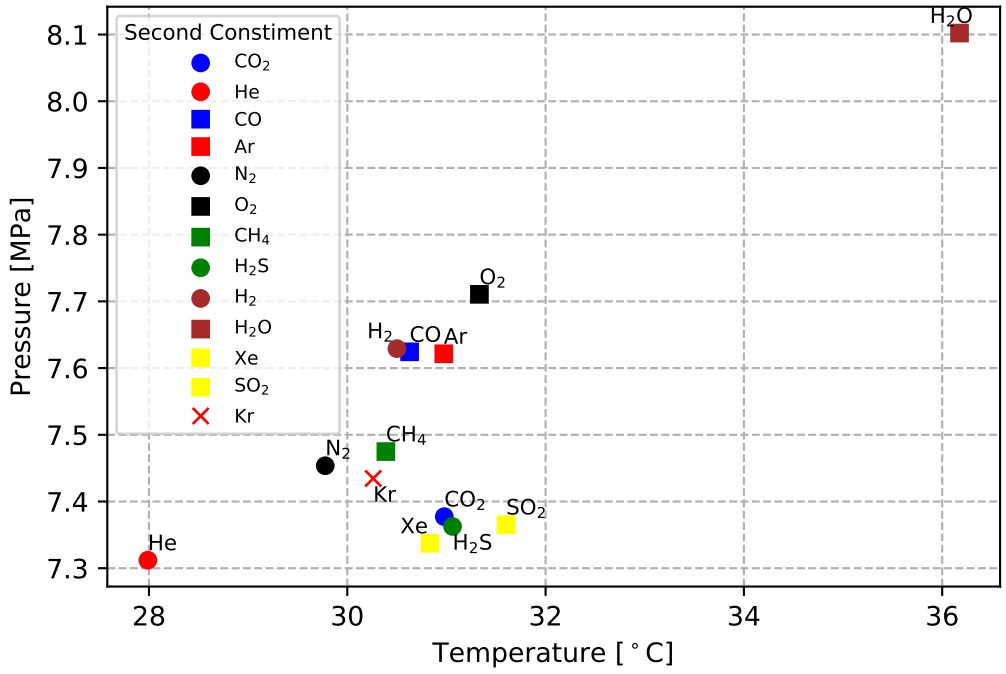

Figure 3.2: The critical point for the binary mixture - 99 % of CO_2.

3.2 Description of Mixtures

The previous research was focused on the effect of specific binary mixtures on the cycle efficiency. One of the research focused on the effect of small amount of He and Air on the cycle. [27] The He was considered as the hypothetical substance for the detection of leaks. The second mixture was Air which is a hypothetical impurity from leaks. Another research was focused on mixtures in SFR (Sodium cooled fast reactor). The substances that were considered were, He, Ar, N_2 and O_2. [28] Other potential substances are Kr and Xe. H_2S is also considered as substance for mixtures. [29]

Other substances such as CO or CH_4 may also be present in the mixtures for the transport, see Table 3.1. The idea is, that this medium with CCS can be used as working medium for the S-CO_2 power cycles. [35], [A.5] For this reason, these substances were also included in the research. There are another substances which has an effect on working medium, for example water or SO_2. Hypothetically propane, methane, butane and many other substances may also occur. [38, 39]

Table 3.1: Recommended composition of the mixture for the transport. [35]

Component	**H_2O**	**H_2S**	**CO**	**CH_4**	**N_2**	**O_2**	**Ar**	**H_2**	**CO_2**
	[ppm]			**[vol.%*]**			**[vol.%*]**		[%]
Pipeline	500	200	2000	<4	<4	-	<4	<4	>95.5
Ship/truck	50	200	2000	<0.3	<0.3	-	<0.3	<0.3	>99.7
*all condensable gases									

Basically, every mixture is a multicomponent mixture which has more different substances. Some multicomponent mixtures are shown in Table 3.2, but these are only a hypothetical mixtures that may occur.

Table 3.2: Multicomponent mixtures. [A.7]

	Air	**M-I**	**M-II**	**M-H**	**Air-H**	**M-IH**
	[mole %]					
CO_2	99.0	99.7	97.1	98.5	98,0	99.72
Ar	0.01	0.03	0.66	-	0.01	0.03
N_2	0.78	0.03	0.66	-	0.78	0.03
O_2	0.21	-	-	-	0.21	-
H_2	-	0.03	0.66	-	-	0.03
CH_4	-	0.04	0.65	-	-	0.04
H_2S	-	0.02	0.02	1	1	-
CO	-	0.15	0.25	-	-	0.15
He	-	-	-	0.5	-	-

The main issue is that it is impossible to predict the exact composition of mixtures, even if the input working medium is known. For this reason, the research on mixtures is very complicated. However, we know which substances may occur in the working medium. Each substance has a different effect on components and the cycle. Therefore it is desirable to describe the effect of the individual substances. The effect of hypothetical multicomponent mixture is than the combination of effects of each substance which occur in the mixture.

For this reason, research in this thesis is focused on the basic binary mixtures with CO_2. The substances that were investigated are: [A.6, A.8]

- Helium
- Argon
- Oxygen
- Hydrogen

- Nitrogen
- Carbon monoxide
- Hydrogen sulfide
- Methane
- Krypton
- Xenon
- Sulfur dioxide

3.3 Description of Substances

The S-CO_2 power cycle operates prartly in the area of critical properties. Especially, the compressors operates very close to the critical point. [3, 5] The supercritical region is located above the critical pressure and temperature, see Figure 2.1. At the critical point, the properties of liquid and gas are equal, and there is no difference between these states. Above the critical temperature a substance may exist only in the gas phase, however, the properties are close to the liquid phase. The critical temperature is defined as the highest temperature at which substance may exist in the liquid state. At the same time at the critical point, the molar volume of the liquid phase can not be greater than the critical volume and the condensation heat at the critical point is zero, see equation 3.1. [40, 41]

$$\left(\frac{\partial p}{\partial V_m}\right)_T = \left(\frac{\partial^2 p}{\partial V_m^2}\right)_T = 0 \tag{3.1}$$

The critical points of investigated substances are shown in Figure 3.1. The range of the critical temperatures is from -300 to 400 °C and the range of the critical pressures is up to 20 MPa. The critical point of mixtures differs. However, this change differs for each substance and its fraction. It also important whether it is a binary or a multiple-component mixture. The critical points for binary mixtures with 99 % CO_2 purity are shown in Figure 3.2. It can be seen, that the temperature and pressure of the critical point of the binary mixtures are is similar, except for H_2O and He. However, even such small change can affect the compression process and therefore the entire power cycle.

3.4 Properties of Mixtures

The most important information for calculation of power cycle are properties of working fluid. There are many different table values of different properties. The data are then used to built equations of state, that describe the behaviour of the substances. This applies to both pure substance and mixtures. For proper application of data for calculation it is necessary to understand each EOS and define which EOS is the best for the investigated mixtures [40–42].

3.4.1 Equation of State

The equation of state is necessary for calculation of substances behaviour. The equation of state describes the relationship between the pressure, temperature and volume of a substance. The state behavior is primarily conditioned by interactions between molecules. The equation of state must meet the conditions resulting from the theoretical concepts and the experimental facts. The first condition is that for the low pressures, Equation 3.2 must result from the equation of state. The second condition is that Equation 3.1 must apply at the critical point. The third condition is that for subcritical temperatures there must be at least three positive values of the molar volume for each pressure value. The EOS for pure gas is defined as Equation 3.3. [40]

$$\lim_{P\to\infty} PV = \lim_{d\to\infty} PV = RT \tag{3.2}$$

$$PV = NR_uT \tag{3.3}$$

where is $\boldsymbol{R_u}$ universal gas constant (8315 J/mol K). The relationships between **P**, **V** and **T** of the real gas pose a more complex problem and other equation of state must be used, e.g. Equation 3.4.

$$PV = ZNR_uT \tag{3.4}$$

where **Z** is the compressibility factor. The compressibility factor can be determined from the EOS. The most accurate expression of the compressibility factor is from the EOS used in the form of an infinite series, according to Equation 3.5. Equation 3.5 is a virival equation

of state. The **B(T)**, **C(T)**, **D(T)**, etc. are function of temperature and are defined as the virial coefficients. [40]

$$z = \frac{PV}{RT} = 1 + \frac{B\,(T)}{V} + \frac{C\,(T)}{V^2} + \frac{D\,(T)}{V^3} + ... \tag{3.5}$$

This applies to both pure substances and mixtures. In the case of mixtures, it is necessary to define other parameters as well. The characterization of the components of the mixture is performed via mole fraction of species i ($\boldsymbol{\chi_i}$) Equation 3.6 and mass fraction of species i (Y_i) Equation 3.7 [42].

$$\chi_i = \frac{N_i}{N_1 + N_2 + ...N_i} = \frac{N_i}{N_{tot}}, \qquad \sum_i \chi_i = 1 \tag{3.6}$$

$$Y_i = \frac{m_i}{m_1 + m_2 + ...m_i} = \frac{m_i}{m_{tot}}, \qquad \sum_i Y_i = 1 \tag{3.7}$$

where, $\mathbf{N}_i$ is the number of molecules and $\mathbf{m}_i$ is the mass of molecules.

The prediction of the relationship of **P**, **V** and **T** for the gas mixture is based on two models. Dalton's law of additive pressure and Amagat's law of additive volumes [42]. Both laws are exact for ideal gas mixture, but only approximate for real gas mixtures. The relationship for real gas mixture can be done with more complex equations of state or by the use of the compressibility factor **Z**, according to Equation 3.4. The compressibility factor **Z** for mixture is defined as follows. [40]

$$Z_m = \sum_{i=1}^{k} y_i Z_i \tag{3.8}$$

The Dalton's law of additive pressure: the pressure of a gas mixture is equal to the sum of the pressures each gas would exert if it existed alone at the mixture temperature and volume. [42]

The Amagat's law of additive volume: the volume of a gas mixture is equal to the sum of the volumes each gas would occupy if it existed alone at the mixture temperature and pressure. [42]

The ideal gas equation of state is very simple, but the range of applicability is limited.

However, it is useful for prediction of behaviour of a substance accurately over a large range of parameters. The equation of state will be naturally more complex for cases of mixtures. There are currently dozens equations of states. The most commonly used equation is the Van der Waals equation, see Equation 3.9. [40, 42]

$$\left(P + \frac{a}{V^2}\right)(V - b) = RT \tag{3.9}$$

This equation of state describes very well state behaviour, but a quantitative description of state behaviour of gas is not very reliable. The compressibility factor for Van der Waals equation of state is 0.375. The constants a and b are calculated according to Equation 3.10.

$$a = \frac{27\left(RT_c\right)^2}{64P_c}, \qquad b = \frac{RT_c}{8P_c} \tag{3.10}$$

For calculation of CO_2 properties a different equations of state is more suitable. These are the REDLICH - KWONGO, the REDLICH-KWONG-SOAVE, the PENG-ROBINSON, the BENEDICT-WEBB-RUBIN-STARLING and the PATEL-TEJA, see below. [40, 42]

The REDLICH - KWONGO (RK) equation of the state, see Equation 3.11, has the constants **a** and **b** are calculated according to Equation 3.12. [40, 42]

$$\left[P + \frac{a}{T^{1/2}V\left(V + b\right)}\right](V - b) = RT \tag{3.11}$$

$$a = 0.4278\frac{R^2T_c^{5/2}}{P_c}, b = 0.0867\frac{RT_c}{P_c} \tag{3.12}$$

Another equation of state is the REDLICH-KWONG-SOAVE equation (SRK), Equation 3.13. The constants **a** and **b** in the SRK equation are calculated according to Equation 3.14. [40, 42]

$$\left[P + \frac{a}{V\left(V + b\right)}\right](V - b) = RT \tag{3.13}$$

$$a = 0.4278\frac{R^2T_c^2}{P_c}, b = 0.0867\frac{RT_c}{P_c} \tag{3.14}$$

The next equation of stage is the PENG-ROBINSON equation of state, Equation 3.15. The constants **a** and **b** in the PR equation are calculated according to Equation 3.16. The commercial softwares also use other equations of state, for example the BENEDICT-WEBB-RUBIN-STARLING (BWRS) or the PATEL-TEJA (PT) and others. The PR and the SRK EOSs are more accurate predictions of properties than other similar equation for CO_2 and the respective mixtures. [3]

$$\left[P + \frac{a}{V\left(V+b\right)+b\left(V-b\right)}\right]\left(V-b\right) = RT \tag{3.15}$$

$$a = 0.4278\frac{R^2T_c^2}{P_c}, b = 0.07780\frac{RT_c}{P_c} \tag{3.16}$$

All of the above equations are equations of state which were developed for pure gas. In the case of mixtures, we can use these EOSs, which have been described above. But, these EOSs are not entirely correct to describe the behavior of the mixtures. Because, the state behavior is primarily conditioned by interactions between molecules. However, in the case of mixtures, consideration must be given to interactions between the same molecules and the molecules of the different substances between them. The EOSs have to be modified for the mixtures. The modification of the EOSs is done using constants **a** and **b**, for example, according to Equation 3.17. [40]

$$a_m = \left(\sum_{i=1}^{n} y_i a_i^{1/2}\right)^2 ; b_m = \sum_{i=1}^{n} y_i b_i \tag{3.17}$$

Equation 3.17 defines constant **a** and **b** of the Van der Waals equation of state. The same principle can be used for other EOSs, for example Equation 3.18. [40]

$$a_m = \sum_{i=1}^{n}\sum_{j=1}^{n} y_i y_j \left(a_i a_j\right)^{1/2} ; b_m = \sum_{i=1}^{n} y_i b_i \tag{3.18}$$

Equation 3.17 defines constants of the REDLICH - KWONGO equation of state. Where, the constants **y**, **a** and **b** defines interactions between the same molecules and the molecules of the different substances.

3.5 Source of Data

The accurate thermo-physical properties of pure CO_2 are known [34, 43]. However, the property database for mixtures is limited and not available for all the mixtures encountered in the real scenario. [33] It is possible to use the existing equations of state, which were written and verified on the real data. [44–47]

For the thermodynamic calculations of the power cycle and the heat exchangers this work used the programming language Python. In the current investigation the properties of gases and mixtures was estimated using the NIST Reference Fluid Thermodynamic and Transport Properties database, Version 9.1. [48] and Open-Source Thermo-physical Property Library CoolProp. [49] The equation TREND 2.0 [44] was applied at the same time. To control the CO_2 mixtures with low concentrations of other substances.

3.6 Summary

The issues of the impurities and mixtures with CO_2 is great and very important for correct understanding of the effect of mixtures on the S-CO_2 power cycle, as can be seen from the foregoing description of the mixtures. The EOSs can be used for calculation, but the molecular interaction for each substance and between the substances has to be considered. For research in this thesis fluid thermodynamic and transport properties databases, which have been developed for both pure substances and for mixtures was used.

Chapter 4

Supercritical Carbon Dioxide Cycle

This chapter is focused on the detail description of the S-CO_2 power cycles. Basic cycle layouts will be introduced. The detail description of the cycle layouts is necessary for future understanding of calculation of the effect of mixtures on the S-CO_2 power cycles in this thesis.

4.1 History of S-CO_2 Cycle

The first research on the use of CO_2 cycles appears in the first half of the 20th century. [4] During this research the interesting properties of CO_2 were identified, but because of the imperfections in construction and materials it has never been tested in practice, despite the broad research on the cycles with supercritical CO_2. With the advent of the modern technology, new materials lead to reconsider the use the of the S-CO_2 power cycles in the new reactors and subsequently in solar and geothermal power plants as well.

4.2 Basic S-CO_2 Cycle Layouts

The S-CO_2 power cycle is a gas power cycle derived from the Ericsson-Brayton cycle, which offers many different layouts for solar, geothermal, nuclear power plants or waste heat recovery systems. Each layout tries to approach the Carnot cycle and its efficiency. The basic layouts considering the use of S-CO_2 are following: [4, 5, 50]

- Simple Brayton cycle
- Re-compression cycle
- Pre-compression cycle
- Split Expansion cycle

- Partial Cooling cycle

The Brayton cycle consists of a compressor **(C)** for isentropic compression, a turbine **(T)** for isentropic expansion. It also consists of a cooler **(CH)** and a heat source **(H)**. The heat source can be a heater or a combustor or other hypothetical system for heating the cycle, according to the application. Basically, the heater is a heat exchanger for indirect S-CO_2 power cycles and the combustor is a component for direct S-CO_2 power cycle. To improve the cycle efficiency the cycles use recuperative heat exchanger, which is used for heat regeneration.

Every cycle has these basic components. However, the number of components is different, because every cycle layout was developed for a specific application or to eliminate certain disadvantage of the other cycle layouts. The basic layout of the S-CO_2 power cycle is the simple Brayton cycle, see Figure 4.1. This cycle is very simple. However, the cycle layout is very problematic due to the pinch point in the heat exchanger **(RH)**. On the other hand the thermal efficiency is improved by introducing the recuperator.

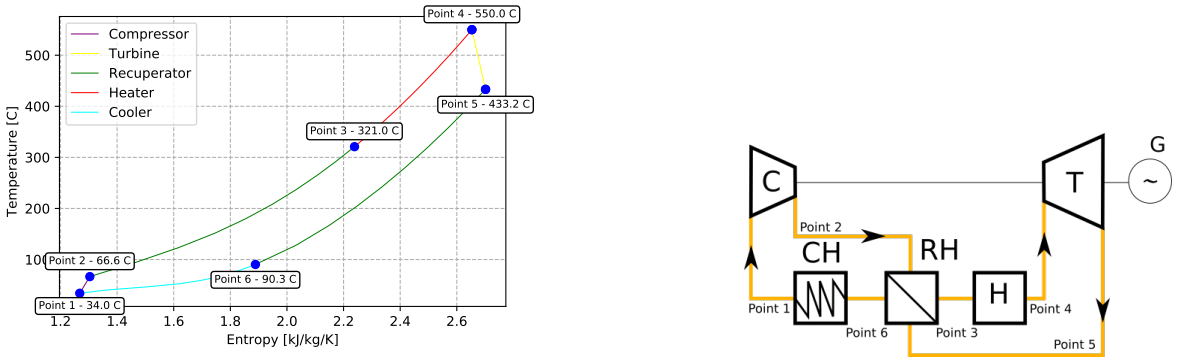

Figure 4.1: T-s diagram and cycle layout of the Simple Brayton cycle

The Re-compression cycle is shown in Figure 4.2. The difference between the simple Brayton cycle and the the Re-compression cycle is the additional compressor and the recuperative heat exchanger. The Re-compression cycle is more complex. The main difference or benefit lies in dividing the flow before cooling into two streams. One stream goes through the cooler to the main compressor and the second stream goes through the re-compressor. This design has an effect on the recuperative heat exchangers **(LTR)** and **(HTR)** and the problem with the pinch point in the **(LTR)** is eliminated, due to mass flow alteration on the hot side. The flow split has to be properly selected.

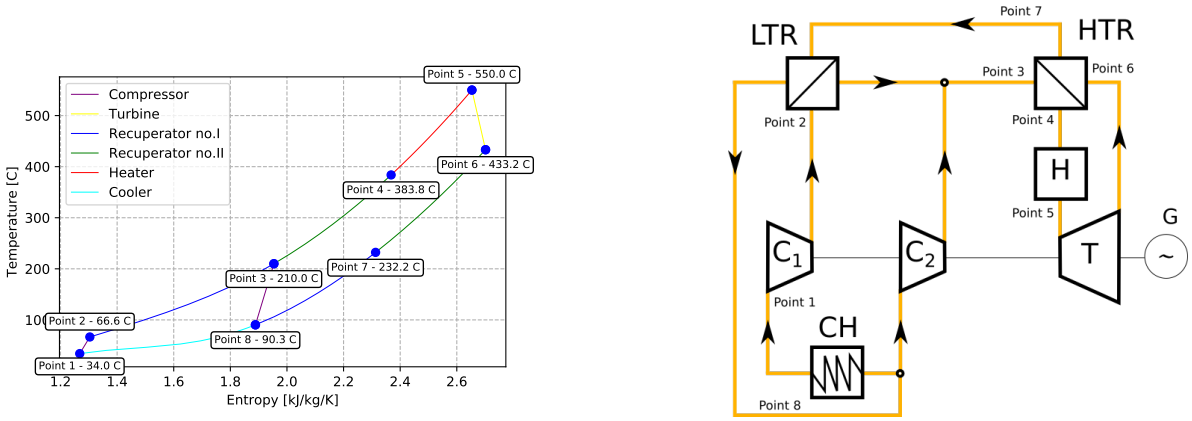

Figure 4.2: T-s diagram and cycle layout of the Re-compression cycle

The Pre-compression cycle is shown in Figure 4.3. The number of components is the same as for the Re-compression cycle. However, the Pre-compression cycle has only one stream. The main advantage of the Pre-compression cycle is in different inlet pressure to main compressor and the turbine outlet pressure. The turbine outlet pressure is thus in the Pre-compression independent on the compressor inlet pressure. At the same time pinch point is avoided by pressure increase between the recuperative heat exchangers.

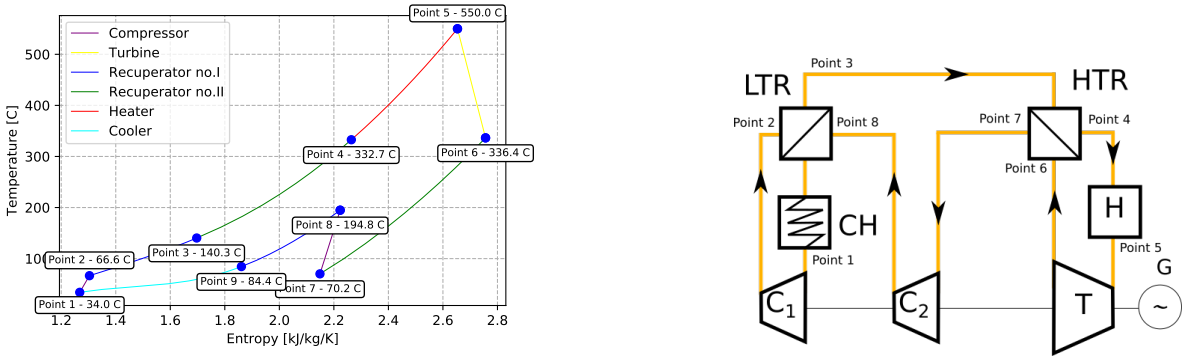

Figure 4.3: T-s diagram and cycle layout of the Pre-compression cycle

The Split Expansion cycle is very similar to the Re-compression cycle. The Split Expansion cycle has two turbines ($\mathbf{T}_1$ and $\mathbf{T}_2$). The Split Expansion cycle is shown in Figure 4.4. The second turbine is used in order to decrease the pressure of the heat source. The stresses are thus decreased. Other benefits are similar as for the Re-compression cycle. The pinch point is avoided. On the other hand cycle efficiency is slightly lower than for the Re-compression cycle.

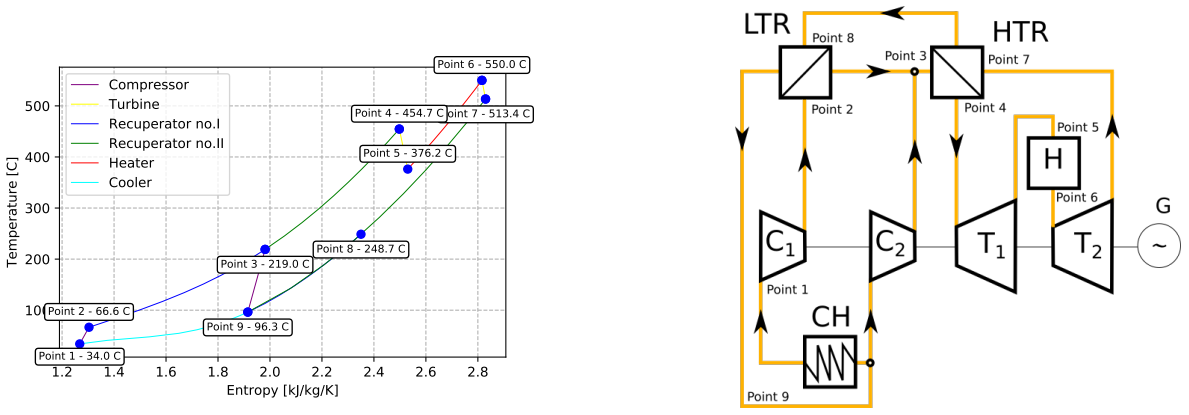

Figure 4.4: T-s diagram and cycle layout of the Split expansion cycle

The Partial Cooling cycle is the last basic cycle layout considered. This cycle has three compressors ($\mathbf{C}_1$, $\mathbf{C}_2$ and $\mathbf{C}_3$) and two coolers ($\mathbf{CH}_1$ and $\mathbf{CH}_2$), the other components are the same as for the other cycle layout. The Partial cooling cycle is shown in Figure 4.5. This cycle is very complicated. It is a hybrid between the Pre-compression and the Re-compression cycles. The benefits of both cycle layouts are integrated in this cycle layout.

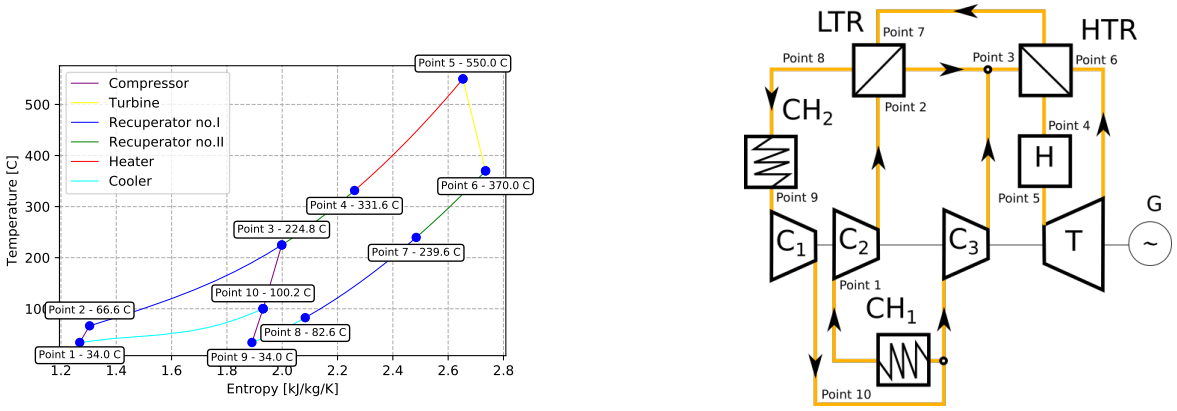

Figure 4.5: T-s diagram and cycle layout of the Partial Cooling cycle

4.3 Advanced S-CO_2 Cycle Layouts

With growing interest in the use of S-CO_2 power cycle new cycle layouts were developed for many applications around the world. These new cycle layouts are developed for special applications.

One of them is a modification of the Partial cooling cycle. The modification improves regeneration. The Partial cooling with improved regeneration is very similar cycle layout as for the Partial cooling cycle. The main different is in the cooler, which is made up of three

streams. This heat exchanger increases the heat removal from the cycle.

Each application needs different cycle layout, because the benefits are different for different applications. With increasing interest in waste heat recovery systems, cycle layouts with multiple heaters were developed. [51–53] These cycles have a better heat utilization, which is important for this application. In addition, these cycle layouts can be used for other application with multiple heat sources, for examples fusion power reactor [54–57]. It appears, that S-CO_2 power cycle is a very interesting cooling system for this application. [A.9]
Some of the advanced S-CO_2 power cycles are following:

- Dual Heater cycle
- Cascade cycle
- Kimzey cycle

One of the advanced cycle layout is the Dual Heater cycle. [58] The Dual heater cycle is shown in Figure 4.6. The Dual heater cycle is based on the Simple Brayton cycle, Figure 4.1. Compared with the Simple Brayton cycle, the Dual heater cycle uses two heat sources. The two heaters have the effect of higher utilization of the heat source. Simultaneously, for this layout the disadvantages of the S-CO_2 cycle are eliminated. Mainly the pinch point is eliminated due to the divided mass flow to the **RH** and $\mathbf{H}_1$. It is obvious that this cycle is very simple cycle with minimum numbers of components. However, due to the use of two heat sources it achieves high performance.

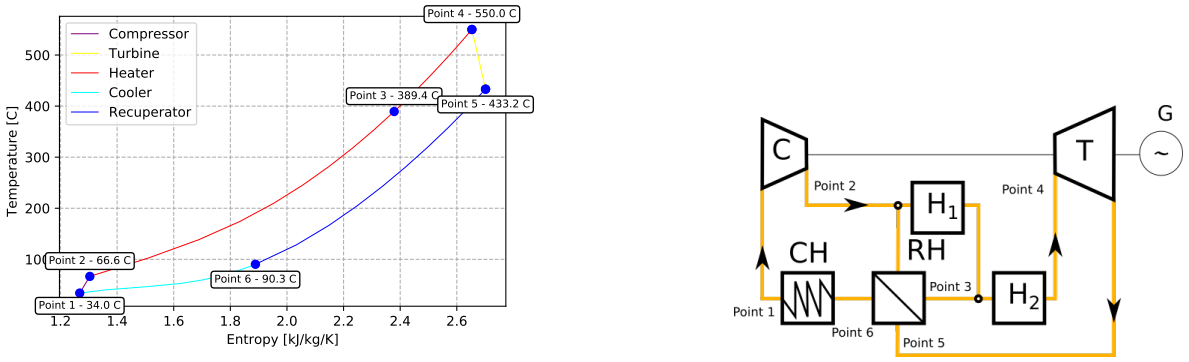

Figure 4.6: T-s diagram and cycle layout of the Dual Heater cycle

The Cascade cycle [58, 59] shown in Figure 4.7 is a very interesting cycle. It consists from two S-CO_2 cycles which are arranged in parallel. There can be many modifications of this cycle layout. It can use different cycle layouts (for example the Simple Brayton cycle and the Re-compression cycle or two Simple Brayton cycles). This depends on the application and parameters of the heat source. Figure 4.7 shows cycle layout of a Cascade cycle for two

heat sources $\mathbf{H}_1$ and $\mathbf{H}_2$. One heater is used for one of the cycle and second heater is used for the second one. The pinch point is eliminated due the division of mass flow for heaters and turbines. There is also increased utilization of the heat source.

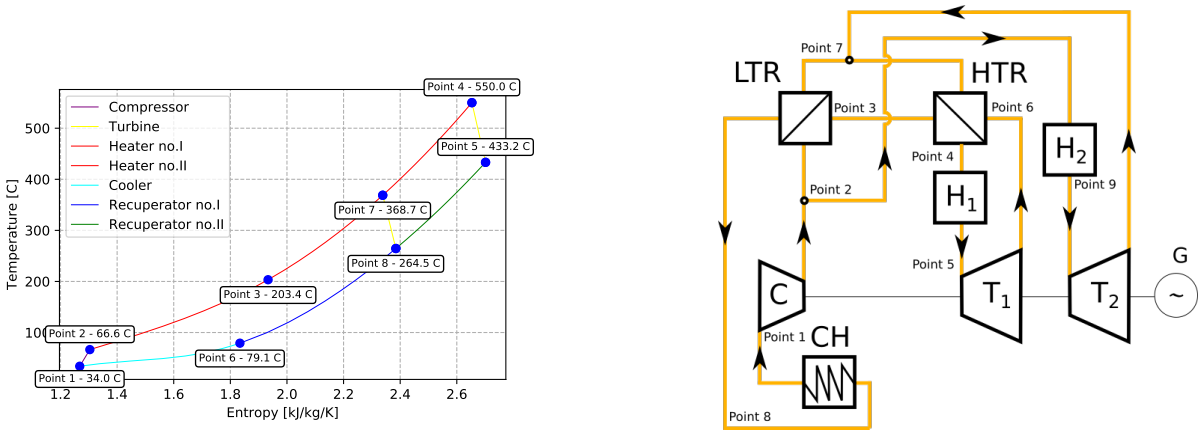

Figure 4.7: T-s diagram and cycle layout of the Cascade cycle

The next cycle layout is the Kimzey cycle. [9] It is shown in Figure 4.8. The Kimzey cycle consists from two compressors ($\mathbf{C}_1$ and $\mathbf{C}_2$), two turbines ($\mathbf{T}_1$ and $\mathbf{T}_2$), two recuperative heat exchangers (**LTR** and **HTR**), two coolers ($\mathbf{CH}_1$ and $\mathbf{CH}_2$) and two heaters ($\mathbf{H}_1$ and $\mathbf{H}_2$). This cycle layout is a combination of the other cycle layouts. It is obvious that this cycle is very complicated, however this layout is one of the best cycles for multiple heat sources. It achieves high utilization of heat source. Simultaneously, for this layout the pinch point is eliminated due to the division of mass flow between the $\mathbf{H}_1$ and $\mathbf{H}_2$.

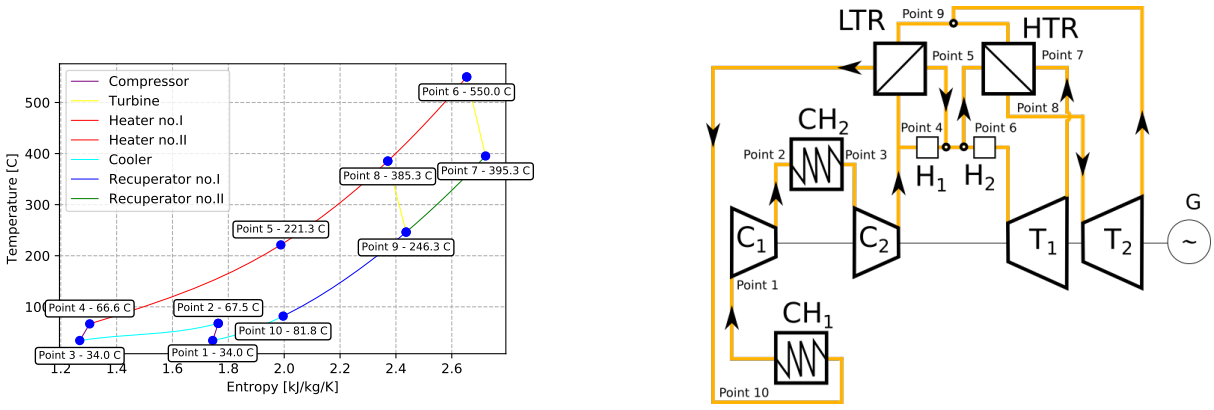

Figure 4.8: T-s diagram and cycle layout of the Kimzey cycle

4.4 Summary

It is evident that the basic cycle layouts for S-CO_2 power cycles have many differences. The differences are in number of the components, in divided stream and design of the components. Furthermore, there are a plethora of other cycle layouts. The many of the new cycle layouts were patented. [10, 60, 61] However, detail design and optimization for specific application, parameters and cooling medium is necessary for all cycle layouts. The description of all cycle layouts is impossible to show in this thesis. However, the effect of mixtures on the power cycle can be shown on the basic cycle layouts, as will be seen in next chapters. For this reason, the effect of mixtures on the power cycle will be shown on the Re-compression, the Pre-compression and the Split Expansion cycle in this thesis.

Chapter 5

Goals of Thesis

The Chapter 2, 3 and 4 showed the overall view of current research of CO_2, current research of mixtures with CO_2 and the cycles layout. Several goals can be defined according to previous chapters. The goals of thesis are following.

The main goal of this research is the detail description of the effect of mixtures on the S-CO_2 power cycle, to identify the substances with negative or positive effect on the cycle and the components and to define the maximum amount of the second substance in CO_2, with still acceptable impact on the cycle.

The other goals of the research are following:

- The physical description of the effect of mixtures on the components - compressor and turbine.
- The description of the effect of mixtures on the pinch point.
- The description of the effect on the heat exchanger type (cooler, heater and recuperative heat exchanger).
- The description of the effect of the compressor inlet temperature on the cycle efficiency and cooling of the cycle.
- The techno-economic evaluation for specific application.

Chapter 6

Effect of Impurities on the S-CO_2 Power Cycle Performance

This chapter is based on the previous chapters and describes of the calculation of the S-CO_2 power cycles. It focuses on the cycle layouts from Chapter 4, especially on the Re-compression, the Pre-compression and the Split Expansion cycle layouts. It means, the calculations of the S-CO_2 power cycle were performed for the close Brayton S-CO_2 power cycle (In-direct S-CO_2 power cycle). This chapter is divided to two part. The first part is focused on the description of calculation and description of calculation code. In the second part the results from calculation of the S-CO_2 power cycle for boundary condition will be presented. The result of this chapter is the detailed description of the effect of mixtures on the cycle efficiency.

6.1 Description of Calculation

The Carnot cycle has the highest thermal efficiency for heat engines which are operating between the same temperature levels. The Carnot thermal efficiency is defined according to Equation 6.1, where $\mathbf{T}_L$ is the temperature of low temperature site and $\mathbf{T}_H$ the temperature of high temperature site. [42]

$$\eta_{Car} = 1 - \frac{T_L}{T_H} \tag{6.1}$$

The closed Brayton gas cycle consists of four internally reversible processes. [42,50] The first process is the isentropic compression, the second is the isentropic expansion, the third is the constant-pressure heat addition and the fourth is the constant-pressure heat rejection. The processes are shown in Figure 6.1.

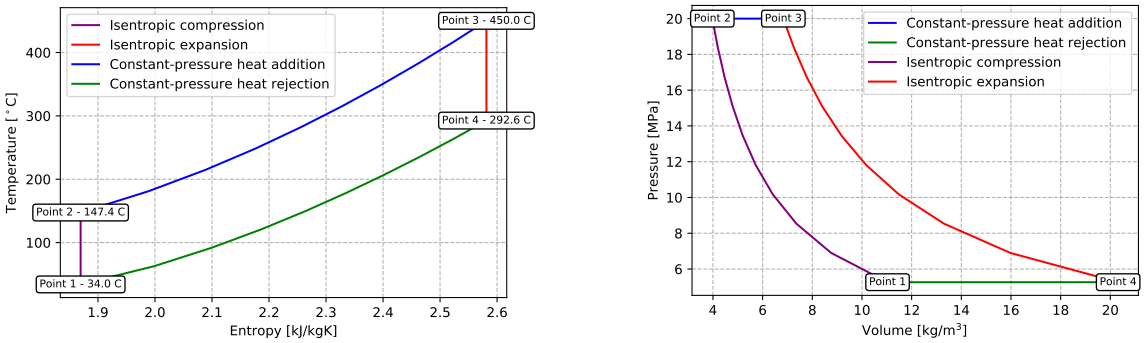

Figure 6.1: T-s diagram and P-v diagram for ideal gas cycle

The Figure 6.1 represent the ideal Brayton cycle. The thermal efficiency is defined according to Equation 6.2. [42]

$$\eta_{th} = \frac{P_{net}}{Q_{in}} = 1 - \frac{Q_{out}}{Q_{in}} \tag{6.2}$$

where $\mathbf{Q}_{in}$ is total the heat input, $\mathbf{Q}_{out}$ is total heat output and $\mathbf{P}_{net}$ is the net power. The net work $\mathbf{P}_{net}$ is defined according to Equation 6.3. [42]

$$P_{net} = P_{tu} - P_c \tag{6.3}$$

where $\mathbf{P}_{tu}$ is turbine output power and $\mathbf{P}_c$ is compressor input power. The $\mathbf{Q}_{in}$ and $\mathbf{Q}_{out}$ defined, according to Figure 6.1, as Equation 6.4. The total heat input and total heat output is between point 2-3, respectively 4-1. [42]

$$Q_{in} = \dot{m}c_p(T_3 - T_2) = \dot{m}(h_3 - h_2), \qquad Q_{out} = \dot{m}c_p(T_4 - T_1) = \dot{m}(h_4 - h_1) \tag{6.4}$$

where $\dot{\boldsymbol{m}}$ is mass flow and $\mathbf{C}_p$ is the heat capacity at constant pressure. The processes between point 1-2 and 3-4 are isentropic compression or expansion respectively. Where $\boldsymbol{\kappa}$ is Poisson constant.

$$\frac{T_2}{T_1} = \left(\frac{P_2}{P_1}\right)^{\left(\frac{(\kappa-1)}{\kappa}\right)}, \qquad \frac{T_3}{T_4} = \left(\frac{P_3}{P_4}\right)^{\left(\frac{(\kappa-1)}{\kappa}\right)} \tag{6.5}$$

The pressure ratio is defined according to Equation 6.6. Where $\mathbf{P}_2$ is the higher pressure level (i.e. the turbine inlet pressure, if pressure drops are not considered) and $\mathbf{P}_1$ is the lower pressure level (i.e. the compressor inlet pressure).

$$Ra = \frac{P_2}{P_1} \tag{6.6}$$

The real Brayton gas cycle differs from the ideal Brayton cycle. The important thing is that the real compressor work will be higher, and the real turbine work will be lower because of the irreversibilities, see Figure 6.2.

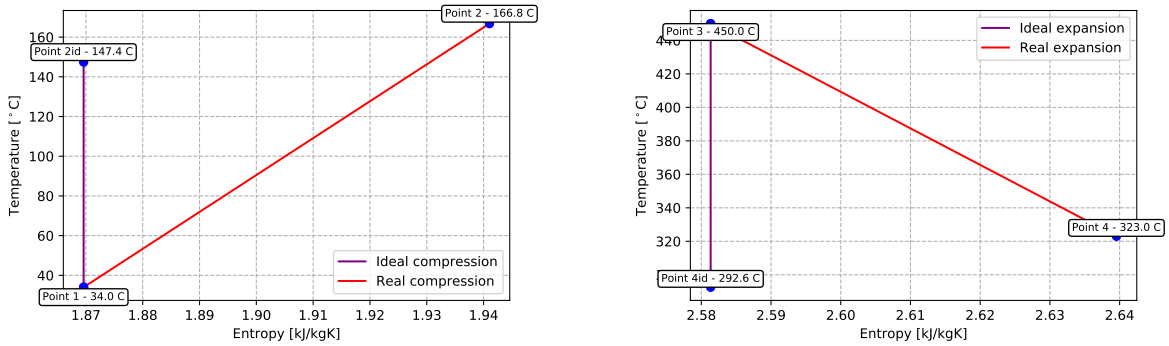

Figure 6.2: Ideal and real compression and expansion

The real compression and expansion are defined according to Equation 6.7, where $\mathbf{h}_i$ is ideal state and $\mathbf{h}_r$ is real state. The turbine and the compressor efficiency is used for the calculation of work. [42]

$$\eta_c = \frac{h_{2i} - h_1}{h_{2r} - h_1}, \qquad \eta_t = \frac{h_3 - h_{4r}}{h_3 - h_{4i}} \tag{6.7}$$

To increase the cycle efficiency the recuperative heat exchanger is used. This is usually a countercurrent-flow heat exchanger. The recuperator effectiveness $\boldsymbol{\eta_{rec}}$ is used for the calculation of regeneration, and is defined according to Equation 6.8. [42]

$$\eta_{rec} = \frac{h_5 - h_2}{h_4 - h_2} \tag{6.8}$$

6.1.1 Description of the Calculation Code

The calculation is made using the calculation code. The code was writen for calculation of the S-CO_2 power cycle and for calculation of the components. The code was written in the Python programming language. The Python is an open-source language for programming.

The code was written using equations defined in chapter 6.1. The equations were converted to Python programming language. The code for calculation was written in version 2.7. The part of the code is in the Appendix B. The code in appendix is the part for calculation of the compressor and the turbine. Both codes have a similar syntax. The simillar parts were written for each component in the cycle. The code uses individual parts using the equations defined in the previous chapter for calculation. The code syntax optimizes the cycle with using the input and the boundary conditions. The minimum $\Delta\mathbf{T}$ and the equation for finding the pinch point are also defined in the code [A.2, A.3]. The code calculates the possible cycles according to the input and the boundary conditions and is looking for the most appropriate result. It is possible to calculate the cycle and optimize each parameters or only some parameters, as the turbine pressure and the pressure ration or the cycle efficiency.

The most important part of the code is the source of gas and mixture properties, according to Chapter 3. The source of gas and mixture properties used was NIST Reference Fluid Thermodynamic and Transport Properties database, Version 9.1. [48] and CoolProp [49]. The CoolProp is the open-Source Thermo-physical Property Library. The PropSI is a command to call tables from NIST or CoolProp. The code used both databases for thermodynamic and transport properties. Because, CoolProp can be used only for pure and pseudo-pure fluid. In the case of calculating the cycle with mixtures, other tables have to be used. The equation TREND 2.0 [44] was applied at the same time.

6.1.2 Boundary Conditions

The boundary conditions are very important information for the calculation. The main input parameters are the compressor inlet temperature $\mathbf{T}_1$, the efficiency of the turbine $\boldsymbol{\eta_{tu}}$ and the efficiency of the compressor $\boldsymbol{\eta_c}$. The calculation was carried out for parameters from Table 6.1. [A.8]

The first part of research is the thermodynamic calculation of the basic cycle layouts. The $\dot{\boldsymbol{m}}$ was considered 1 kg/s, as specific conditions. The $\boldsymbol{\eta_c}$ and $\boldsymbol{\eta_{tu}}$ were selected as realistic, which the real compressor and turbine for S-CO_2 application may achieve. However, selection of the efficiencies have small or no effect on the general impact of mixtures on the cycle thermodynamic.

Table 6.1: Boundary conditions [A.7, A.8]

Compressor inlet temperature	$\mathbf{T}_1$	34	[°C]
Turbine inlet temperature	$\mathbf{T}_4$	550	
Turbine efficiency	$\boldsymbol{\eta_{tu}}$	0.79	[-]
Compressor efficiency	$\boldsymbol{\eta_c}$	0.68	
Recuperator effectiveness	$\boldsymbol{\eta_{reg}}$	0.9	
Mass flow	$\boldsymbol{\dot{m}}$	1.0	**[kg/s]**

The investigated variables are the turbine inlet pressure $\mathbf{P}_2$ and the compressor pressure ratio **Ra**. The pressure drops were not considered in this case. The **Ra** was examined within the range from 1.5 to 3.0. The $\mathbf{P}_2$ was examined in the range from 15 MPa to 30 MPa. The best cycle conditions may hypothetically be located outside of these boundary conditions. However, the effect of mixtures will still have the same trend. The reference case is the pure CO_2. The results of calculations were compared to the reference case with pure CO_2. The investigated parameter is the cycle efficiency $\boldsymbol{\eta_{th}}$.

6.2 Results of Calculation

The investigated mixtures are binary mixtures, with the fraction of the second substance up to 5 %. The results ot the analysis show the effect on the cycle efficiency, i.e. whether the cycle efficiency increases or decreases. The difference of cycle efficiency between pure CO_2 and mixture was calculated according to Equation 6.9. [A.8] The unit of $\boldsymbol{\Delta\eta}$ is %.

$$\Delta\eta = \eta_{mixture} - \eta_{pureCO_2} \tag{6.9}$$

The total cycle efficiency for the re-compression and the pre-compression cycles are shown in Figure 6.3 and Figure 6.4. [A.8] The maximum cycle efficiency for the re-compression cycle for the boundary conditions, from Chapter 6.1.2, is 33.44 %. The parameters for the maximum cycle efficiency are folowing: $\mathbf{P}_2$ is 27 MPa and **Ra** is 3.0. However, the total maximum cycle efficiency can be outside of the boundary conditions (chapter 6.1.2). The pre-compression cycle has the maximum cycle efficiency 44.44 %. The parameters for the maximum cycle efficiency are folowing: $\mathbf{P}_2$ is 30 MPa and **Ra** is 1.65. It is obvious that, the pre-compression cycle has higher cycle efficiency for the same boundary conditions. However, the parameters for the maximum cycle efficiency are different.

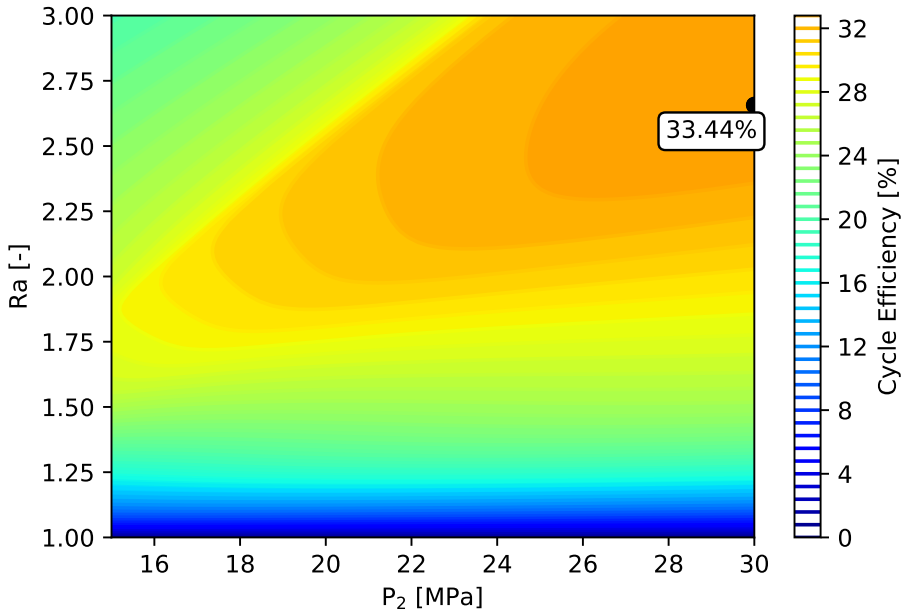

Figure 6.3: The cycle efficiency of the Re-compression cycle.

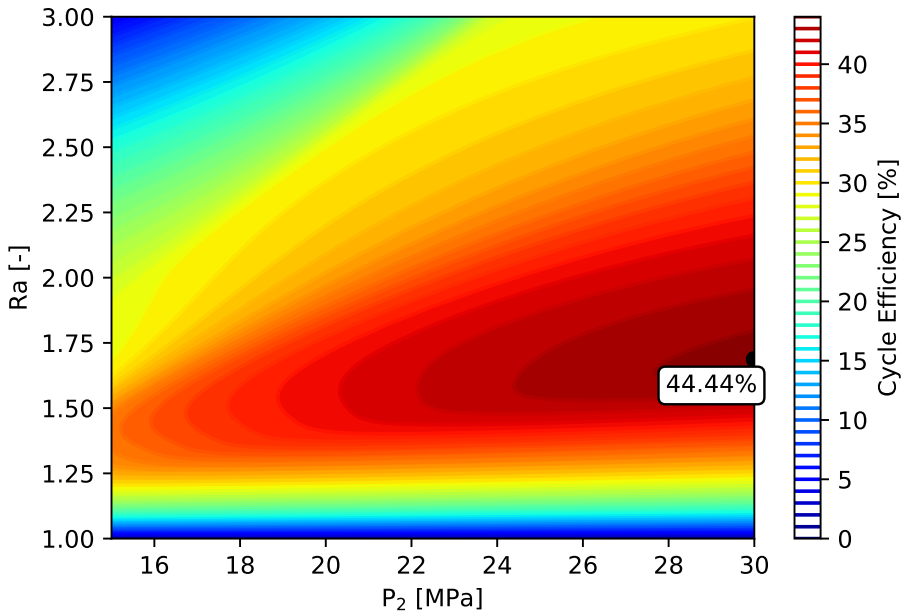

Figure 6.4: The cycle efficiency of the Pre-compression cycle.

The effect of mixtures is shown in Figure 6.5 and Figure 6.6. [A.8] The results are for 1 % of impurities (Ar and He). The negative effect is observed for both substances, but He has a higher negative effect, which is about -3.75%. The decrease of the cycle efficiency is -2.63% for Ar. The area, where the biggest decrease of cycle efficiency is observed, is the same for each substance being investigated.

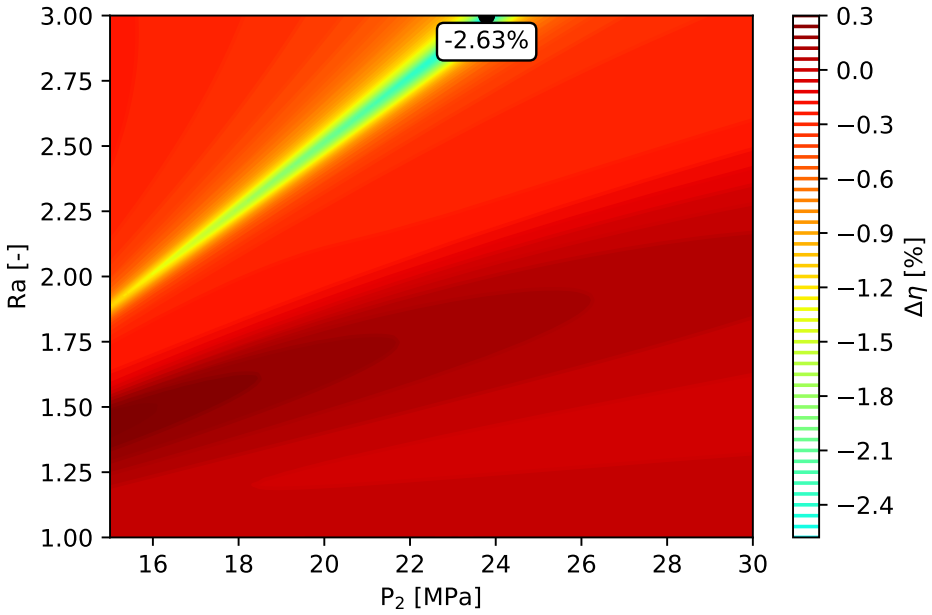

Figure 6.5: The $\boldsymbol{\Delta\eta}$ - the Re-compression cycle - 1% of Ar.

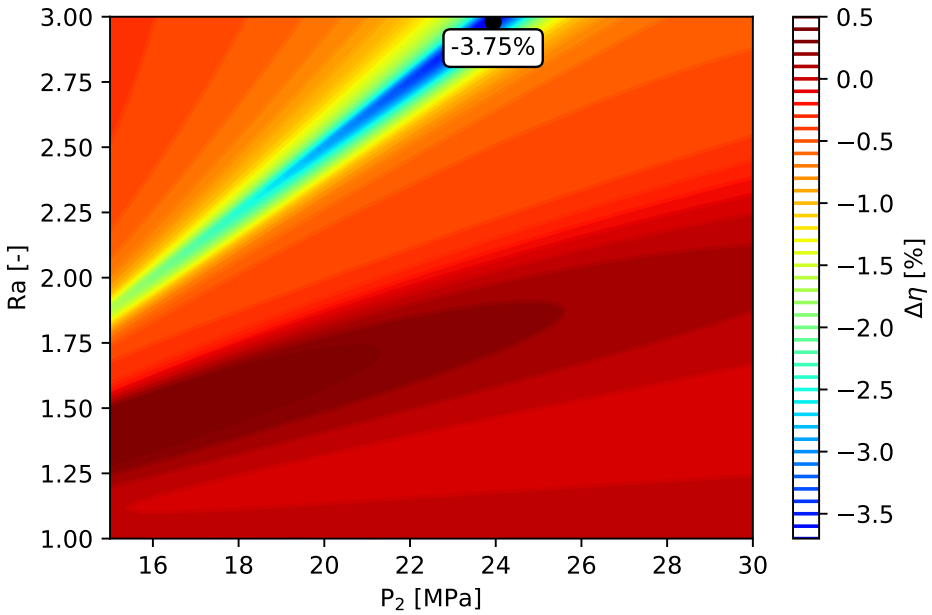

Figure 6.6: The $\boldsymbol{\Delta\eta}$ - the Re-compression cycle - 1% of He.

A very similar result are obtained, if the amount of the second substance is increased. The results for 5 % of impurities are shown in Figures 6.7 and 6.8. [A.8] The decrease of cycle efficiency for each mixture increased approximately twofold. Apparently, there is a dependence between the amount of the second substance and the decrease of the cycle efficiency.

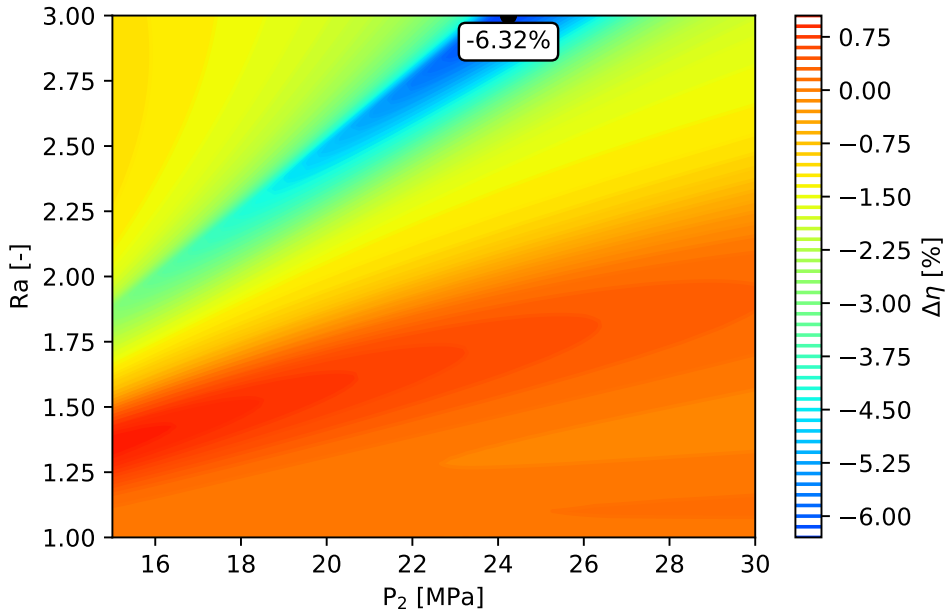

Figure 6.7: The $\boldsymbol{\Delta\eta}$ - the Re-compression cycle - 5% of Ar.

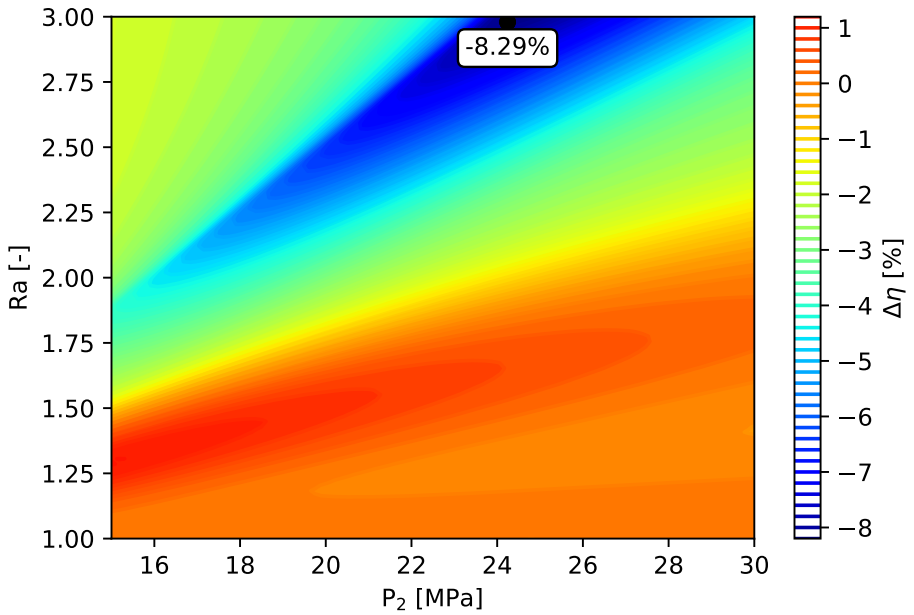

Figure 6.8: The $\boldsymbol{\Delta\eta}$ - the Re-compression cycle - 5% of He.

The difference between the cycle efficiency is shown in Figure 6.9. The difference is shown for Ar, He, O_2 and H_2S. It is evident, decrease/increase of cycle efficiency shows a dependence on the concentration of CO_2. The difference between the cycle efficiency appears to be linear, for contrecation of CO_2 from 100 % to 99 %, except H_2S. The increase of cycle efficiency for H_2S appears to be linear for all contrecation of CO_2. The decrease of the cycle

efficiency can be approximated by exponential function. Conclusion can be drawn, which describes the maximum amount of a secondary substance, which has a minimum effect on the cyclic efficiency. The optimum amount of the second substance is up to 1 %. For this amount the negative effect of binary mixture is small. [A.8] Also, decrease of the concentration of CO_2 can have a negligible effect on decrease of the cycle efficiency for He and concentration of CO_2 under 90 %.

The results in Figure 6.9 are for the Re-compression cycle with the pressure ratio of 2.6, the turbine inlet pressure 20 MPa, mass flow rate 200 kg/s and power of 38 MW. The power is constant for all cases and all substances.

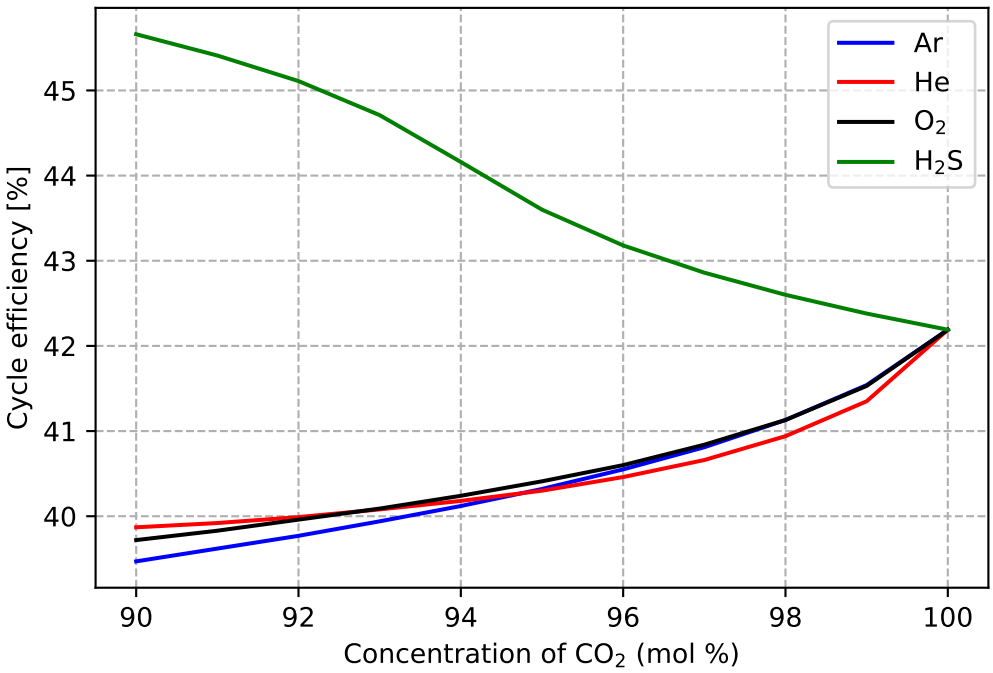

Figure 6.9: The cycle efficiency for the Re-compression cycle.

Most the investigated substances have always a negative effect on the cycle efficiency. Three substances H_2S, Xe and SO_2 have a positive effect on the cycle efficiency see Figure 6.10 and Figure 6.11. [A.8] The results are for H_2S and Xe.

The cycle efficiency increased when these substances were added. The maximum increase of the cycle efficiency was 0.47 % for H_2S and 0.26 % for Xe. In addition, it is obvious that the increase occurs in the same area, where the decrease occurs for other substances. The same results can be observed for the case with higher fraction of the second substance, as in Figure 6.7 and Figure 6.8. The results for 5 % of H_2S and Xe in S-CO_2 are shown in Figure 6.12 and Figure 6.13. The effect of H_2S and Xe on the cycle efficiency is positive and has linear dependence, see Figure 6.9

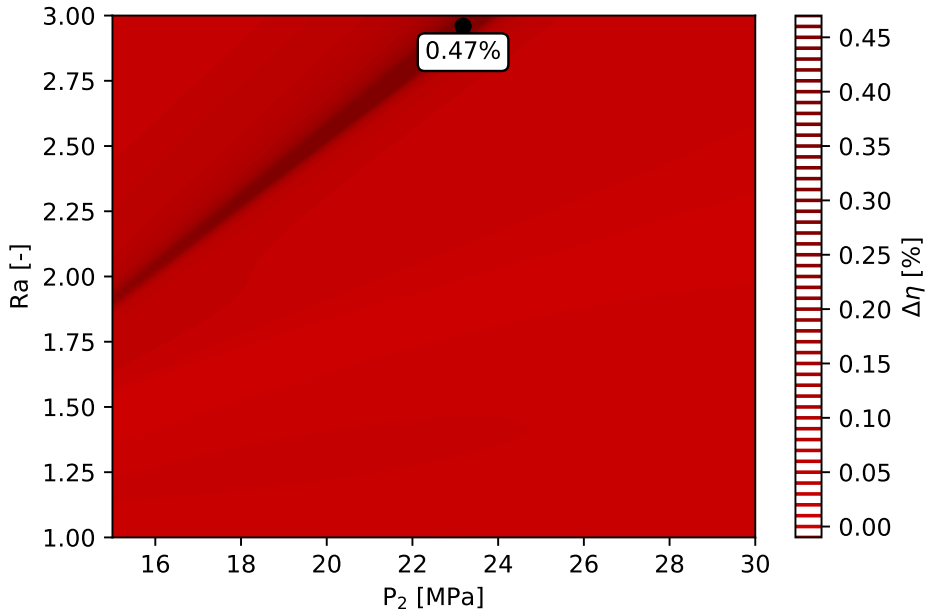

Figure 6.10: The $\boldsymbol{\Delta\eta}$ - the Re-compression cycle - 1% of H_2S.

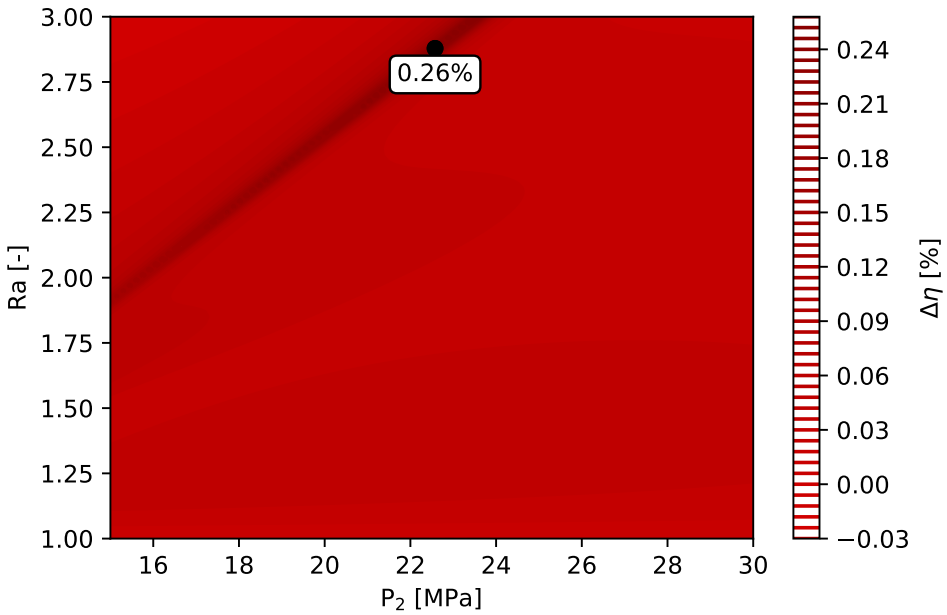

Figure 6.11: The $\boldsymbol{\Delta\eta}$ - the Re-compression cycle - 1% of Xe.

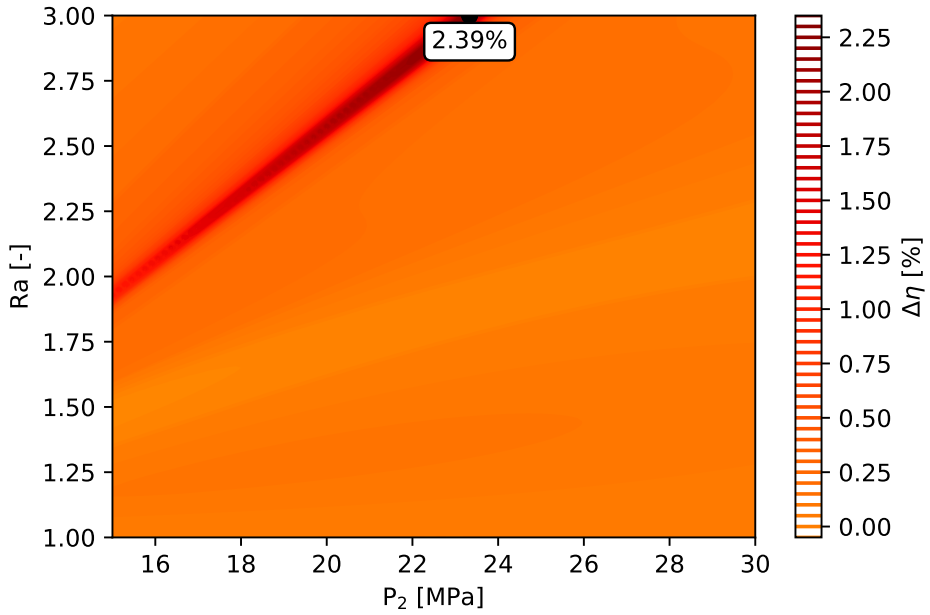

Figure 6.12: The $\boldsymbol{\Delta\eta}$ - the Re-compression cycle - 5% of H_2S.

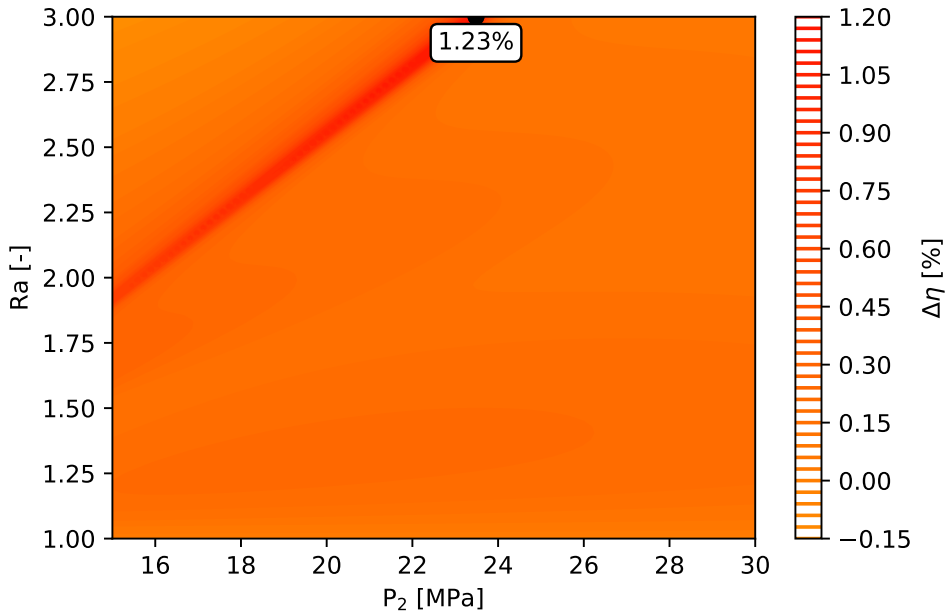

Figure 6.13: The $\boldsymbol{\Delta\eta}$ - the Re-compression cycle - 5% of Xe.

The Pre-compression cycle has a very similar results for each substance. The negative effect on the cycle efficiency is for Ar and He it is shown in 6.14 and Figure 6.15. The positive effect is for H_2S and Xe it is shown in Figure 6.16 and Figure 6.17. [A.8]

The similar results can be observed. The maximum decrease/increase of the cycle efficiency occurs in the same area as for the re-compression cycle. The area with maximum

decrease/increase can be found for each cycle layout and for each binary mixtures. The He has a higher negative effect, which is about -6.04%. The negative effect for Ar is -4.18%. The H_2S has the biggest positive effect on the cycle efficiency, for the investigated substances. The positive effect for H_2S is 0.71% and for Xe is 0.33%.

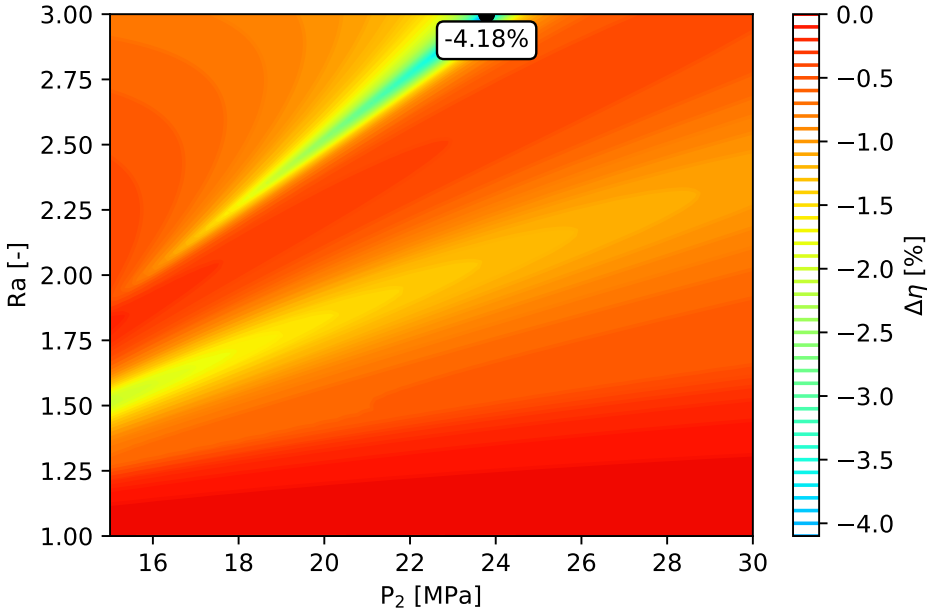

Figure 6.14: The $\boldsymbol{\Delta\eta}$ - the Pre-compression cycle - 1% of Ar.

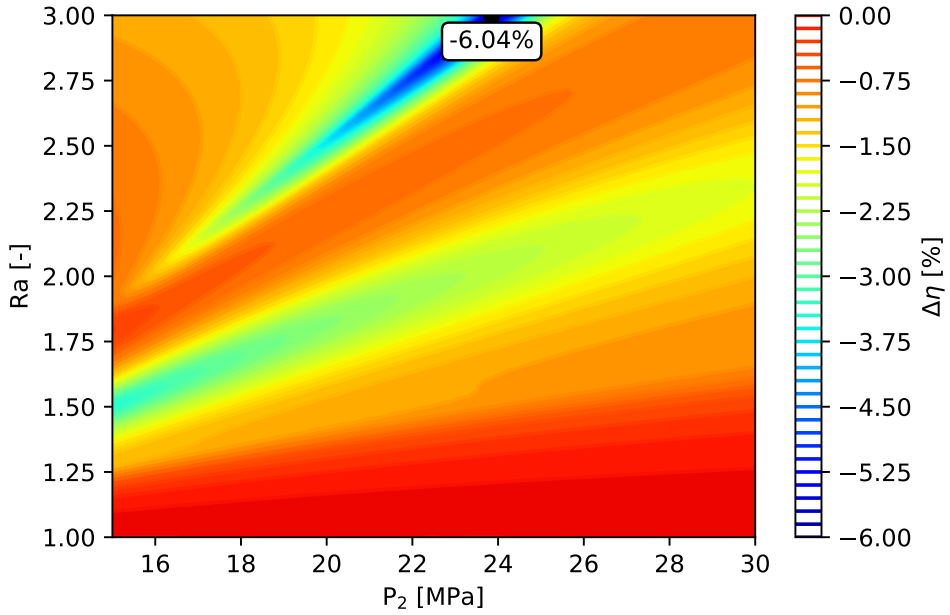

Figure 6.15: The $\boldsymbol{\Delta\eta}$ - the Pre-compression cycle - 1% of He.

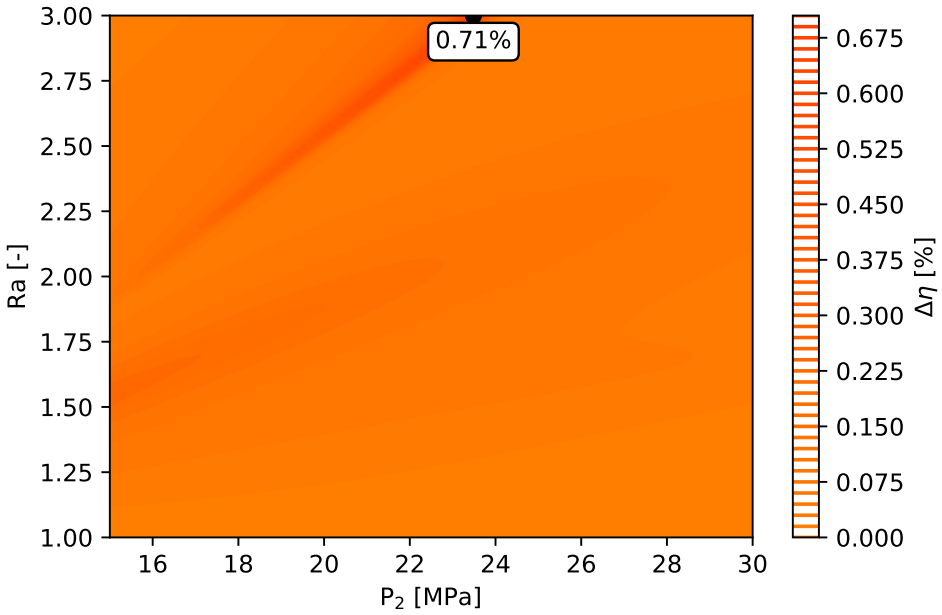

Figure 6.16: The $\boldsymbol{\Delta\eta}$ - the Pre-compression cycle - 1% of H_2S.

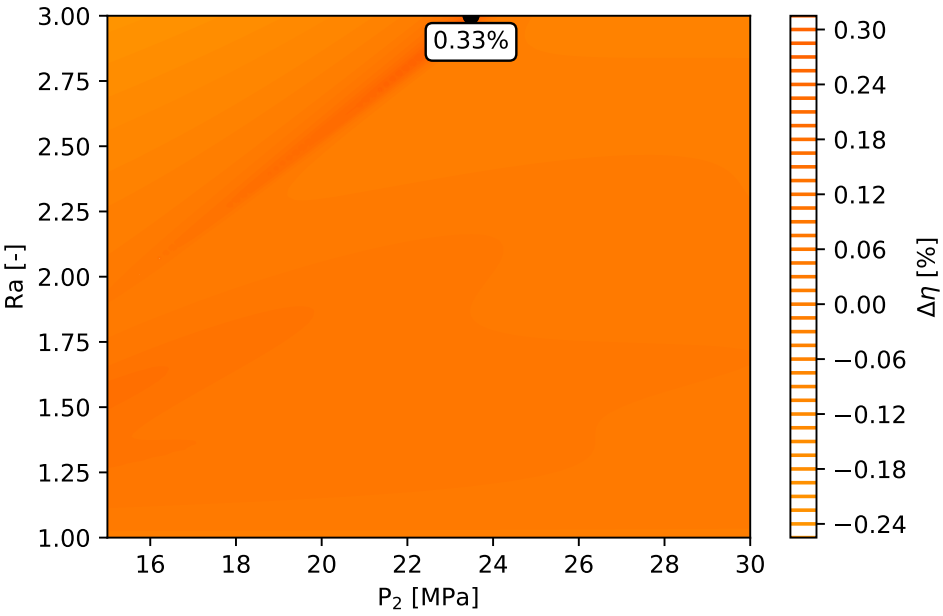

Figure 6.17: The $\boldsymbol{\Delta\eta}$ - the Pre-compression cycle - 1% of Xe.

The last investigated cycle layout is the split expansion cycle. The cycle layout of the spilt expansion cycle is very similar to the re-compression cycle. The results may be essentially the same as for the re-compression cycle for this reason. The results for the split expansion cycle are shown in Figure 6.18 and Figure 6.19. These results are for Ar and He, i.e. substances with negative effect on the cycle efficiency. The positive effect of H_2S and Xe is shown in Figure 6.20 and Figure 6.21.

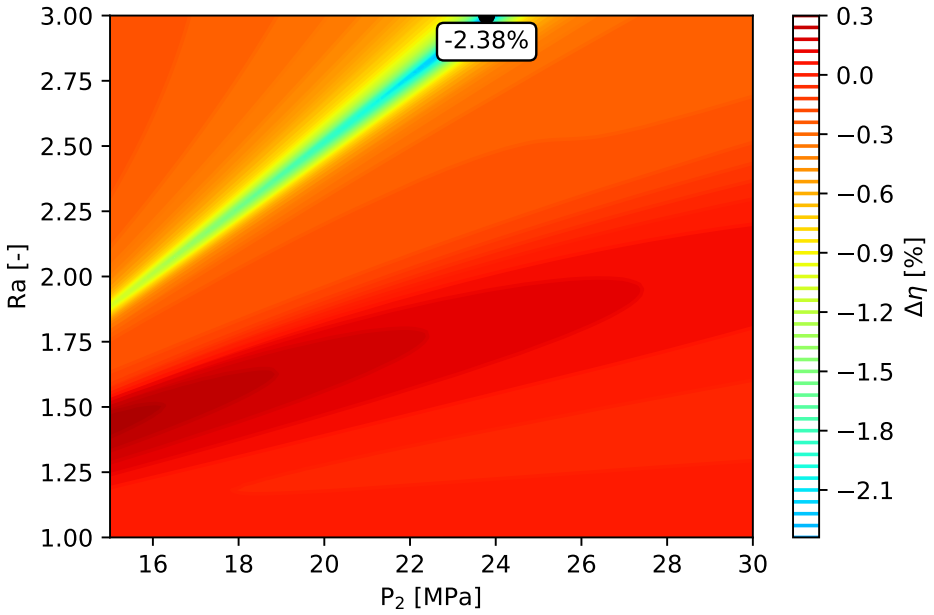

Figure 6.18: The $\boldsymbol{\Delta\eta}$ - the Split expansion cycle - 1% of Ar.

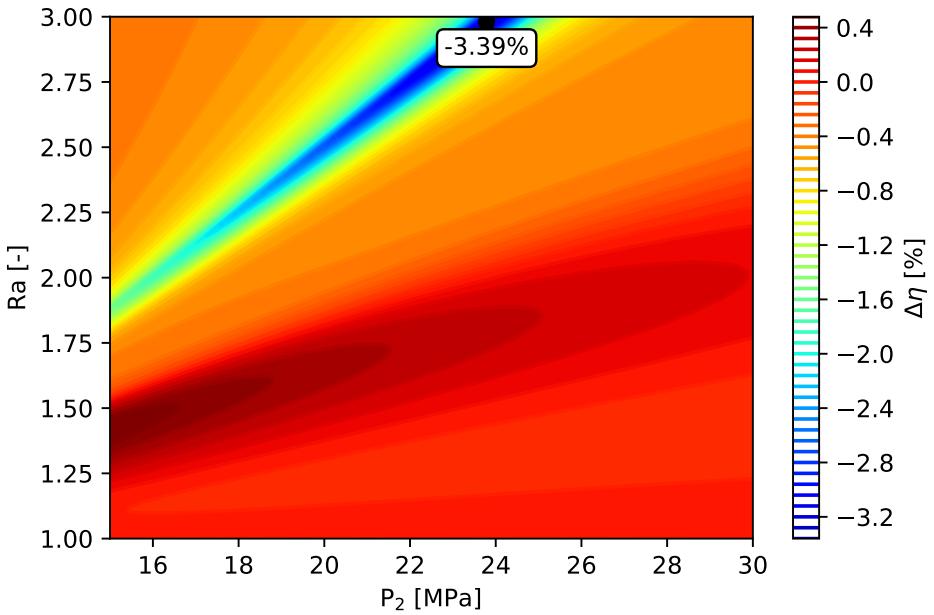

Figure 6.19: The $\boldsymbol{\Delta\eta}$ - the Split expansion cycle - 1% of He.

The negative effect for He is -3.39% and for Ar is -2.38%, see Figure 6.18 and Figure 6.19. The negative effect is very simillar as for the re-compression cycle. The negative effect is -3.75% for He and -2.63% for Ar. The H_2S has again the biggest positive effect on the cycle efficiency. The positive effect for H_2S is 0.43% and for Xe it is 0.24%. The positive effect for the re-compression cycle is 0.47% for H_2S and 0.26% for.

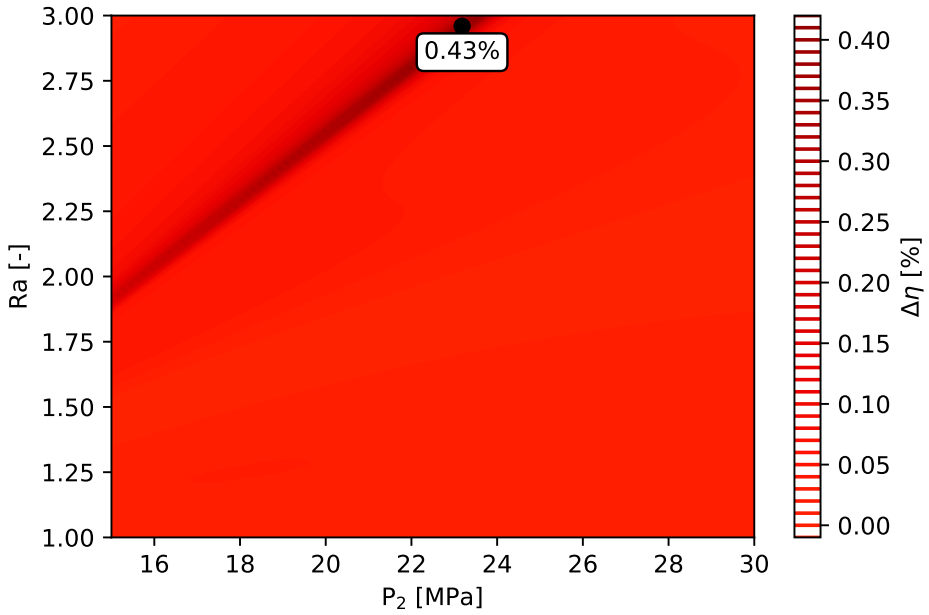

Figure 6.20: The $\boldsymbol{\Delta\eta}$ - the Split expansion cycle - 1% of H_2S.

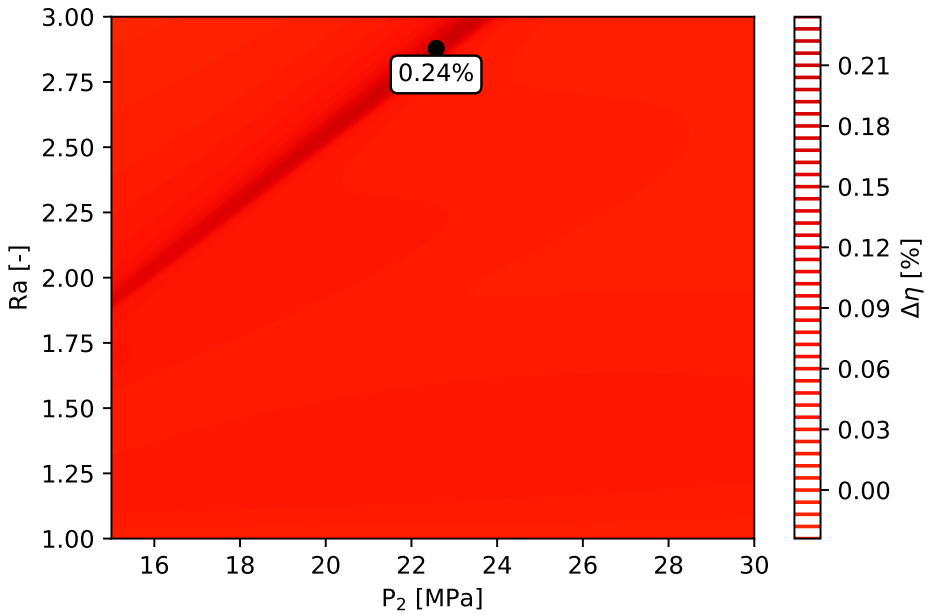

Figure 6.21: The $\boldsymbol{\Delta\eta}$ - the Split expansion cycle - 1% of Xe.

The effect of the mixtures is quite small for the split expansion cycle. It is evident that the results of the re-compression and the split expansion cycles are very similar. The reason is lies in similar cycle layout. [A.7, A.8] The only difference is that the split expansion cycle has the second turbine to reduce the pressure stress on the heater.

The results of the effect of the mixtures on the cycle efficiency are similar for each cycle layout from Chapter 4. The largest negative effect on the cycle efficiency is caused by He, followed by O_2 and CO, see Table 6.2. The largest positive effect on the cycle efficiency is caused by SO_2, followed by H_2S and Xe. The results in Table 6.2 were obtained for 1 % fraction of impurity. It was pointed out that the maximum effect on the cycle efficiency occur in the area where the cycles achieve the highest efficiency for pure CO_2 (for boundary conditions from Table 6.1 [A.7]).

Table 6.2: The maximum effect on the cycle efficiency. [A.7]

η_{pureCO_2}	**Rec**	**Pre**	**Split**
[%]	33.44	44.44	29.83
$\Delta\eta$	[%]	[%]	[%]
He	-0.9	-1.3	-1.0
H_2	-0.4	-0.9	-0.5
CO	-0.5	-1.0	-0.52
O_2	-0.56	-1.1	-0.6
Ar	-0.36	-0.8	-0.4
N_2	-0.39	-0.9	-0.42
CH_4	-0.24	-0.6	-0.26
H_2S	0.04	0.14	0.06
Xe	0.036	0.08	0.04
Kr	-0.23	-0.7	-0.25
SO_2	0.16	0.25	0.2

The similar dependence as for binary mixtures can be observed for all mixtures, as well as multi-component mixtures. [A.7, A.8] The effect of the multi-component mixtures will be described in Chapter 8.

6.3 Conclusion on the Effect of Impurities on the S-CO_2 Power Cycle Performance

The impurities have an effect on the S-CO_2 power cycle performance as was shown in this chapter. It is possible to derive the conclusion that all investigated substances, except for H_2S, Xe and SO_2 have a negative effect on the cycle and the cycle efficiency, as was shown in Figure 6.9 and Table 6.2. This effect is different for each cycle layout. The decrease/increase of cycle efficiency is appears to be linear (H_2S, Xe and SO_2) or approximately exponencial

with depends the operating parameters, substances and cycle layouts [A.7, A.8].

The reason for the biggest decrease/increase of the cycle efficiency in the respective areas can be explained by the properties of CO_2 and its mixtures, due to changes of properties near the critical point. The critical point, temperature and pressure is changed for each mixture, as shown in Figure 3.1. With the shift of the critical point, the area near the critical point also changes. This subsequently affects the cycle performance. According to Equation 6.2 for calculating the cycle efficiency, it is obvious, that the most influencing parameter is the compressor power. The required compression power will change depending on the position to the critical point. The description of the compression power will be show in next chapter.

The results of the effect of the mixtures on the S-CO_2 power cycle performance are published in papers: *Effect of Multicomponent Mixtures on Cycles with Supercritical Carbon Dioxide* [A.7] and *Effect of Gaseous Admixtures on Cycles with Supercritical Carbon Dioxide.* [A.8]

Chapter 7

Effect of Mixtures on the Cycle Components

As shown previously, the effect of impurities on the cycle efficiency is not negligible. It should be considered when designing the S-CO_2 cycle. The largest negative effect on the cycle efficiency is caused by He, followed by O_2 and CO, see Table 6.2 in Chapter 6. As shown in the previous chapter, some substances have a positive effect on the cycle efficiency. The largest positive effect on the cycle efficiency is caused by SO_2, followed by H_2S and Xe. The effect of each substance can be observed regardless of the cycle layout.

The mixtures have an effect on each component of the cycle. The cycle efficiency, defined by to Equation 6.2., is strongly effected by component performance, especially the compressor and the turbine, which determine the net power of the cycle. The cooler and heater, which determine $\boldsymbol{Q}_{in}$ and $\boldsymbol{Q}_{out}$, are also important. For this reason, a detailed description of the effect on individual cycle component is necessary.

This chapter shows the effect on each individual cycle component. The first part is focused on the descritpion of the effect on the compressor performance and the turbine performance. The second part shows the effect on the heat exchangers, esspecially on the recuperative heat exchanger, the cooler and the heater. The results are for the same boundary conditions as in Chapter 6, see Table 6.1.

7.1 Effect of Mixtures on the Compressor Performance

Compressor is the most important component for the S-CO_2 cycles. The reduction of compressor work due to its operation near the critical point was shown in Figure 2.2. This has a significant effect on the cycle efficiency and net power. However the compressor design is quite complex. The problem for the compressor design is the large changes in CO_2 properties close to critical point. The power consumption needed for compression of CO_2 increases

as the compressor operation range moves away from the critical point. For this reason, the optimization and design of the compressor operation point is necessary.

Figure 7.1 and Figure 7.2 show compressor power for compressor number 1 and compressor number 2 in the re-compression cycle, see Figure 4.2. The boundary conditions are based on Table 6.1. From these figures the difference of compressor power is obvious. For the case with the maximum cycle efficiency (the pressure $\mathbf{P}_2$ is 27 MPa and the pressure ratio **Ra** is 3.0) the compressor power of compressor number 1 is lower than the compressor power of compressor number 2. The compressor number 1 (the main compressor) has lower power because it operates closer to the critical point, while, the compressor number 2 operates far away from the critical point. In the area where the properties are already not so favorable. [A.10]

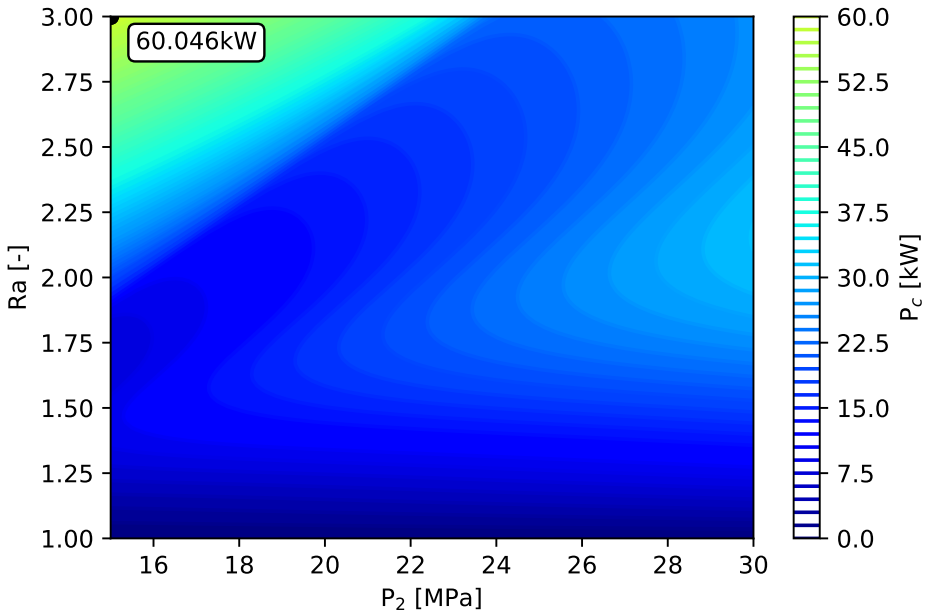

Figure 7.1: The $\mathbf{P}_c$ no.1 - the Re-compression cycle.

For each investigate binary mixtures a very similar results can be observed as for the cycle efficiency. Figure 7.3 and Figure 7.4 show the difference between compressor power for mixtures and compressor power for pure CO_2, the results are for 1 % of Ar. It is obvious that, the difference for the compressor number 1 has very similar profile as the cycle efficiency. On the other hand, the difference for the compressor number 2 is very different. [A.10] This is due to changes of CO_2 properties near the critical point of CO_2 and mixtures.

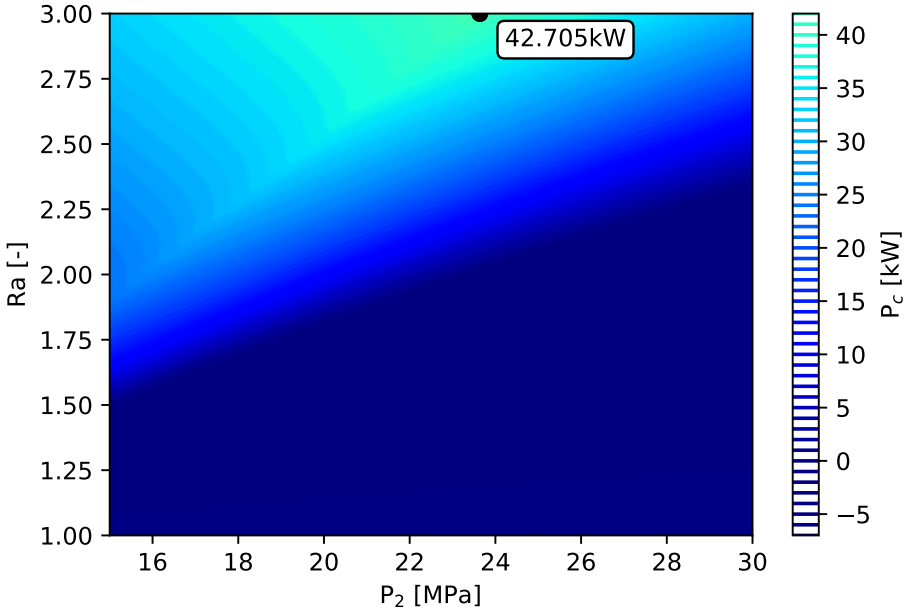

Figure 7.2: The $\mathbf{P}_c$ no.2 - the Re-compression cycle.

.

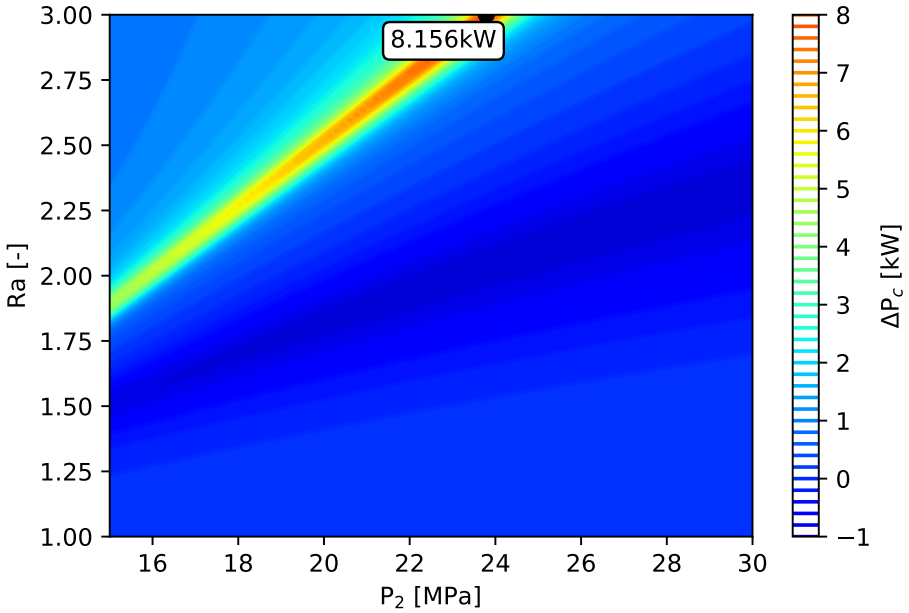

Figure 7.3: The $\Delta\mathbf{P}_c$ no.1 - the Re-compression cycle.

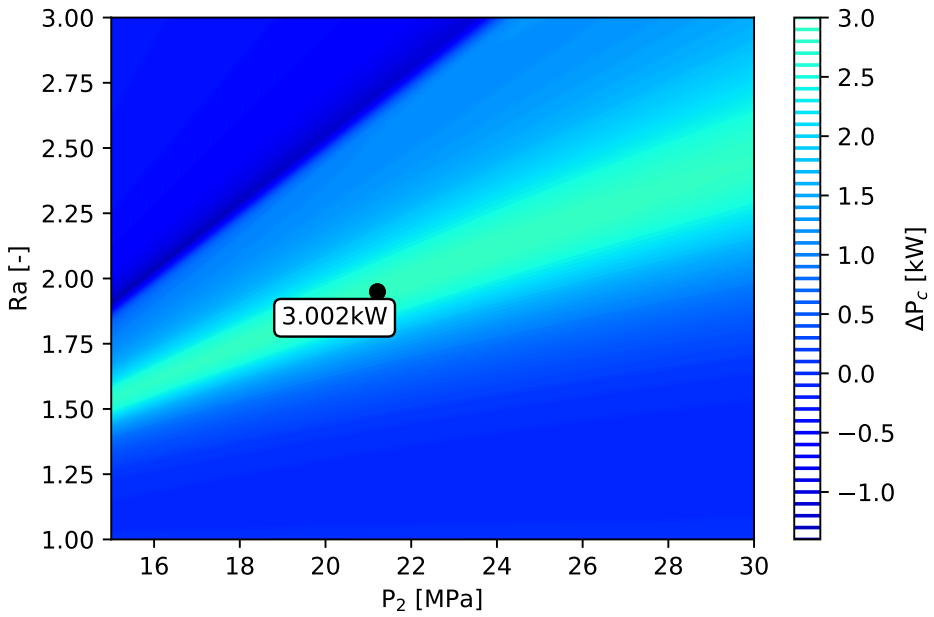

Figure 7.4: The $\Delta \mathbf{P}_c$ no.2 - the Re-compression cycle.

Basically, if we consider ideal isentropic compression, this isentropic compression is defined according to Equation 6.5. A very important variable in this equation is the Poisson constant $\boldsymbol{\kappa}$, which is defined according to Equation 7.1.

$$\kappa = \frac{C_p}{C_v} = \frac{c_p}{c_v} \tag{7.1}$$

Therefore, Equation 7.1 depends on the heat capacity at constant pressure ($\mathbf{C}_p$) and the heat capacity at constant volume ($\mathbf{C}_v$). $\mathbf{C}_p$ and $\mathbf{C}_v$ also change near the critical point as other properties of CO_2. This changes are shown in Figure 7.5 and Figure 7.6. Based on the figures, it is obvious that the Poisson constant $\boldsymbol{\kappa}$ will change with the change of $\mathbf{C}_p$ and $\mathbf{C}_v$ This affects the compressor outlet temperature. The real compression has similar results. The Poisson constant $\boldsymbol{\kappa}$ is shown in Figure 7.7.

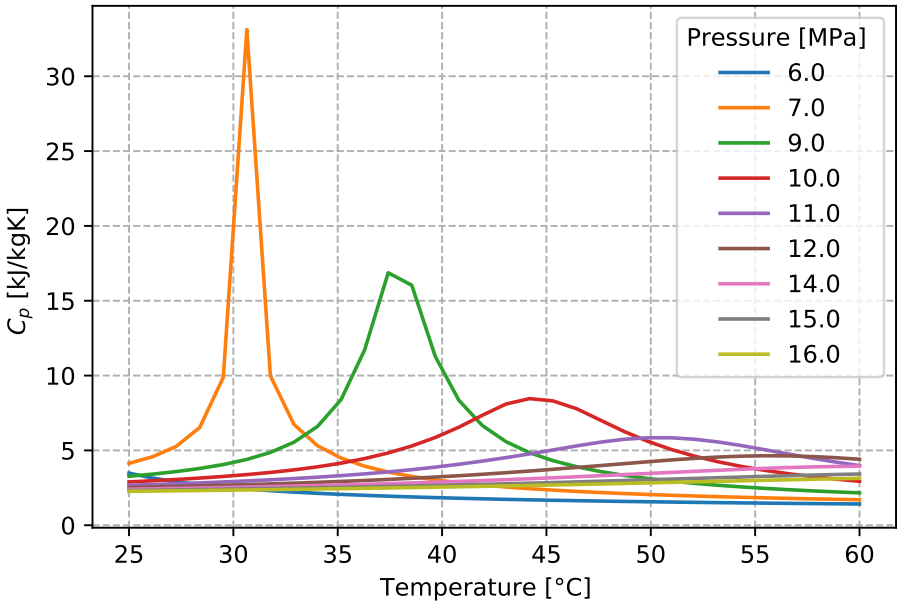

Figure 7.5: The $\mathbf{C}_p$ of pure CO_2.

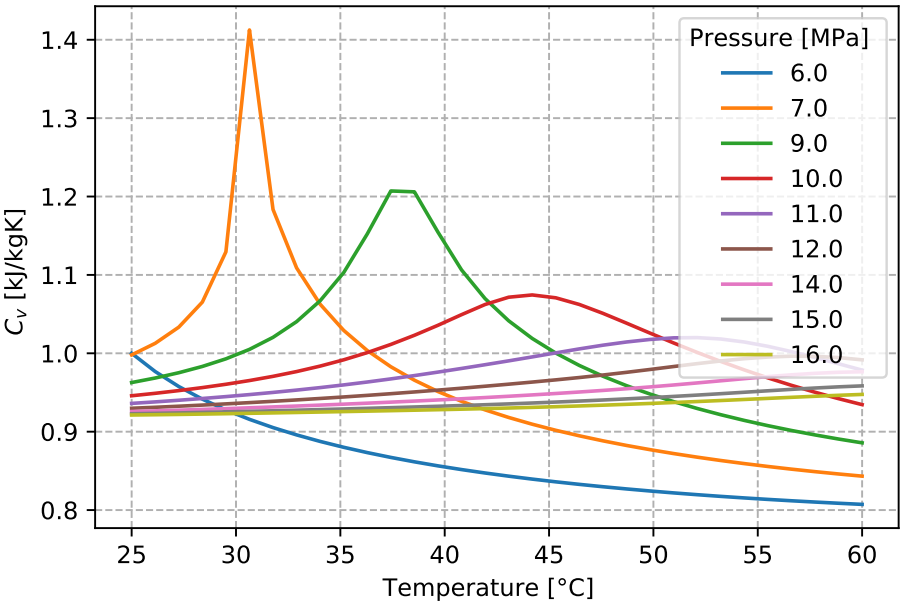

Figure 7.6: The $\mathbf{C}_v$ pure CO_2.

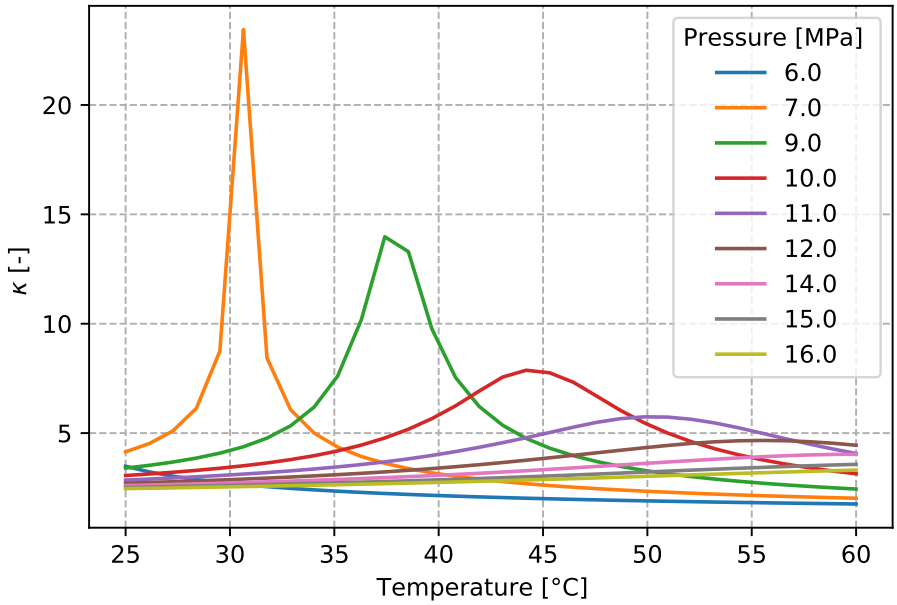

Figure 7.7: The $\boldsymbol{\kappa}$ pure CO_2.

The $\mathbf{P}_c$ total for the Re-compression cycle is shown in Figure 7.8. The change of $\mathbf{P}_c$ is shown in Figure 7.9. It has a very similar results as for the $\mathbf{P}_c$ of the compressor number 1. This again proves the importance and effect of the compressor number 1. Approximately the same results can be found for other mixtures. The He has the highest negative effect and H_2S, Xe and SO_2 have the positive effect. [A.10]

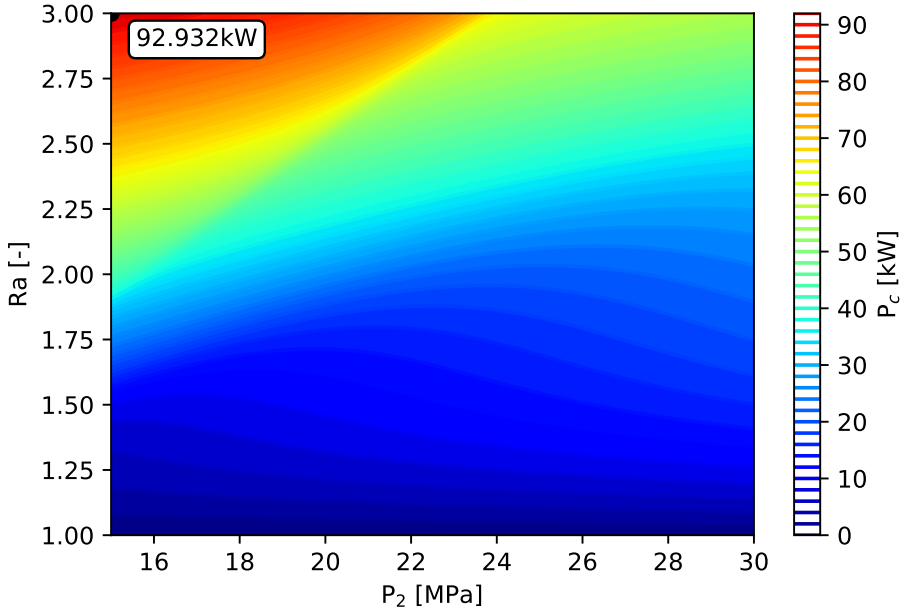

Figure 7.8: The $\mathbf{P}_c$ total - the Re-compression cycle.

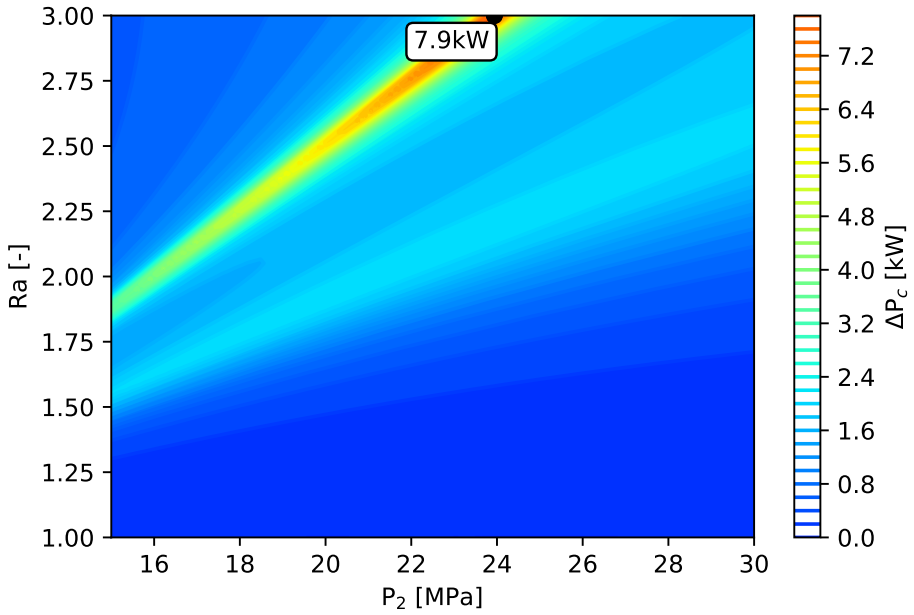

Figure 7.9: The $\Delta \mathbf{P}_c$ total - the Re-compression cycle.

The results for the Pre-compression cycle are similar as for the re-compression cycle, except for the compressor number 2. The increase of compressor number 2 power has a similar profile as for the compressor number 1, see Figures 7.10 and 7.11. It results from the pre-compression cycle layout, according to Figure 4.3.

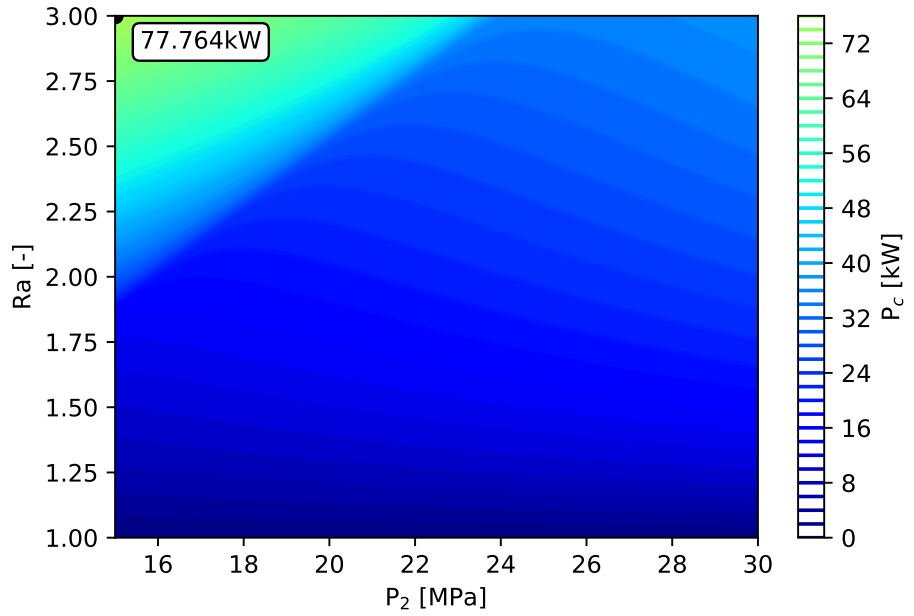

Figure 7.10: The $\mathbf{P}_c$ no.1 - the Pre-compression cycle.

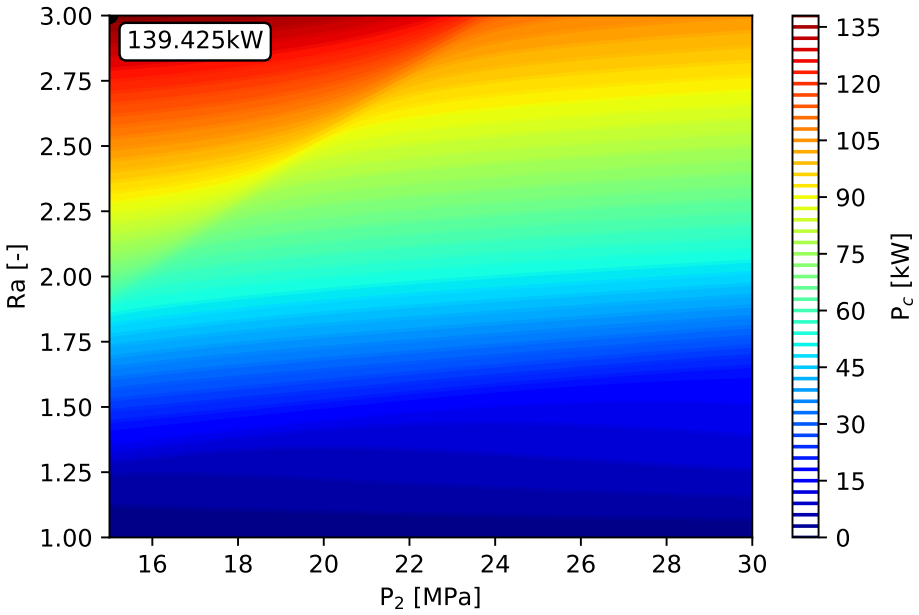

Figure 7.11: The $\mathbf{P}_c$ no.2 - the Pre-compression cycle.

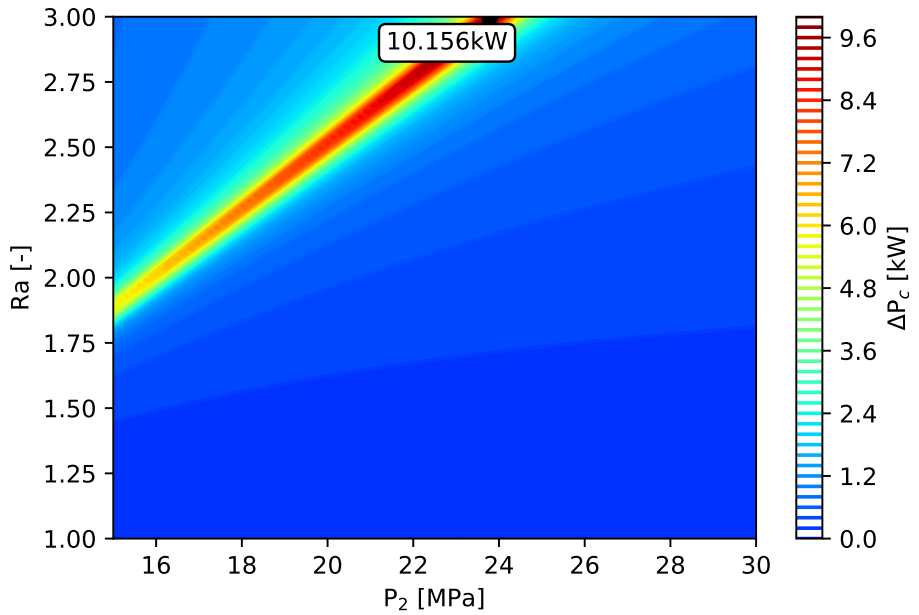

Figure 7.12: The $\Delta\mathbf{P}_c$ no.1 - the Pre-compression cycle.

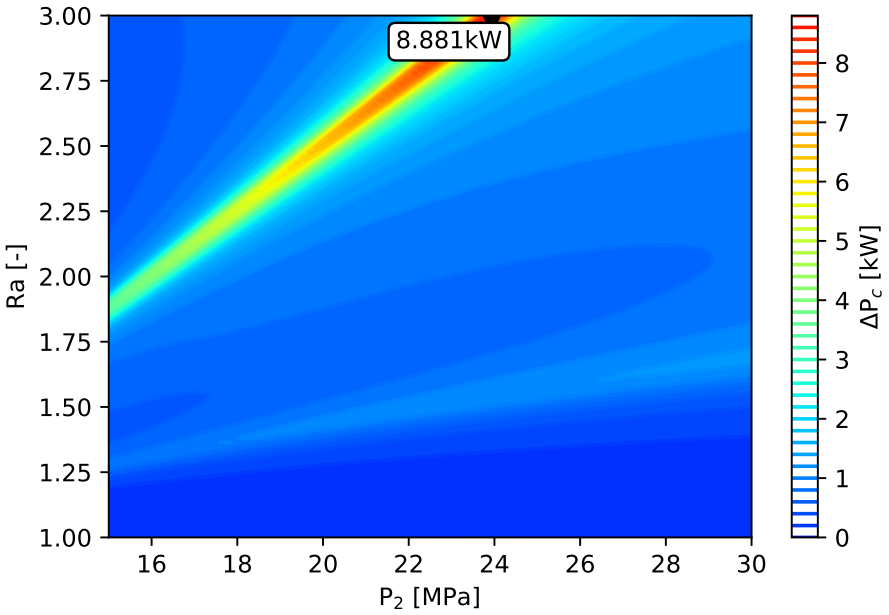

Figure 7.13: The $\Delta \mathbf{P}_c$ no.2 - the Pre-compression cycle.

The compressors are arranged in series in this cycle layout. For this reason, the compressor number 2 operates close to the critical conditions, especially close to the critical temperature. Also, the compressor number 2 operates in the area affected by the critical pressure, for boundary parameters. Thus, the compressor number 2 operates with similar parameters as the compressor number 1. Hence, the results are similar for both compressors. The change of the $\mathbf{P}_c$ is shown in Figures 7.12 (the compressor number 1) and 7.13 (the compressor number 2).

7.2 Effect of Mixtures on the Turbine Performance

The turbine is another component, which affects on the cycle efficiency and the net power. Unlike the compressor a positive effect of mixtures was observed for the turbine power. However, the increase of the turbine power for all investigated mixtures is negligible. Nevertheless, it can greatly affect the resulting cycle efficiency and net power. The turbine power for the re-compression cycle is shown in Figure 7.14. The difference of the turbine power is shown in Figure 7.15. According to these figures, this positive effect of mixtures is visible. The results are for 1 % of Ar.

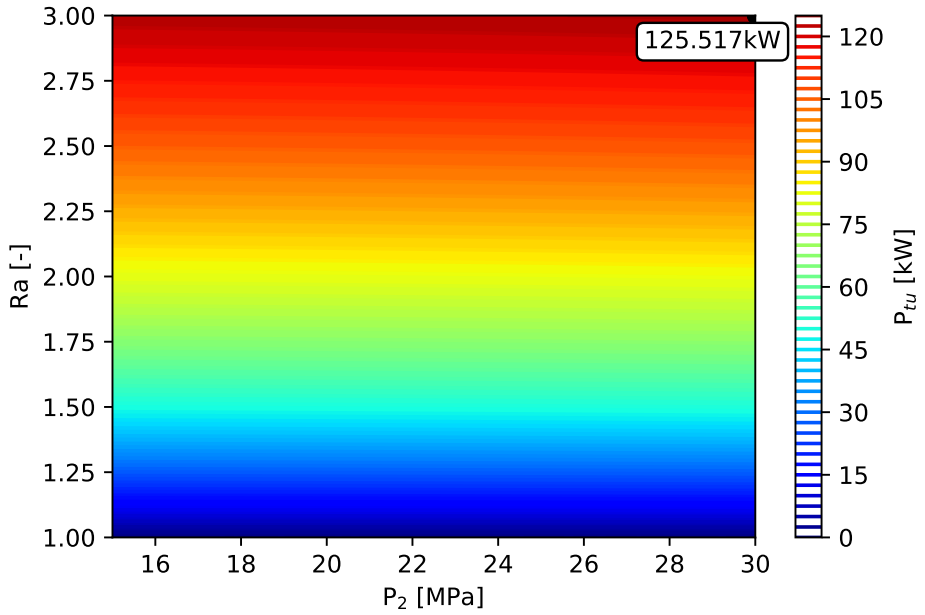

Figure 7.14: The $\mathbf{P}_{tu}$ - the Re-compression cycle.

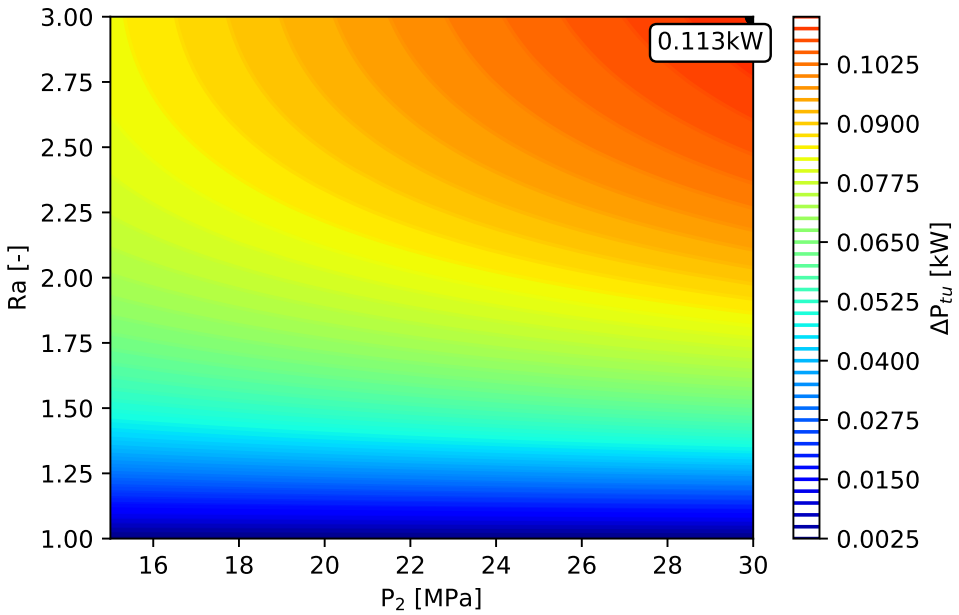

Figure 7.15: The $\Delta\mathbf{P}_{tu}$ - the Re-compression cycle.

The reason why turbine power increase, is again due to the properties of CO_2. If we consider the ideal isentropic expansion, it is defined according to Equation 6.5. It can be observed, that the very important variable in this equation is once again the Poisson constant $\boldsymbol{\kappa}$, which is defined according to Equation 7.1. This leads to $\mathbf{C}_p$ and $\mathbf{C}_v$, which have effect on the Poisson constant $\boldsymbol{\kappa}$. According to Figure 7.16 and Figure 7.17, it is obvious that

the change of $\mathbf{C}_p$ and $\mathbf{C}_v$ is significantly smaller when compared to the change near the critical point. However even such a this small change affects the exponent of Equation 6.5, thereby affecting the outlet temperature of the turbine. The turbine outlet temperature is smaller. Therefore, more work is done and thus the turbine power increase. In the case of a compressor, it is the opposite. The Poisson constant $\boldsymbol{\kappa}$ is shown in Figure 7.18.

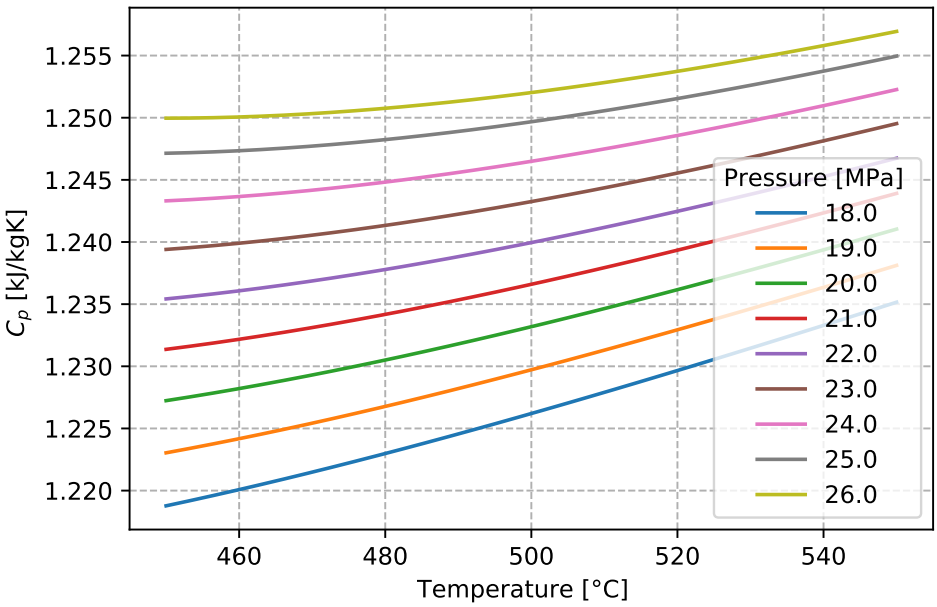

Figure 7.16: The $\mathbf{C}_p$ of pure CO_2.

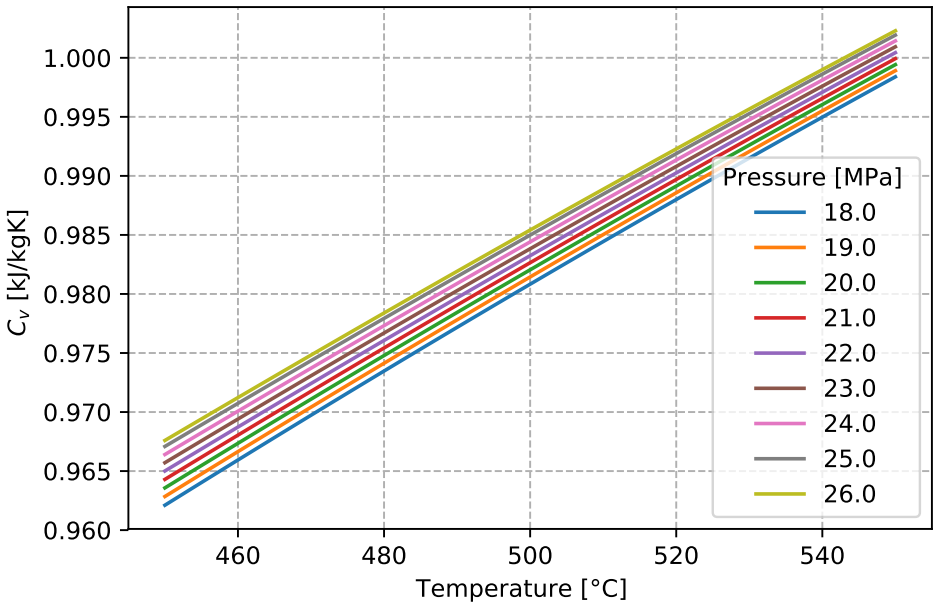

Figure 7.17: The $\mathbf{C}_v$ pure CO_2.

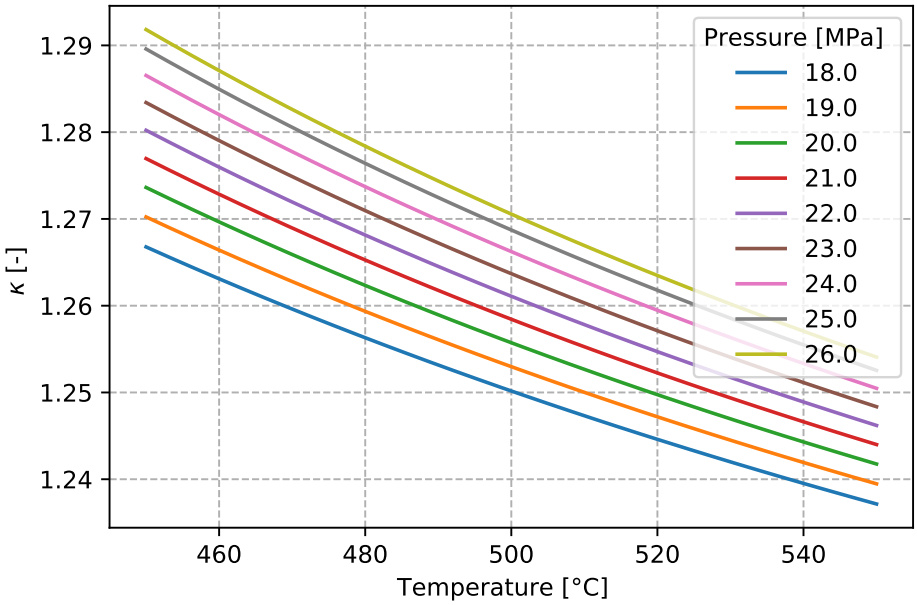

Figure 7.18: The $\boldsymbol{\kappa}$ pure CO_2.

The similar results can be observed for other cycle layouts. Figure 7.19 and Figure 7.20 shows the results for the pre-compression cycle. The increase of the turbine power is sightly positive. The biggest increase is in the area close to the area of maximum cycle efficiency for the operation conditions from Table 6.1.

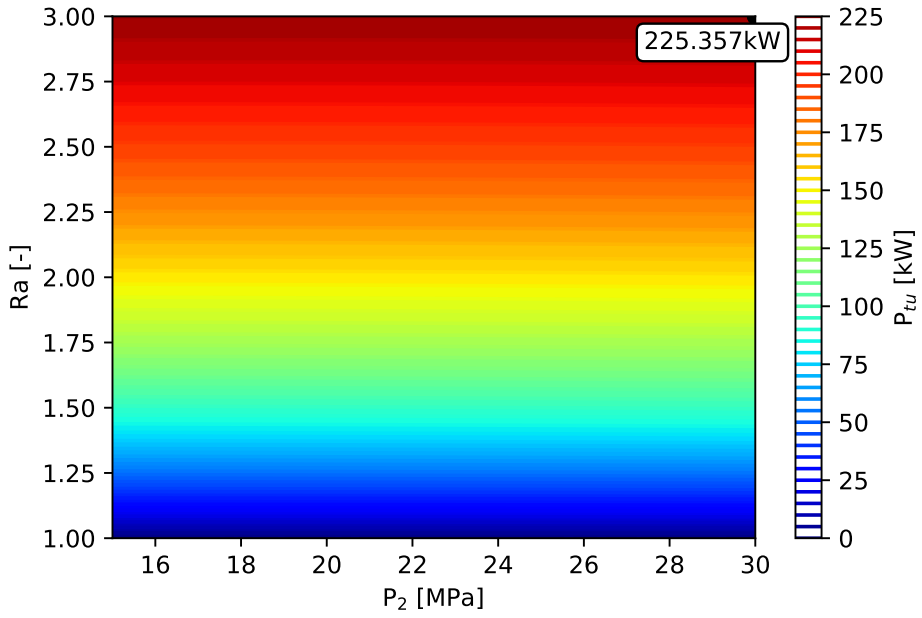

Figure 7.19: The $\mathbf{P}_{tu}$ - the Pre-compression cycle.

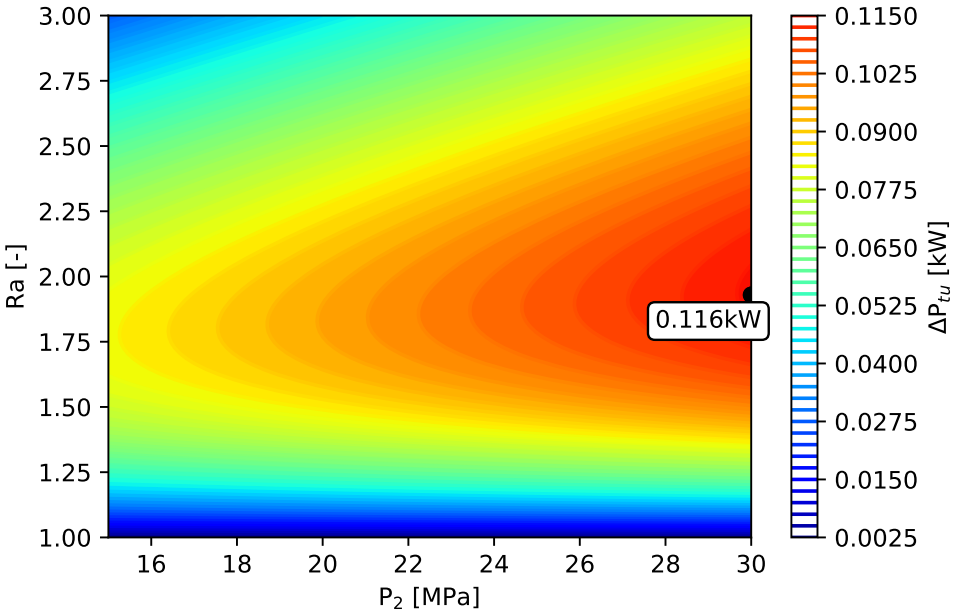

Figure 7.20: The $\Delta \mathbf{P}_{tu}$ - the Pre-compression cycle.

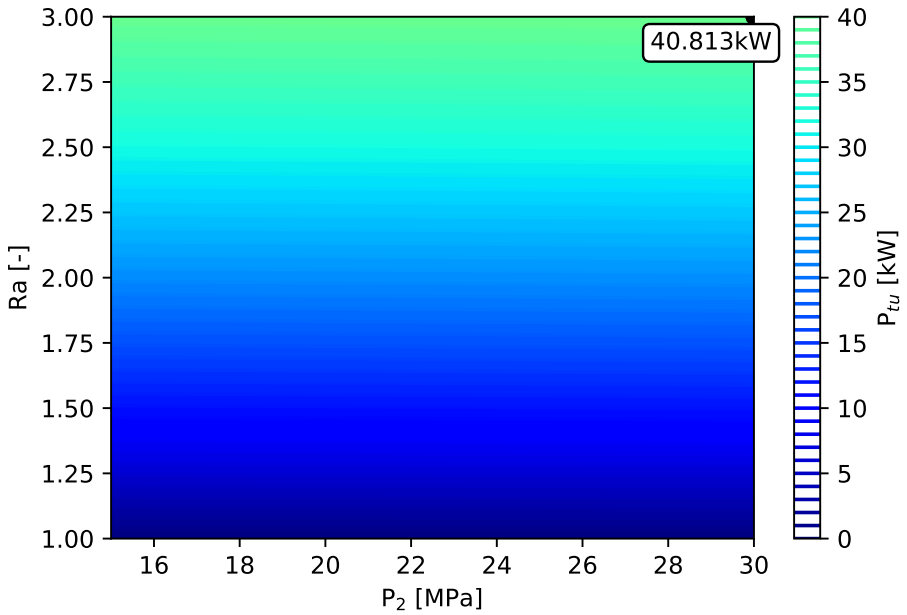

Figure 7.21: The $\mathbf{P}_{tu}$ no.2 - Sthe Split expansion cycle.

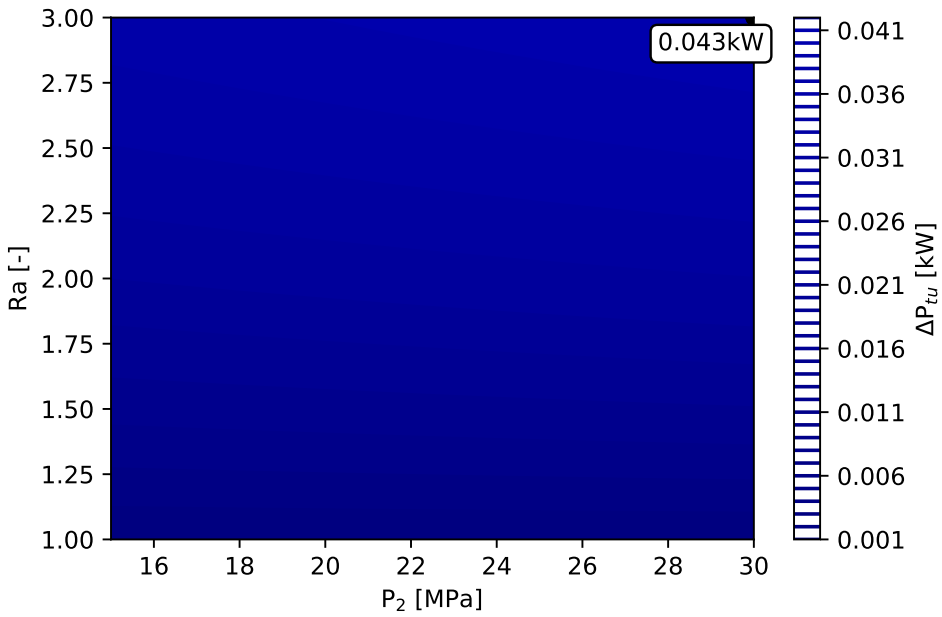

Figure 7.22: The $\Delta\mathbf{P}_{tu}$ no.2 - the Split expansion cycle.

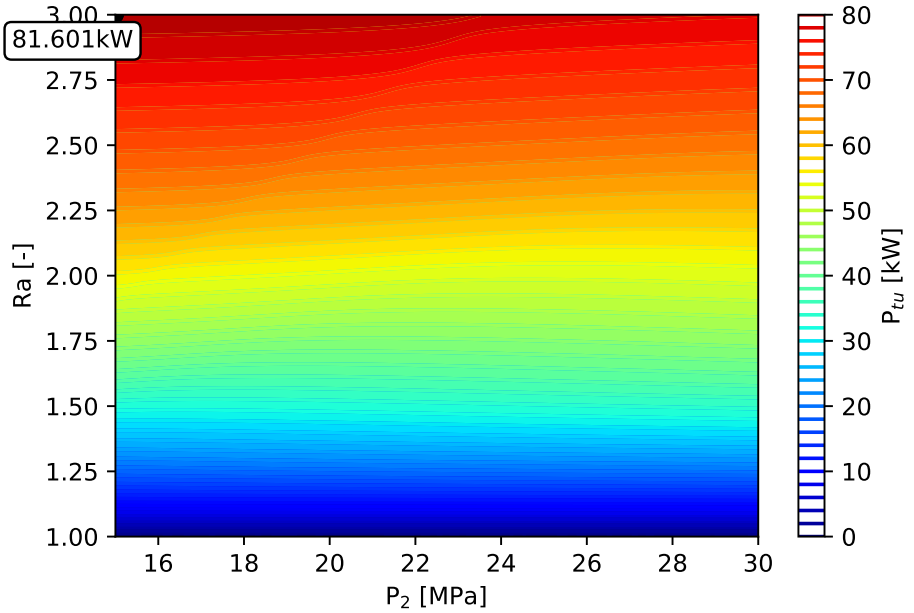

Figure 7.23: The $\mathbf{P}_{tu}$ no.1 - the Split expansion cycle.

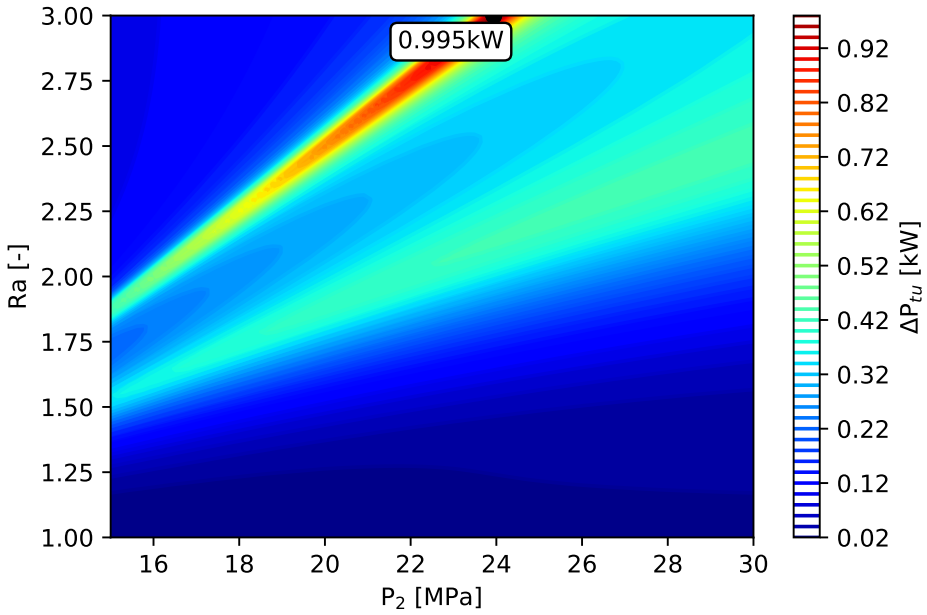

Figure 7.24: The $\Delta \mathbf{P}_{tu}$ no.1 - the Split expansion cycle.

Figure 7.21 and Figure 7.22 shows the results for the Split expansion cycle. The results are for turbine number 2. The result are similar to the Re-compression cycle. This turbine has the same operating parameters, like the turbine in the Re-compression cycle, except the turbine inlet pressure. The turbine inlet pressure is lower than that of the Re-compression cycle. The results for the turbine number 1 are different, but the resulting effect is the same. The largest increase is in the different area than for the turbine number 2., see Figure 7.23 and Figure 7.24. The results for other mixtures are similar. All investigated mixtures have the positive effect. He has the larges effect.

7.3 Effect of Mixtures on the Heat Exchangers Design

Other important components of the S-CO_2 power cycle are heat exchangers. The S-CO_2 power cycle has three different types of heat exchangers, see Chapter 4. The first type of the heat exchanger is the recuperative heat exchanger (**RH**, **LTR** and **HTR**). The second type of the heat exchanger is the cooler. The last type of the heat exchanger is the heater, (only for indirect S-CO_2 power cycle). The direct S-CO_2 power cycle is without heater. The heat source for this type of S-CO_2 cycle is a combustion chamber or other direct heat source.

To explain the effect of mixtures on heat exchangers let us use the Re-compression cycle layout. The Re-compression cycle was optimized for the best cycle efficiency in this case 42.1 % and the net power of 16.06 MW. If the working medium for the same parameters and cycle layout consists of 99 % CO_2 and 1 % Ar, the cycle efficiency is reduced to 41.76 % and

the net power to 15.7 MW. The T-s diagram of the re-compression cycle is show in Figure 7.25.

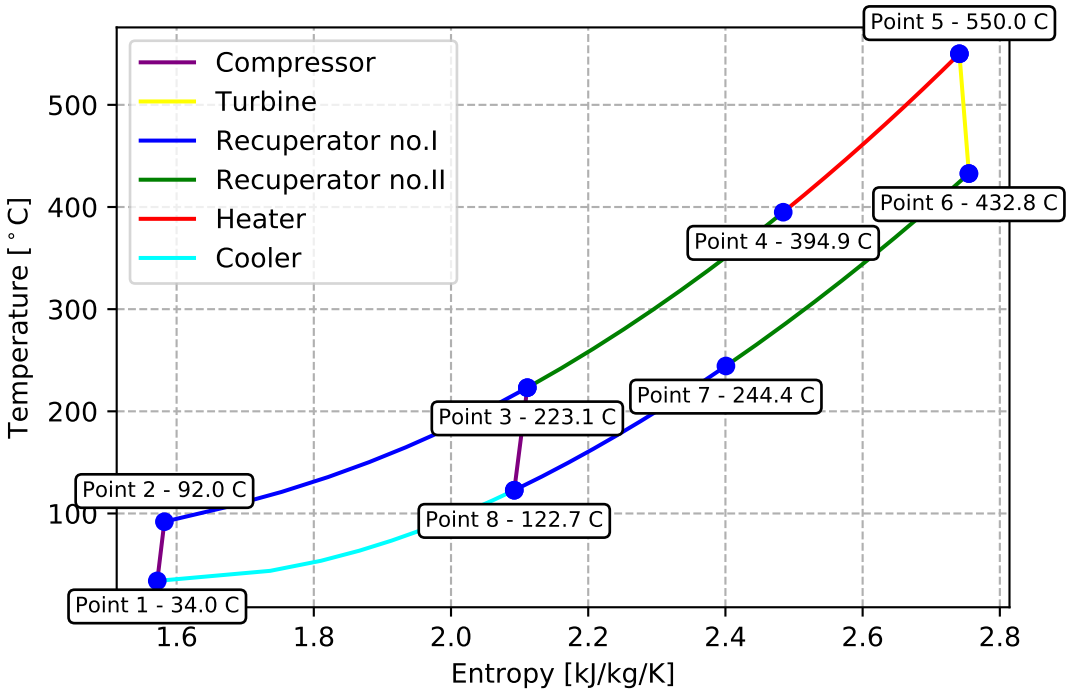

Figure 7.25: T-s diagram of the Re-compression cycle. [A.10]

The re-compression cycle consists from two recuperative heat exchangers (**LTR** and **HTR**), a cooler and a heater. [5] The most important and problematic heat exchanger is the recuperative heat exchanger, especially **LTR**, due to the pinch point issue. The pinch point is very undesirable in the heat exchanger.

The design of heat exchanger is different for each type. However, all heat exchangers in the investigated cases are the countercurrent the arrangement. The recuperative heat exchanger is of PCHE (Printed Circuit Heat Exchanger) type. [19] It is a heat exchanger with zigzag and semi-circular channels. The prime manufacturer is Heatric (Heatric Division of Meggitt UK Ltd). Other heat exchangers are shell and tube. Except for the air cooler [62] [63], manufactured by ALFA laval, and the heater for exhaust gas for gas turbine (waste heat recovery systems).

7.3.1 Recuperative Heat Exchangers

As has been previously described, one of the reasons for this research is the possibility of eliminating the effect of the pinch point in the heat exchangers. Therefore first results are shown for the recuperative heat exchanger, since they have a major problem with the pinch point. However, removing the pinch point may affect the cycle efficiency, by reduction of the

net power. The effect is shown on three different types of heat exchangers (different operation parameters), where the pinch point occurs. The results are shown on the low temperature recuperative heat exchangers (**LTR**), where the pinch point usually occurs.

The first heat exchanger is a recuperative heat exchanger from Figure 2.6. This recuperative heat exchanger has the negative $\Delta\mathbf{T}$. The results for this heat exchanger are shown in Figure 7.26 and Figure 7.27. The $\Delta\mathbf{T}$ is the temperature difference between the hot and the cold side. [A.3] The theoretical negative temperature difference can be removed using mixtures. [A.2] Each substance has a different effect on the temperature difference. The effect of the mixtures on the pinch point is opposite compare to the effect on the cycle efficiency and the net power. The highest positive effect on $\Delta\mathbf{T}$ has He, the highest negative effect have H_2S, Xe and SO_2, i.e. substances that have a positive effect on the cycle. [A.2] In Figure 7.26 and Figure 7.27, it is possible to observe the effect on the minimum $\Delta\mathbf{T}$, for recuperative heat exchangers where negative $\Delta\mathbf{T}$ theoretically occurs.

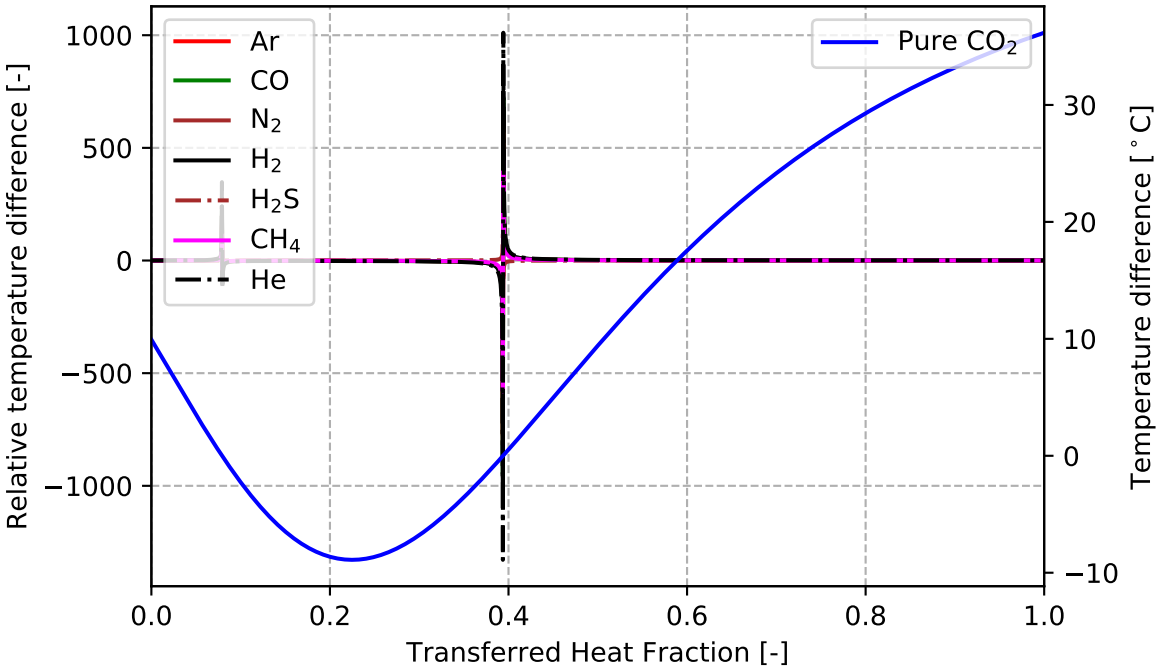

Figure 7.26: The $\Delta\mathbf{T}$ for the binary mixture with the pinch point (negative $\Delta\mathbf{T}$).

Figure 7.28 and Figure 7.29 show two recuperative heat exchangers, with different minimum $\Delta\mathbf{T}$ and different pressure 7.6 MPa (Figure 7.28) and 10 MPa (Figure 7.29). These heat exchangers have the same design as the recuperative heat exchanger from Figure 2.6. The results for recuperative heat exhcangers with different minimum $\Delta\mathbf{T}$ (Figure 7.28 and Figure 7.29) are slightly different result.

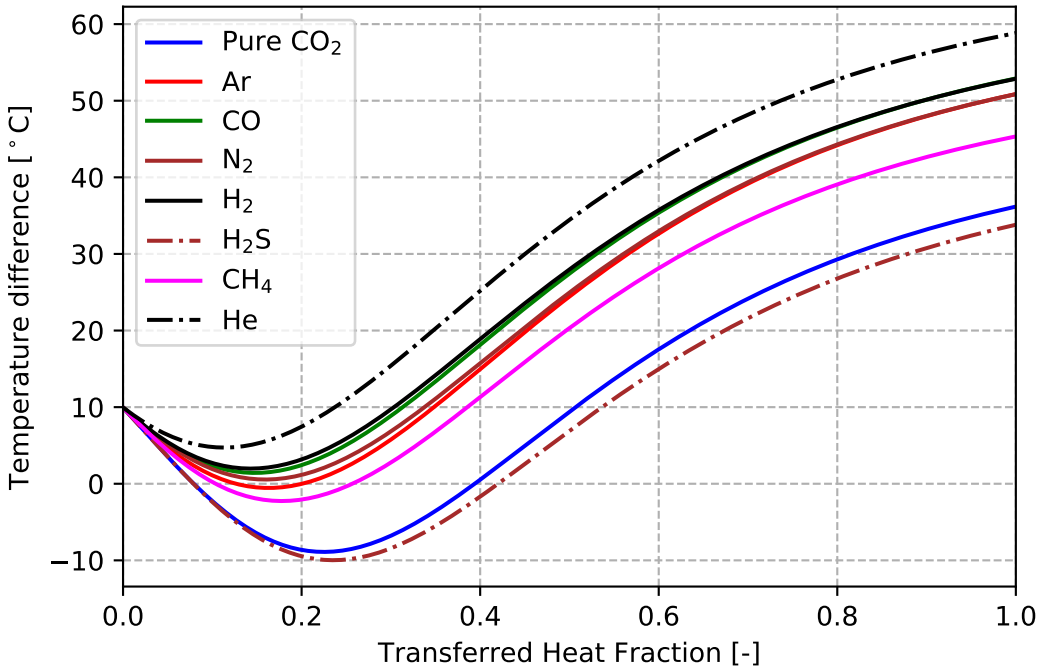

Figure 7.27: The $\Delta\mathbf{T}$ for the binary mixture with the pinch point (negative $\Delta\mathbf{T}$).

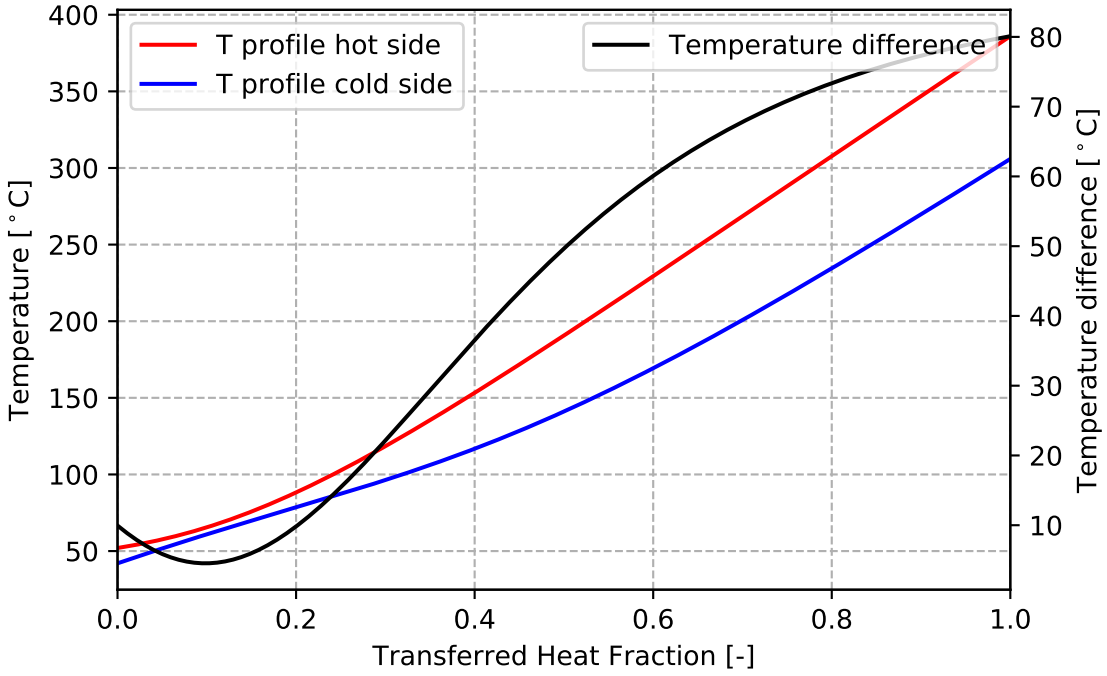

Figure 7.28: The temperature profiles and $\Delta\mathbf{T}$ with the pinch point (minimum $\Delta\mathbf{T}$).

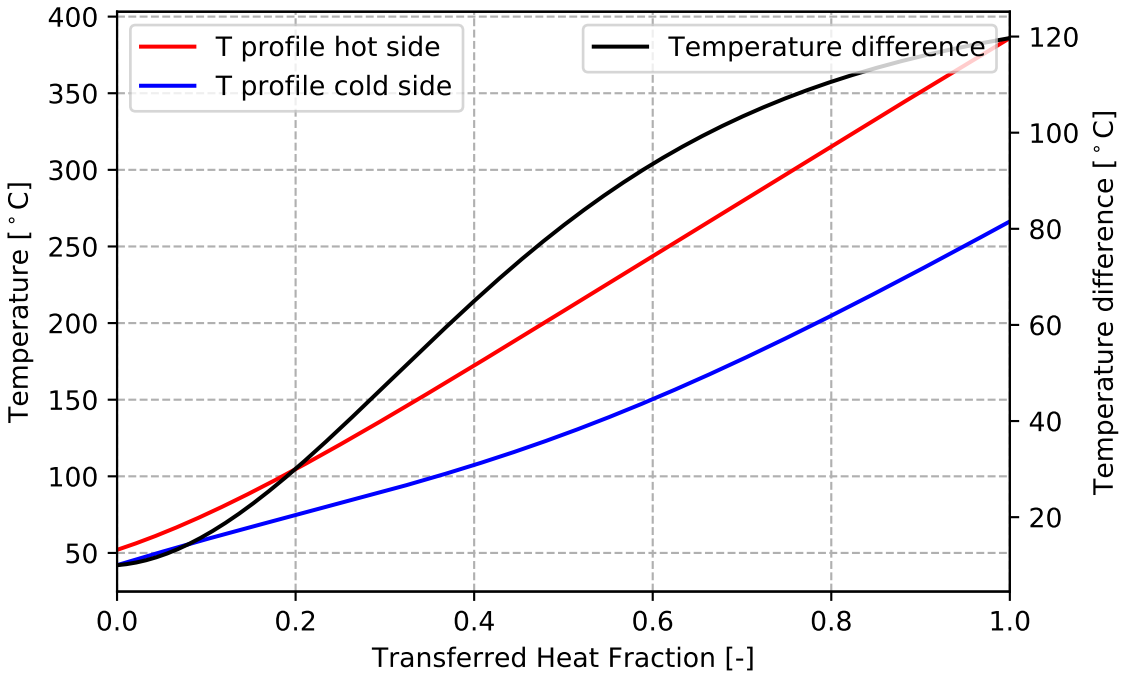

Figure 7.29: The temperature profiles and $\Delta\mathbf{T}$ with minimum $\Delta\mathbf{T}$.

The effect of mixtures of the recuperative heat exchanger from 7.28 is shown in Figure 7.30 and Figure 7.31. The results are for 95 % pure CO_2. The results are very similar to the previous case. He still has the maximum positive effect on increasing the minimum $\Delta\mathbf{T}$ and Xe, H_2S and SO_2 have the effect of decreasing the heat exchanger $\Delta\mathbf{T}$.

The effect of mixtures on heat exchanger $\Delta\mathbf{T}$ is different for the third case, see Figure 7.29. The results are for 95 % pure CO_2. The result are shown Figure 7.32 and Figure 7.33. In this case He and other substances with generally positive effect on $\Delta\mathbf{T}$ do not have this effect in the whole range, because there is no the pinch point.

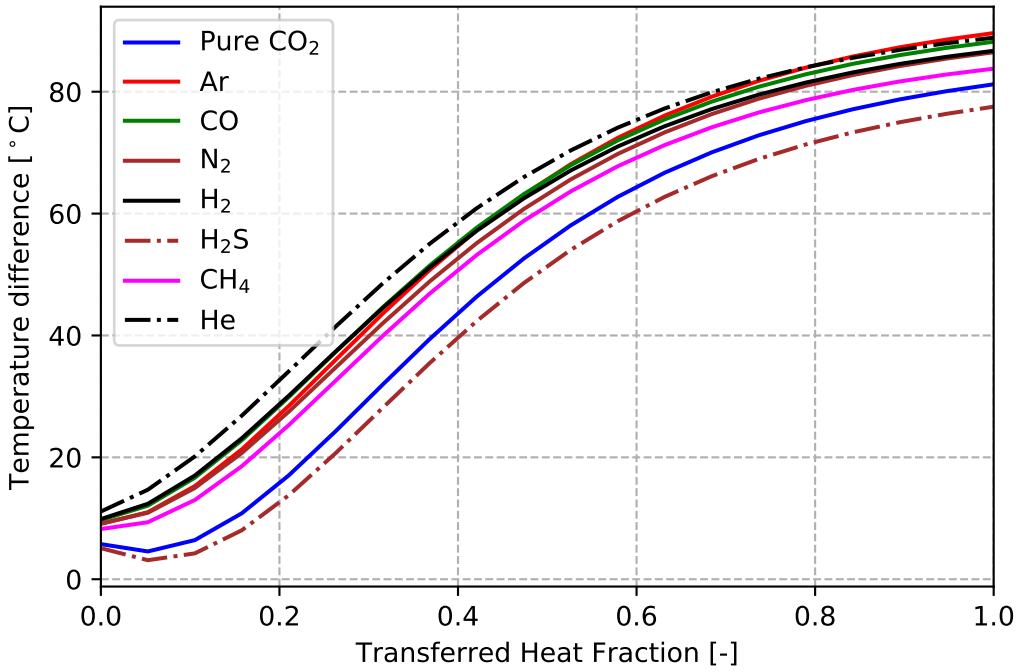

Figure 7.30: The $\Delta\mathbf{T}$ for the binary mixture with minimum $\Delta\mathbf{T}$.

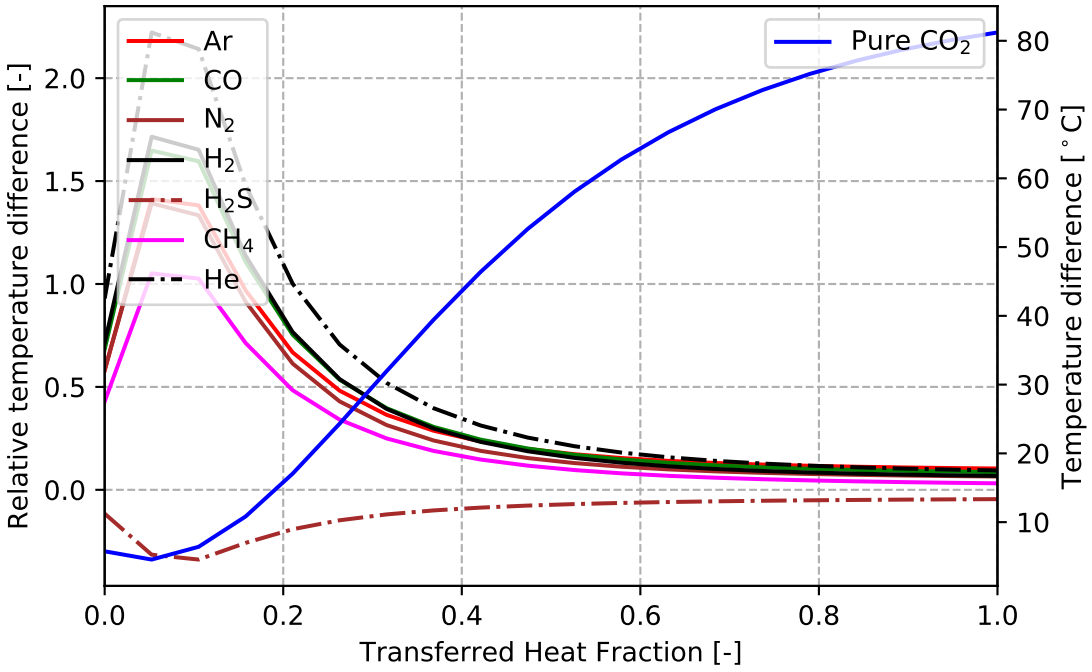

Figure 7.31: The $\Delta\mathbf{T}$ for the binary mixture with minimum $\Delta\mathbf{T}$.

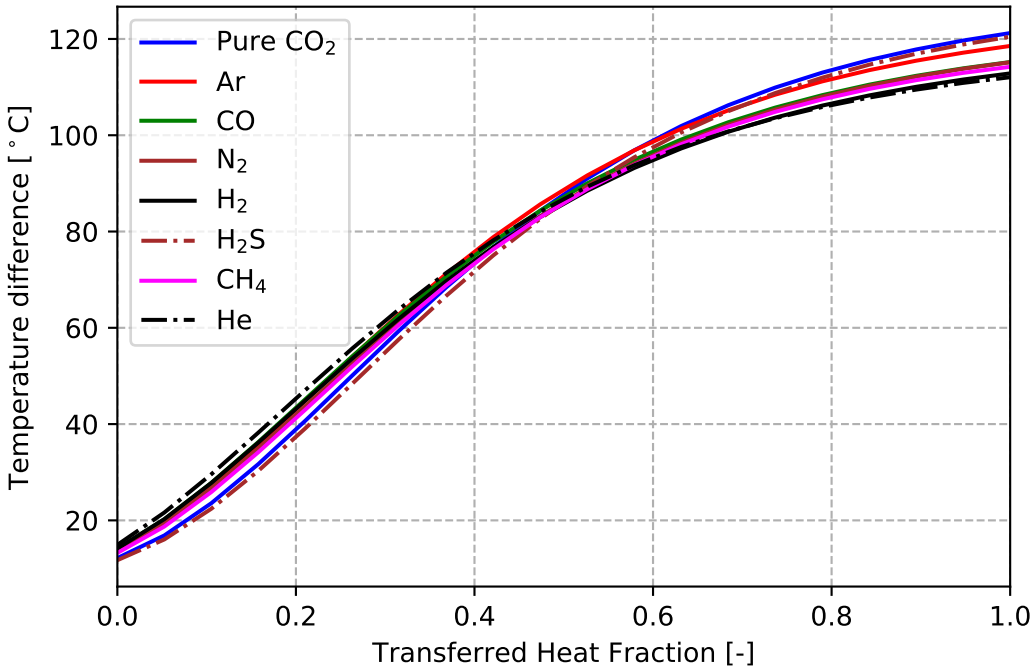

Figure 7.32: The $\Delta\mathbf{T}$ for the binary mixture with minimum $\Delta\mathbf{T}$.

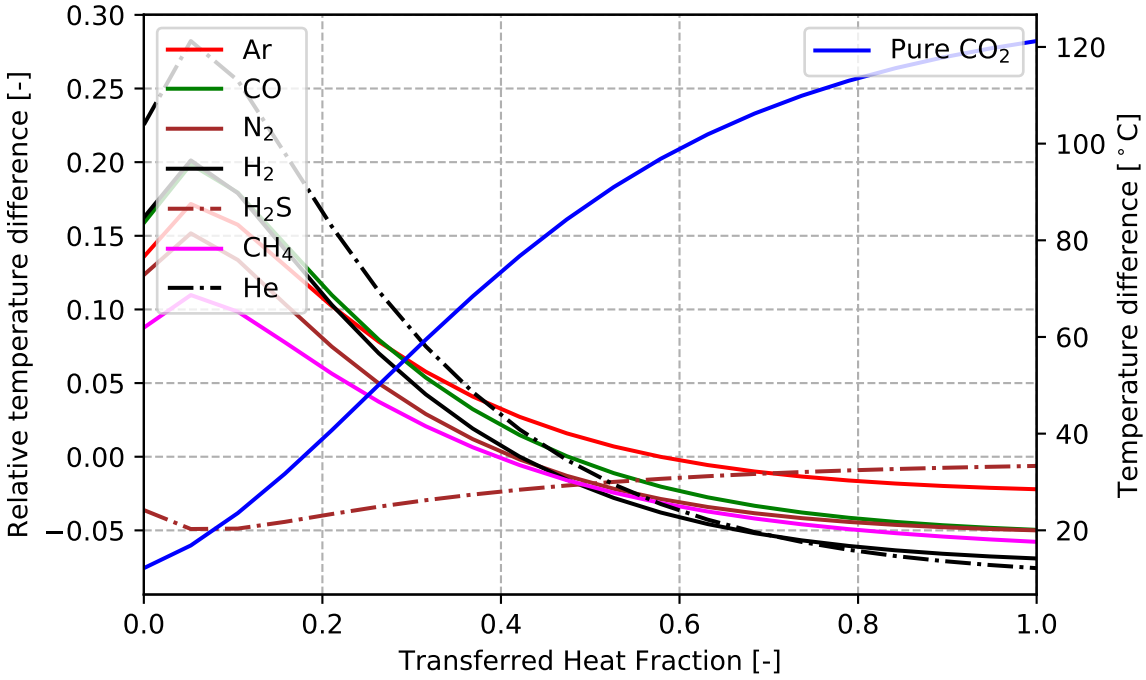

Figure 7.33: The $\Delta\mathbf{T}$ for the binary mixture with minimum $\Delta\mathbf{T}$.

The above described results are for the recuperative heat exchanger with small $\Delta\mathbf{T}$ or with the pinch point. However, it was a case study to describe the effect of mixtures on the pinch point in a hypothetical heat exchanger. In the real life it is necessary to focus on the recuperative heat exchangers in a real power cycle, such as for example the cycle from Figure 7.25. In this cycle there are two recuperative heat exchangers with the same working pressures, pressure losses are neglected, but with different temperatures. The first recuperativeheat exchanger is **LTR** (low temperature recuperative heat exchanger), the second is **HTR** (high temperature recuperative heat exchanger). The effects of mixtures on these heat exchangers are shown in Figure 7.34, Figure 7.35 and Figure 7.36, Figure 7.37.

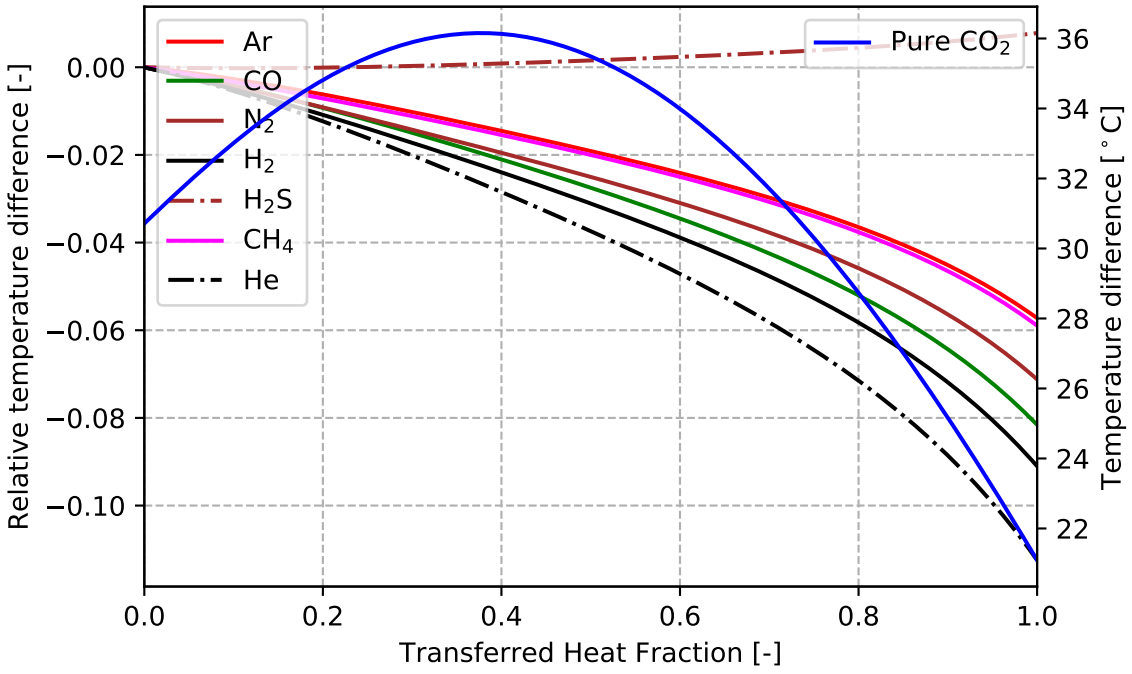

Figure 7.34: The $\Delta\mathbf{T}$ for recuperative heat exchanger **LTR**.

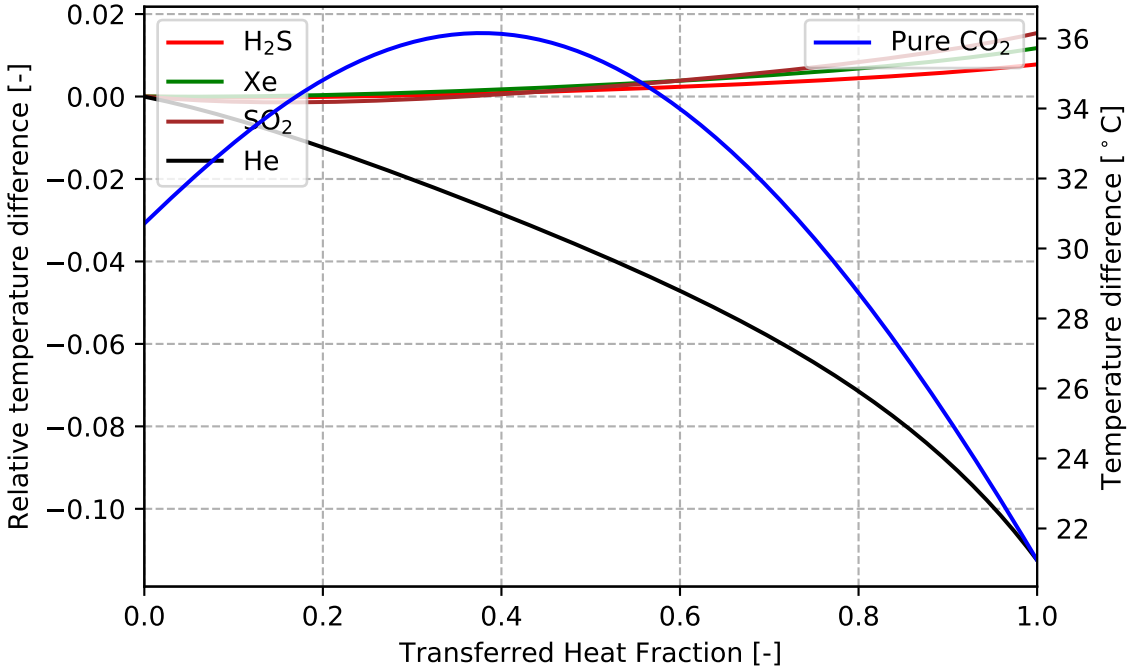

Figure 7.35: The $\Delta\mathbf{T}$ for recuperative heat exchanger **LTR**.

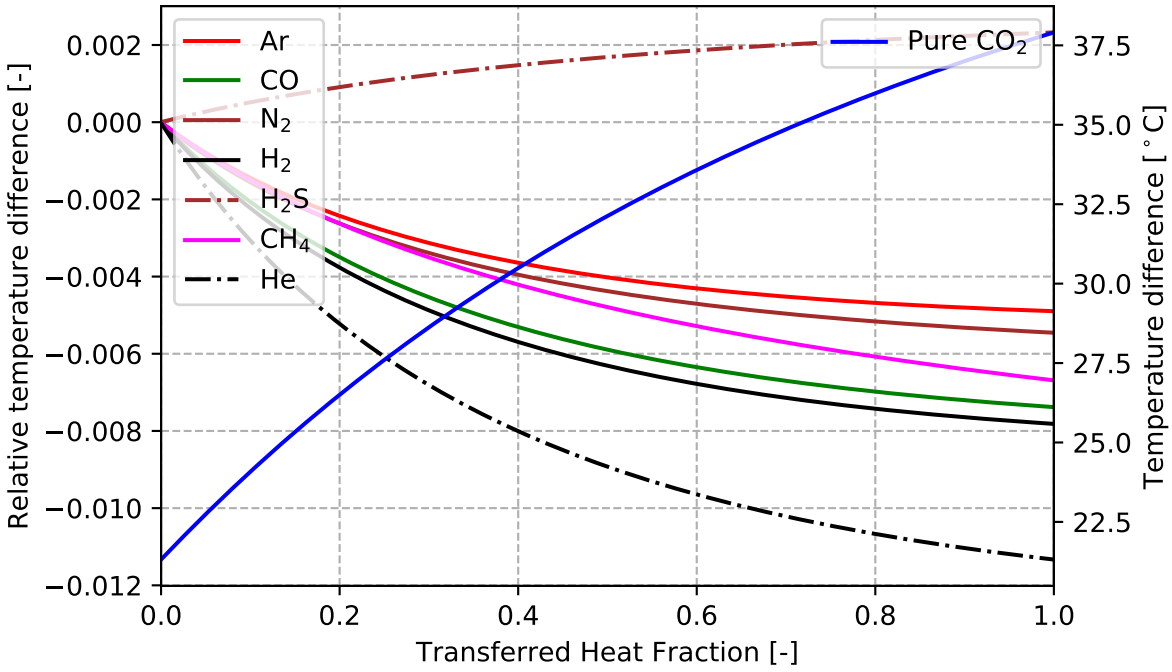

Figure 7.36: The $\Delta\mathbf{T}$ for recuperative heat exchanger **HTR**.

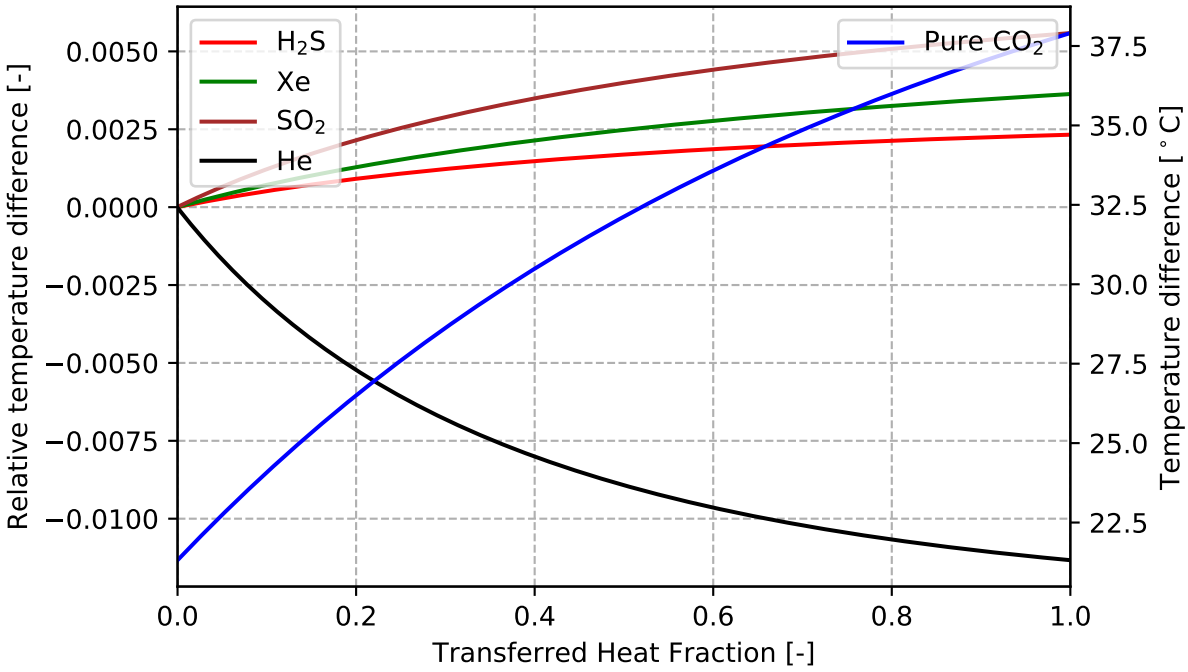

Figure 7.37: The $\Delta\mathbf{T}$ for recuperative heat exchanger **HTR**.

It is apparent that the effect of mixtures on $\Delta\mathbf{T}$ and heat transfer has the opposite trend when compared to the recuperative heat exchanger with the pinch point. These results can be observed for both cases (**LTR** and **HTR**). The effect is very small, in the case of **HTR** it is almost neglible. The results are for 99 % CO_2 purity. When the purity is further reduced, the difference increases but the trend remains the same. The main conclusion for the recuperative heat exchanger **LTR** and **HTR**) is the substance with positive effect on the cycle efficiency has the positive effect on the $\Delta\mathbf{T}$ (increase of $\Delta\mathbf{T}$) and the substance which has the negative effect on the cycle efficiency has the negative effect on the $\Delta\mathbf{T}$ (decrease of $\Delta\mathbf{T}$). This means that, using the CO2 with substance which have positive effect on cycle efficiency, the $\Delta\mathbf{T}$ in recuperative heat exchanger increase. The $\Delta\mathbf{T}$ decrease with substance which have negative effect on cycle efficiency.

7.3.2 Coolers and Heaters

This chapter investigates coolers and heaters. For coolers the focus is on water and air cooling. Each cooler has a different design. For water the design is the PCHE heat exchanger. [19] This is the same type of the heat exchanger as for the recuperative heat exchanger. However, the PCHE heat exchanger using the different material compared to the recuperative heat exchanger due to the operation parameters (pressure and temperature).

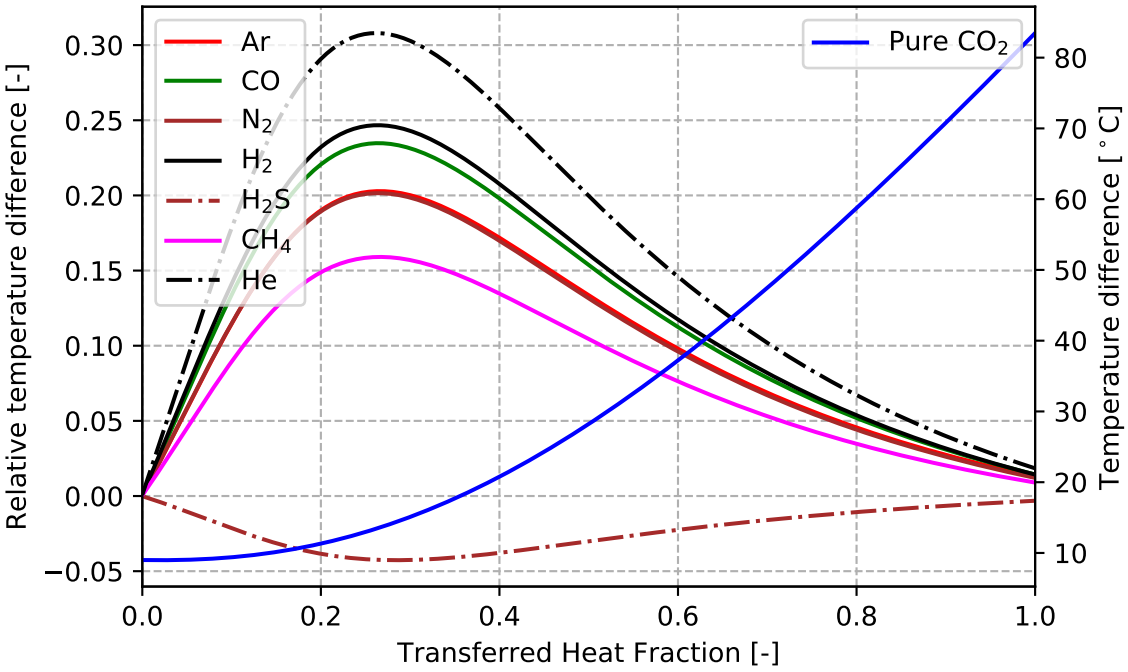

Figure 7.38: The $\Delta\mathbf{T}$ for water cooler. [A.10]

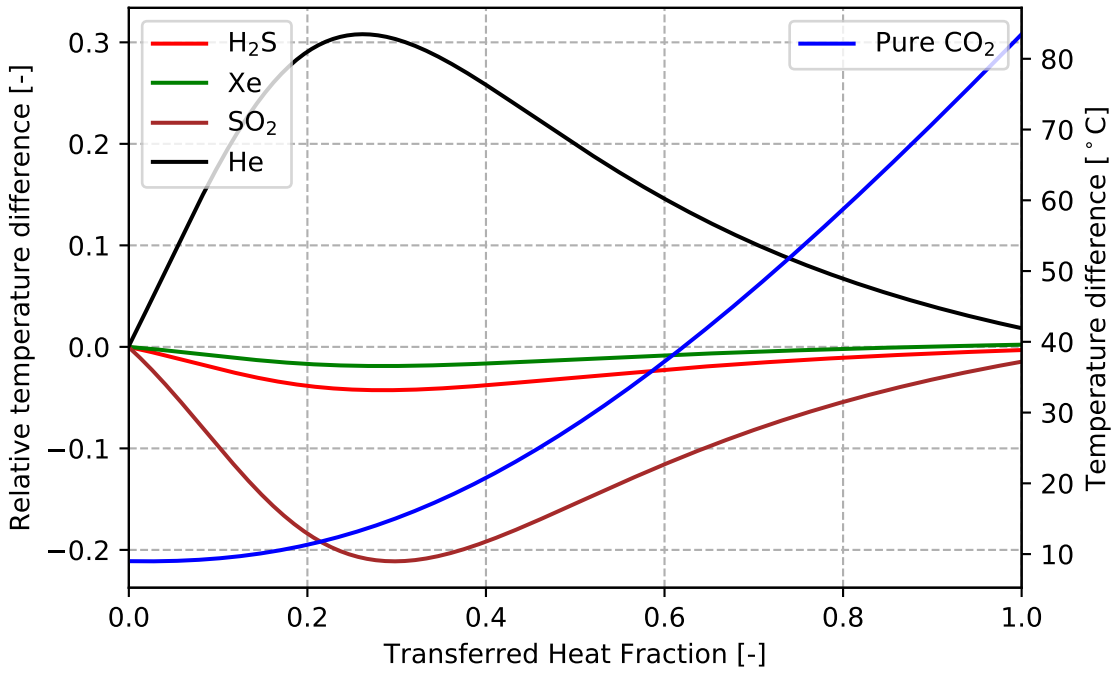

Figure 7.39: The $\Delta\mathbf{T}$ for water cooler.

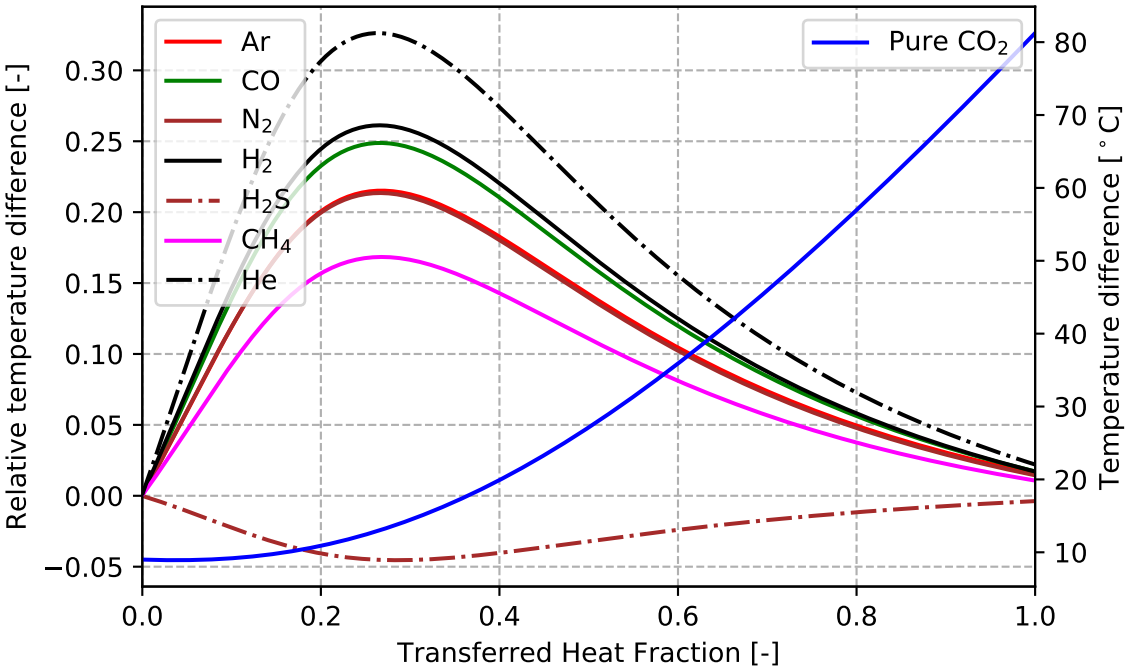

Figure 7.40: The $\Delta\mathbf{T}$ for air cooler. [A.10]

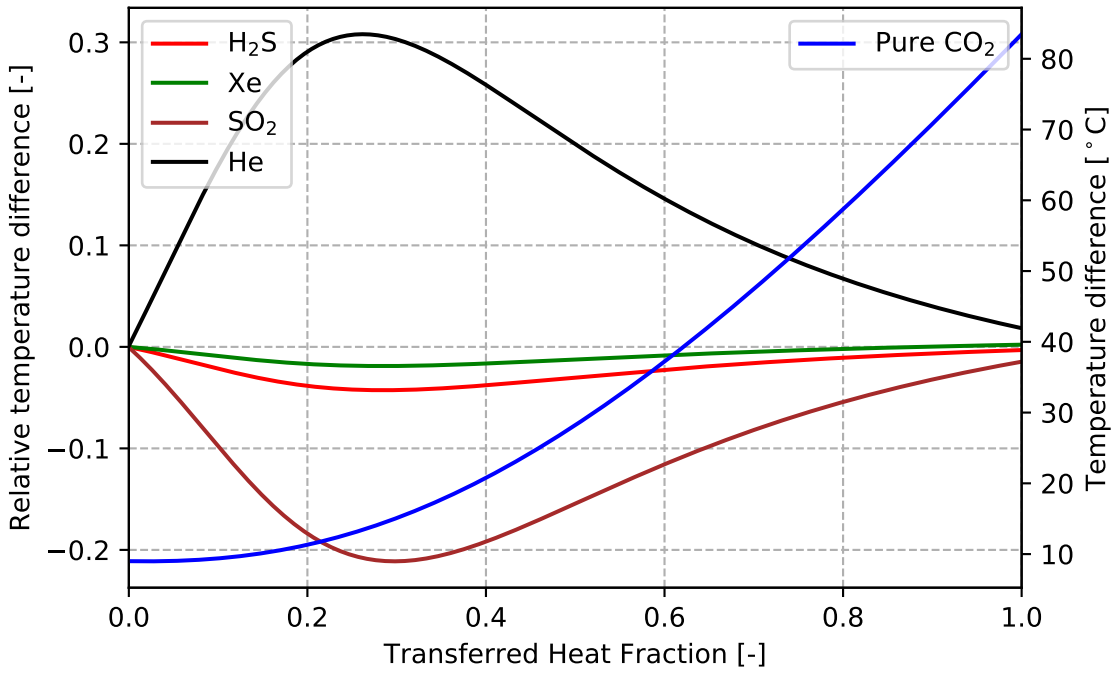

Figure 7.41: The $\Delta\mathbf{T}$ for air cooler.

The results for 99 % pure CO_2 are shown in Figure 7.38 and Figure 7.39, as can be seen

the results are very similar to the results for the recuperative heat exchanger with the pinch point. This means that, the substance with the positive effect on the cycle has the negative effect on the $\Delta\mathbf{T}$ (decrease of $\Delta\mathbf{T}$) and the substance which has the negative effect on the cycle has the positive effect on the $\Delta\mathbf{T}$ (increase of $\Delta\mathbf{T}$) [A.2, A.10].

The results for air cooler are very similar. The same trends as for water cooler can be observed. The results are shown in Figure 7.40 and Figure 7.41 [A.10].

The last type of the heat exchanger is the heater. Two cases of heaters were investigated. The first case is the heater with He as working medium. The result is shown in Figure 7.42 and Figure 7.43. The results are also for 99 % pure CO_2 and the results are the same as for cooler. This means that the substance with the positive effect on the cycle has the negative effect on the $\Delta\mathbf{T}$ (decrease of $\Delta\mathbf{T}$) and the negative effect on the $\Delta\mathbf{T}$ (increase of $\Delta\mathbf{T}$) has the substance with negative effect on the cycle.

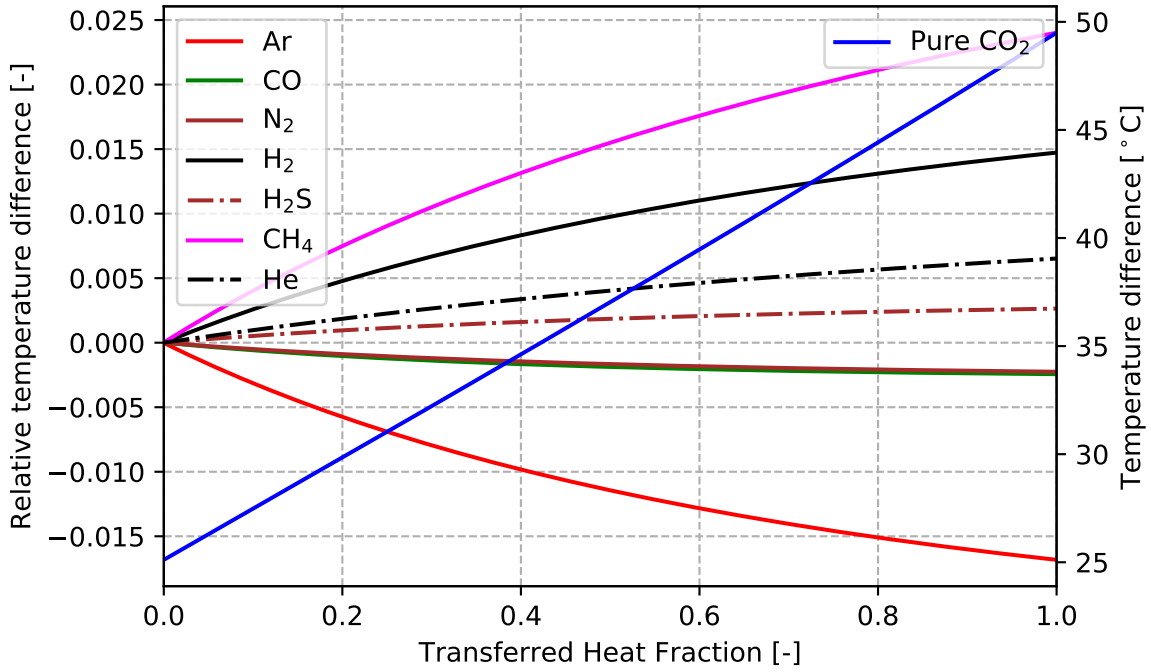

Figure 7.42: The $\Delta\mathbf{T}$ for He heater.

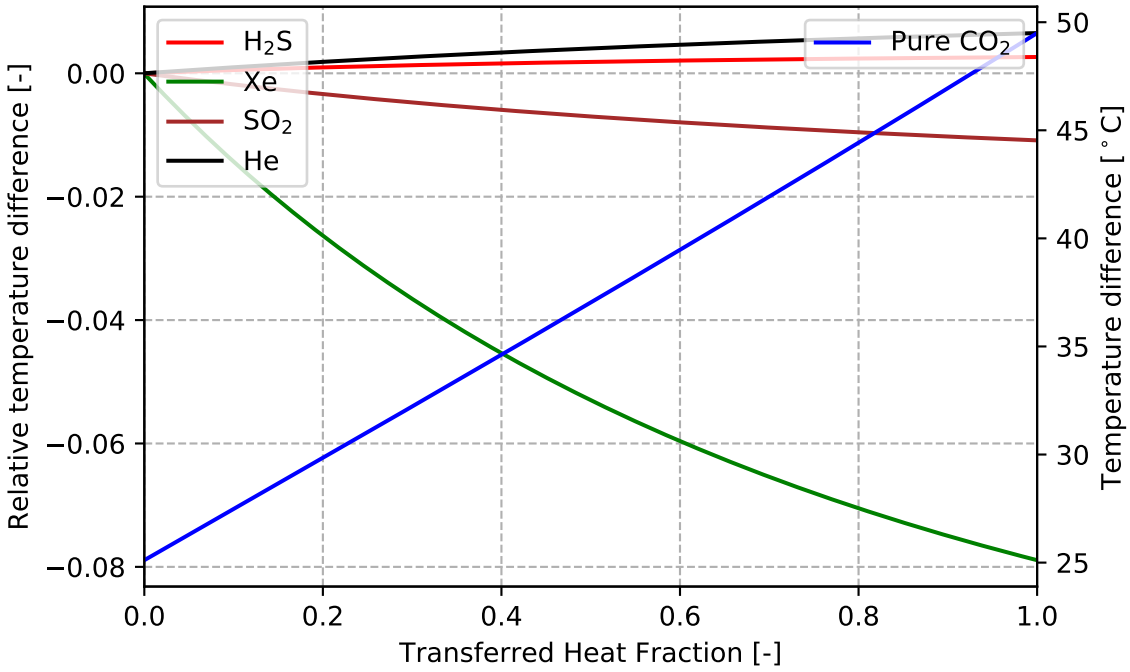

Figure 7.43: The $\Delta\mathbf{T}$ for He heater.

The same results are for heater with exhaust gas from gas turbine (waste heat recovery systems). The results are shown in Figure 7.44. Again, the substance with positive effect on the cycle has the negative effect on the $\Delta\mathbf{T}$ (decrease of $\Delta\mathbf{T}$) and the substance with the negative effect on the cycle has the positive effect on the $\Delta\mathbf{T}$ (increase of $\Delta\mathbf{T}$). For this reason, it can be stated that working medium of heat source has a small effect on heat transfer to mixtures in the S-CO_2 cycle. However, this conclusion applies only to indirect S-CO_2 power cycle. In the case of a direct cycle, it will be a completely different effect because, the heater is not considered due to the different arrangement and direct connection to the heat source.

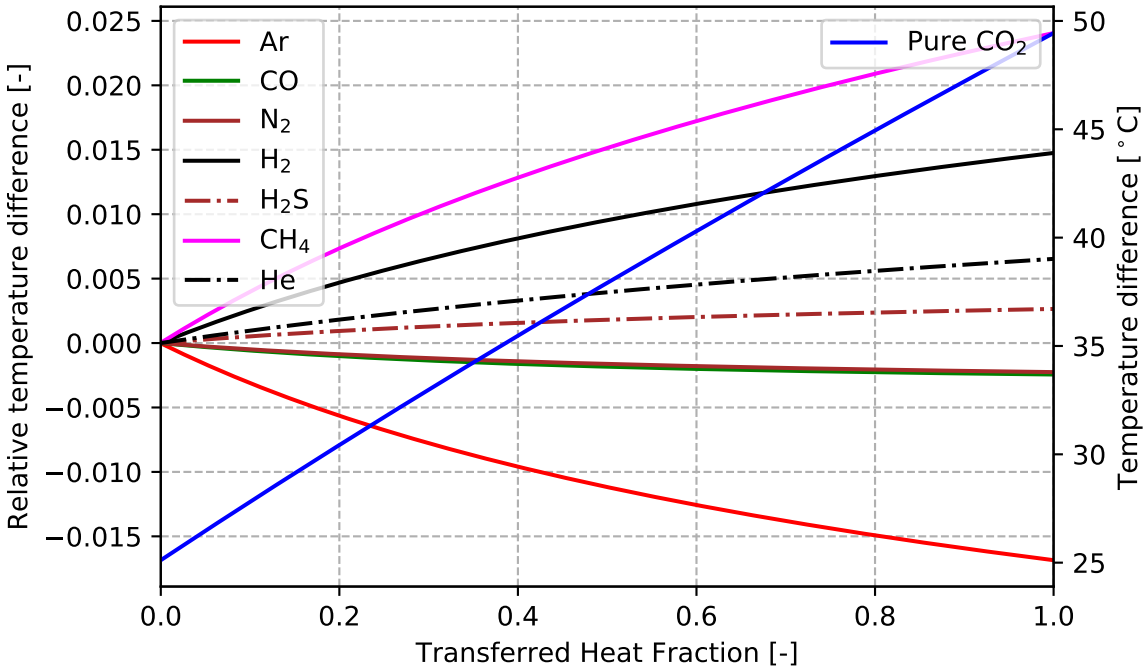

Figure 7.44: The $\Delta\mathbf{T}$ for heater (WHR).

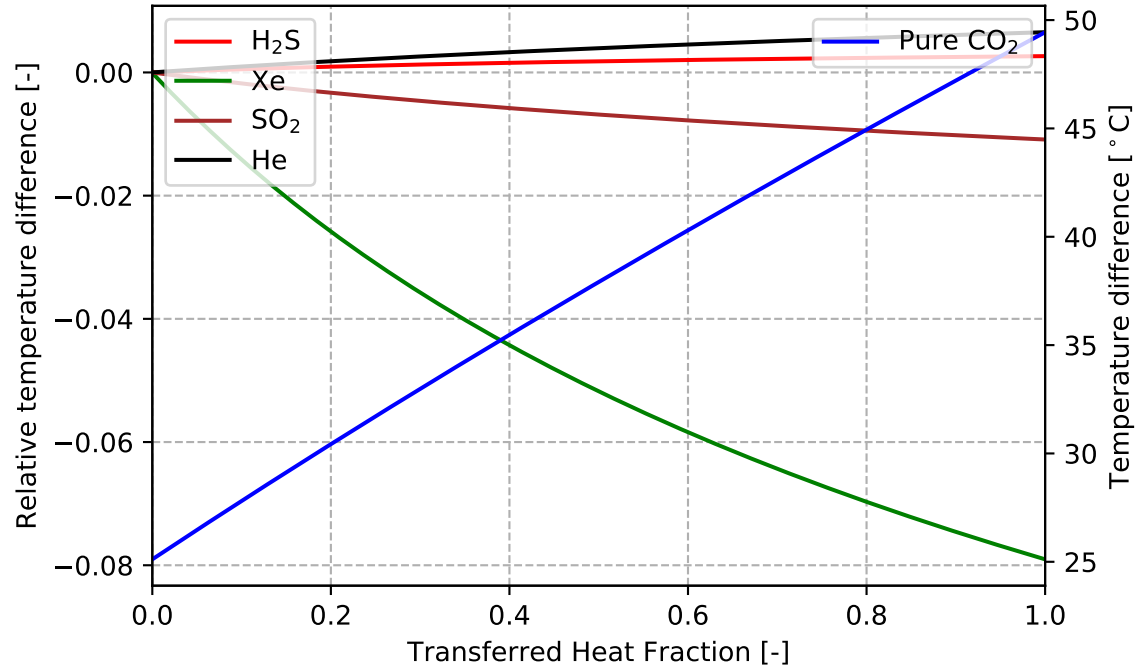

Figure 7.45: The $\Delta\mathbf{T}$ for heater (WHR).

7.3.3 Physical Description of the Effect on the Heat Exchangers

In the previous text different effects of mixtures on the heat exchanger, the compressors and the turbines performance were observed. The effect is connected to the thermo-physical properties of CO_2 and mixtures with CO_2. However, the results were described only for $\Delta\mathbf{T}$. The $\Delta\mathbf{T}$ is defined from temperature on the hot and cold side. The temperature is connected to enthalpy and pressure. The $\Delta\mathbf{T}$ is one of the parameters, which have an effect on the heat transfer and the final design of the heat exchanger. The properties of CO_2 such as enthalpy, have an effect on the calculation, especially on heat flux, overall heat transfer coefficient and other parameters, which are necessary for the design of the heat exchanger. The heat exchanger and heat transfer are calculated according to the following equations. [64] The main parameter is the thermal power, Equation 7.2.

$$q = UA\Delta T_d \tag{7.2}$$

where **U** is the overall heat transfer coefficient, $\Delta\mathbf{T}$ is the temperature difference and **A** is the surface area for each fluid side. The thermal power is also calculated from the balance equation of the heat exchanger. The balance equation is defined byo Equation 7.3, [64]

$$q = m_h \left(h_{h,i} - h_{h,0}\right) \quad q = m_c \left(h_{h,0} - h_{h,i}\right) \tag{7.3}$$

where **m** is the mass flow on the hot and the cold side and **h** is the enthalpy of the hot and the cold side on inlet and outlet of the heat exchanger. The calculation is done such that the heat exchanger is divided to elementary volumes. Each elementary volume has the same thermal power. The description of the calculation of the elementary volume is shown in Figure 7.46. The heat exchangers for this study were divided into 2000 elements. The heat exchanger is divided in order to control the minimum $\Delta\mathbf{T}$. For this reason, the difference between the temperature of the hot side and the temperature of the cold side can be used. The same procedure was applied to each element.

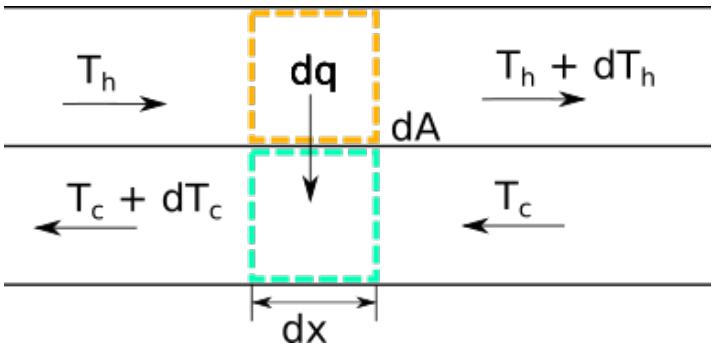

Figure 7.46: The temperature distributions for a counterflow heat exchanger.

The overall heat transfer coefficient is defined as, [64]

$$U = \frac{1}{\left(\frac{1}{\alpha_h} + \frac{w_t}{\lambda_t} + \frac{1}{\alpha_c}\right)} \tag{7.4}$$

where $\boldsymbol{\alpha}$ is the heat transfer coefficient for the hot and the cold side, $\mathbf{w}_t$ is the wall thickness and $\boldsymbol{\lambda_t}$ is the thermal conductivity. Equation 7.4 is writen for the specific case of PCHE heat exchanger. [19] The $\boldsymbol{\alpha}$ is calculated from the Nusselt number, by Equation 7.5. [64]

$$\alpha = \frac{\lambda_{CO_2} Nu}{d} \tag{7.5}$$

where $\boldsymbol{\lambda}$ is the conductivity of CO_2, **d** is the characteristic dimension and **Nu** is the Nusselt number. The same procedure was applied to each element. The Nusselt number is further calculated according to the criterion equations. Equation 7.6 is the criterion equations for the Nusselt number and for the PCHE design with zigzag and semi-circular channels. [19]

$$Nu = 0.1696 * Re^{0.629} Pr^{0.317} \tag{7.6}$$

where **Re** is the Reynolds number and **Pr** is the Prandl number. The large number of correlations for calculation of the **Nu** exists. However, only limited number of correlations are applicable to S-CO_2. [65] Examples include the Dittus-Boelter correlation [65], the Gnielinski correlation [66] [67] or other modification of correlations for laminar or turbulent flow and different design of channels and heat exchanger. The effect of mixtures can be observed for each correlation, the effect of the correlation on calculation is always the same, but the **Nu**

is different for each substance. The Nusselt number is affected by the **Re** and the **Pr**. The **Re** is calculated based on Equation 7.7. [64]

$$Re = \frac{cd\rho}{\mu} \tag{7.7}$$

where **c** is the velocity, **d** is the characteristic dimension, $\boldsymbol{\mu}$ is the dynamic viscosity and ρ is the density of CO_2. The **Re** is the ratio of the inertia and viscous forces. The **Pr** is defined as the ratio of the momentum and thermal diffusivities. [64]

$$Pr = \frac{\nu}{\alpha_t} \tag{7.8}$$

where $\boldsymbol{\nu}$ is the kinematic viscosity and $\boldsymbol{\alpha_t}$ is the thermal diffusivity. The **Pr** is the last parameter which has an effect on the calculation of a heat exchanger. The calculated parameter of the heat exchanger is the length of channel. The length of channels for **LTR** heat exchanger is shown in Figure 7.47 and Figure 7.48. The effect of mixtures is similar for each design and operating parameters of the heat exchanger.

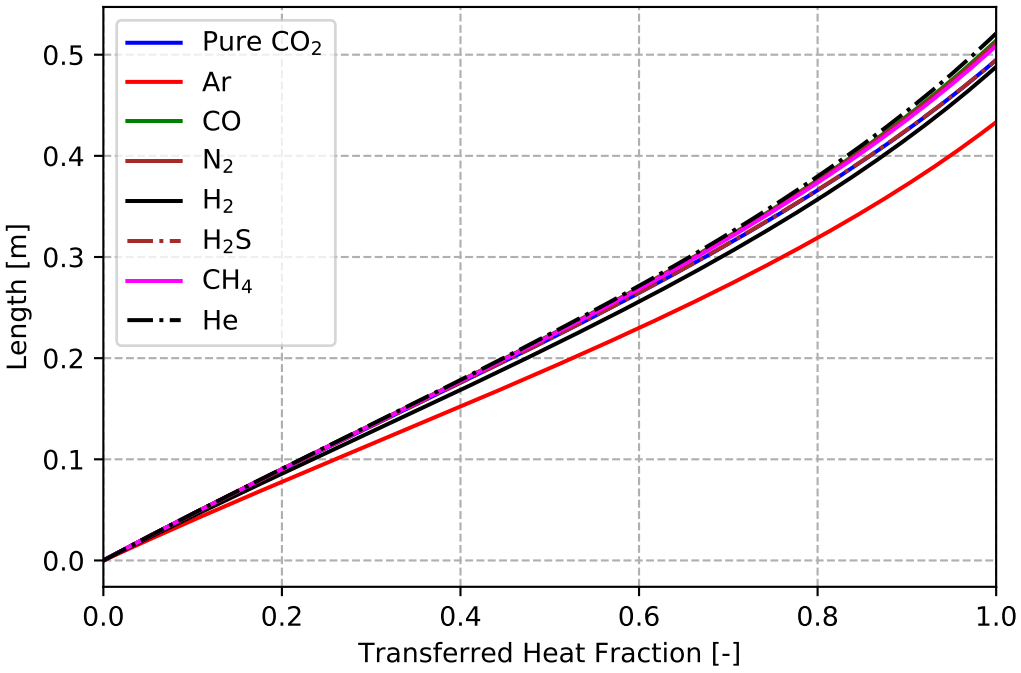

Figure 7.47: The length of channel for **LTR** heat exchanger.

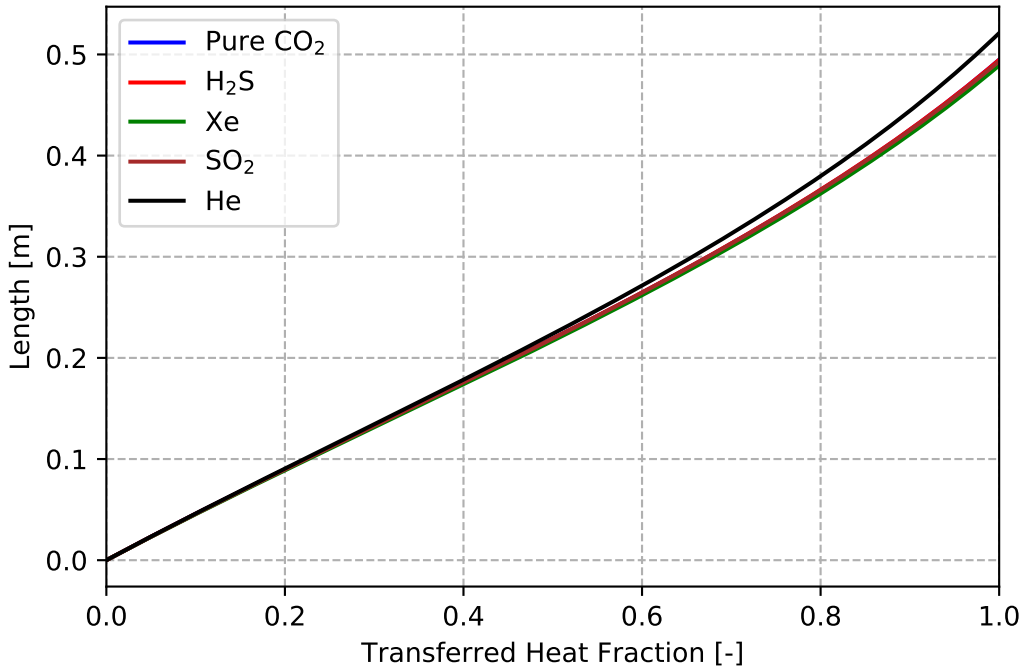

Figure 7.48: The length of channel for **LTR** heat exchanger.

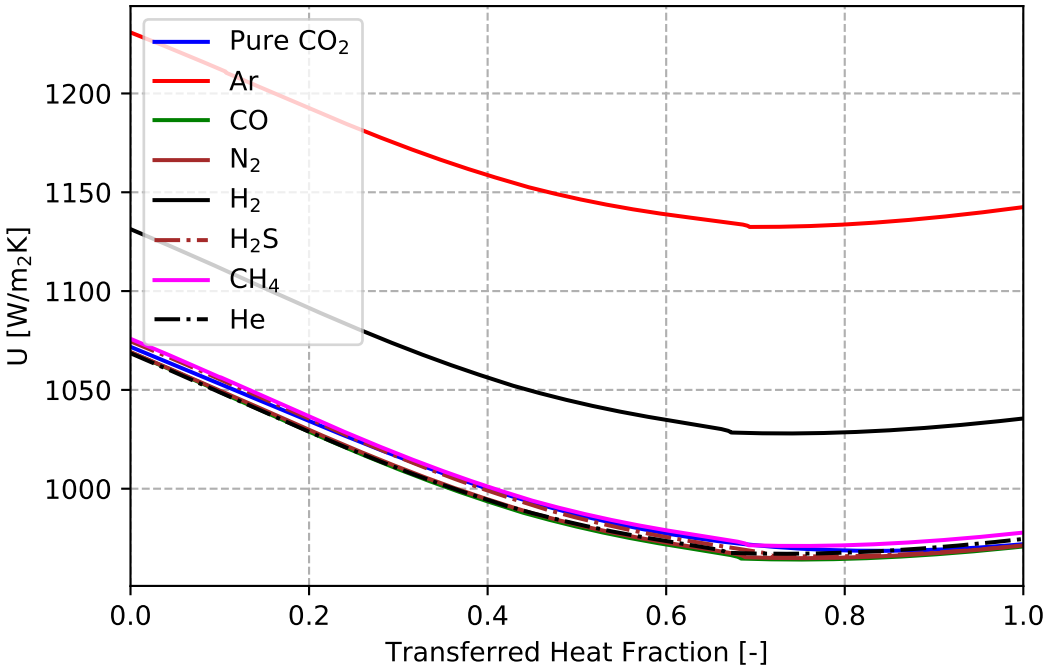

Figure 7.49: The **U** for **LTR** heat exchanger.

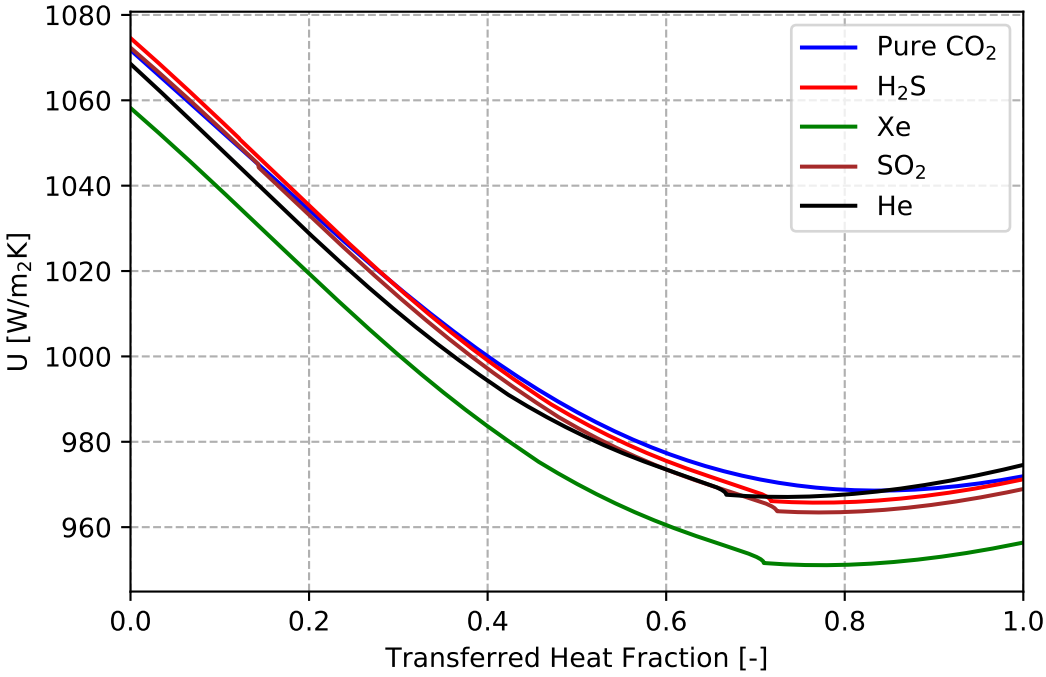

Figure 7.50: The **U** for **LTR** heat exchanger.

According to Figure 7.47 and Figure 7.48, it is obvious, that the effect on length is negligible for this case. The length is calculated from Equation 7.2, therefore the length is affected by $\Delta\mathbf{T}$ and **U**. The thermal power is the same for each element. The effect on the $\Delta\mathbf{T}$ was described before. The effect on the overall heat transfer coefficient is shown in Figure 7.49 and Figure 7.50.

It is clear, that the effect on U is much more pronounced. The largest positive effect has CO and H_2. This corresponds to the final length as shown in Figure 7.47 and Figure 7.48. Xe has a negative effect. Other substances which have positive effect on the cycle have negligible effect. The **U** is defined according to Equation 7.4. The effect is the same for both side. The effect on the **Re** is very small, but the effect on the **Nu** and the **Pr** is not negligible. The effect on **Nu** is shown in Figure 7.51. The **Pr** is shown in Figure 7.52. The results for the heat transfer coefficient for hot and cold side calculated from Equation 7.5, are shown in Figure 7.53 and Figure 7.54 respectively. It follows that the properties that have the greatest influence on the heat transfer are the following: viscosity (dynamic and kinematic), conductivity and density. This properties have the largest effect on heat transfer.

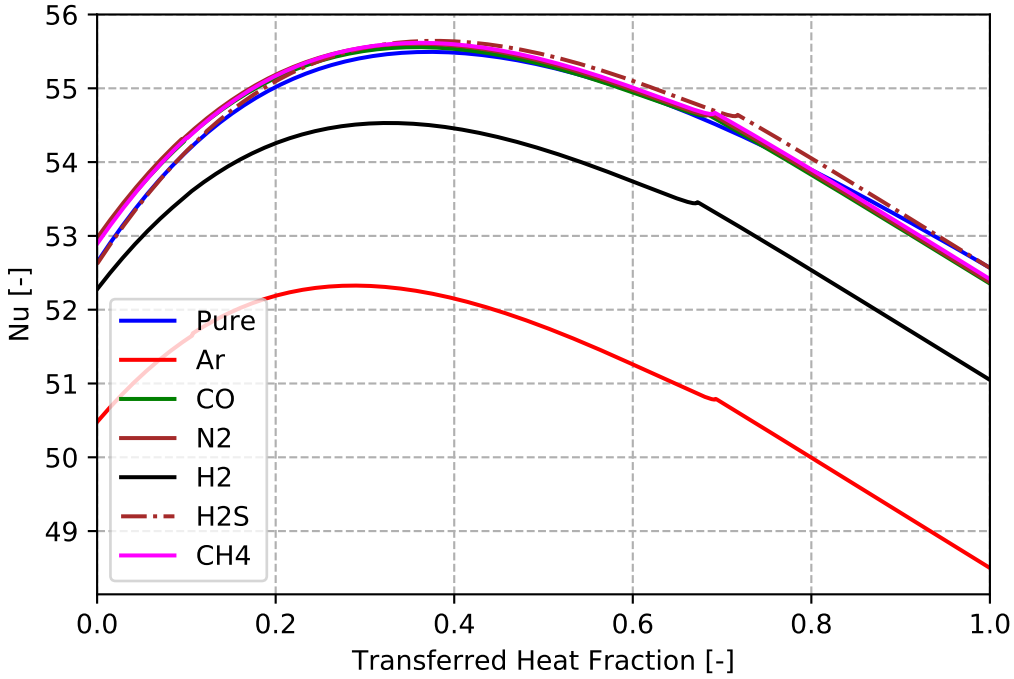

Figure 7.51: The **Nu** for cold side of **LTR**.

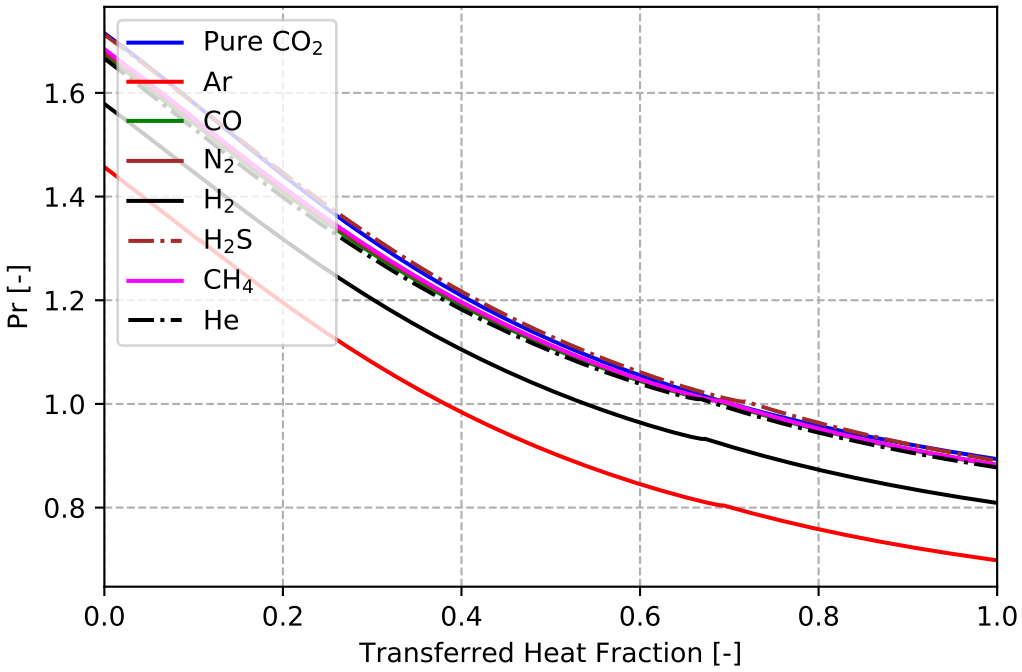

Figure 7.52: The **Pr** for cold side of **LTR**.

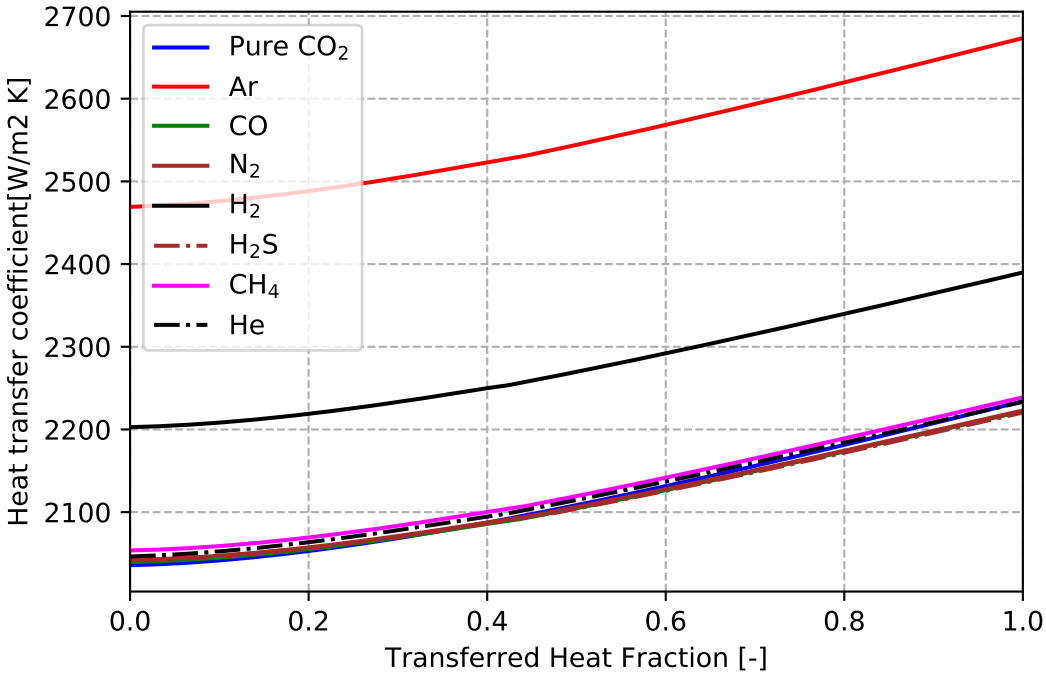

Figure 7.53: The $\boldsymbol{\alpha}$ for hot side.

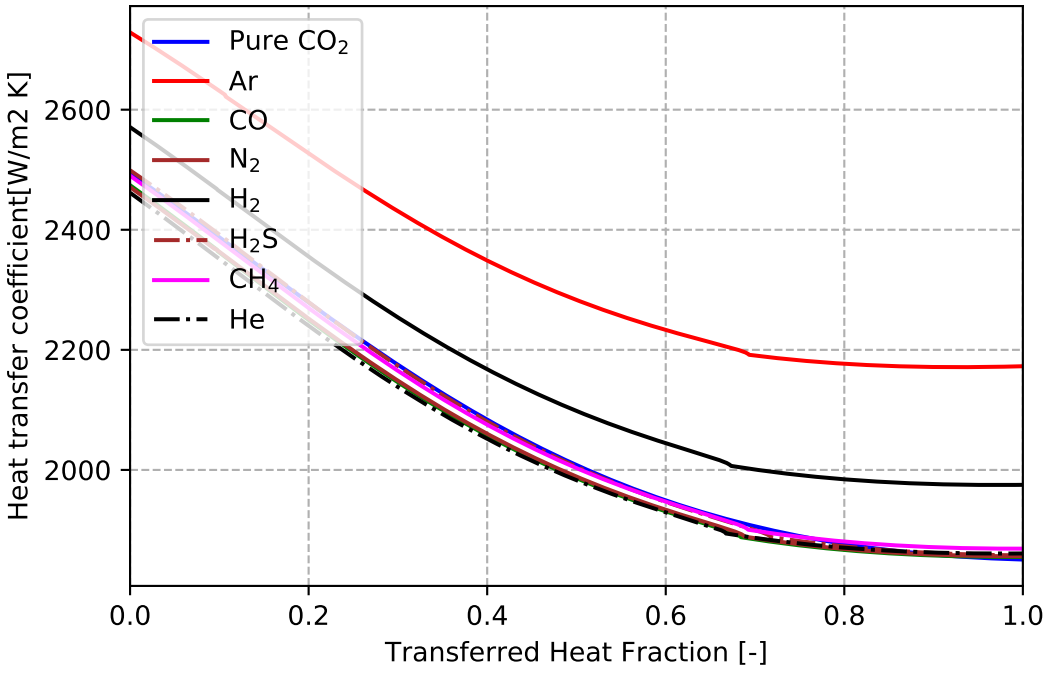

Figure 7.54: The $\boldsymbol{\alpha}$ for cold side.

However, it can not be said generally, that the effect will be the same for each heat

exchanger. The effect on the coolers, which operates with similar operating conditions has similar results. This also applies to other heat exchangers, but it is not possible to explicitly determine the effect of a mixture on the heat exchanger. The detail calculation and design of heat exchanger is necessary for each case and working medium.

7.4 Conclusion of the Effect of Mixtures on the Cycle Components

This chapter showed the effect of mixtures on the components of the S-CO_2 power cycle. The chapter was focused on the compressor, the turbine and three heat exchangers. Several conclusions can be determined from the results.

The first conclusion is for the compressor performace. We can observe very similar results as for the cycle efficiency for each investigated binary mixture. It can be seem, that the effect of the mixtures on the compressor performance for the compressor operation near the critical point has very similar profile as for the cycle efficiency. The effect of the mixtures on the turbine performance is negligibly positive.

The design of the compressor is very important for the S-CO_2 power cycle. Designing the compressor with regard to the effect of mixtures on the compressor performance is necessary. Focusing on the effect of the mixtures on the components, especially with different compressor input temperature is very important for the design of the compressor. The detailed description of the effect of the mixture on the compressor performance with regard to the compressor input temperature will be discussed in the next chapter.

The effect of mixtures on the heat exchangers is different for different type of the heat exchangers. Conclusion for the recuperative heat exchanger is the following. The substance with positive effect on the cycle efficiency has the positive effect on the $\Delta\mathbf{T}$ (increase of $\Delta\mathbf{T}$) and the substance which has the negative effect on the cycle efficiency has the negative effect on the $\Delta\mathbf{T}$ (decrease of $\Delta\mathbf{T}$) [A.2, A.6].

The results for the cooler and heater have the opposite trend. The substance with positive effect on the cycle has the negative effect on the $\Delta\mathbf{T}$ (decrease of $\Delta\mathbf{T}$) and the substance with the negative effect on the cycle has the positive effect on the $\Delta\mathbf{T}$ (increase of $\Delta\mathbf{T}$) [A.2, A.10].

The main conclusion for this chapter is that the effect of mixtures on the components is noticeable [A.2, A.7, A.8, A.10]. The effect of mixtures must be taken into account when designing the S-CO_2 power cycle. The optimization for each application of the S-CO_2 power cycle depending on the previous results is very important when designing of the S-CO_2 power cycle. The optimization of the S-CO_2 power cycle will described in next chapter.

The results of the effect of the mixtures on the compressor performance are published in paper: *Effect of Mixtures on Compressor and Cooler in Supercritical Carbon Dioxide Cycles.* [A.10] The results for recuperative heat exchangers are published in papers: *Pinch Point Analysis of Heat Exchangers for Supercritical Carbon Dioxide with Gaseous Admixtures in CCS Systems* and *Research on the Effect of the Pinch Point Shift in Cycles with Supercritical Carbon Dioxide.* [A.2, A.6] The results for coolers are published in papers: *Pinch Point Analysis of Heat Exchangers for Supercritical Carbon Dioxide with Gaseous Admixtures in CCS Systems* and *Effect of Mixtures on Compressor and Cooler in Supercritical Carbon Dioxide Cycles.* [A.2, A.10]

Chapter 8

Optimization of the Power Cycles

The optimization of a power cycle is the most important part in the design of any new system. According to Chapter 7, the effect of mixtures on the components is noticeable and the effect of mixtures must be taken into account when designing the S-CO_2 power cycle.

The important parameter of the S-CO_2 power cycle is the cycle efficiency and the $\boldsymbol{P}_{net}$, i.e. the power which will be generated from the system. The cycle efficiency and net power are connected by the Equation 6.2. The decrease or increase of the cycle efficiency and the $\boldsymbol{P}_{net}$ depends on the $\boldsymbol{P}_c$ and the $\boldsymbol{P}_{tu}$, since, the $\boldsymbol{P}_{net}$ is defined as the difference between the $\boldsymbol{P}_c$ and the $\boldsymbol{P}_{tu}$. The $\boldsymbol{P}_c$ increases for each investigated substances (negative effect on cycle) and the $\boldsymbol{P}_{tu}$ also increases (positive effect on cycle).

The optimization have to be done for each cycle layout and application. That means, for boundary conditions such as heat source, place of construction (cooling systems), operation parameters and intended use. All of the above conditions affect the resulting system performance and output power. The problem occurs when the optimization is performed for pure CO_2 and the potential effect of impurities is not taken into account.

This chapter shows the optimization of the power cycle and the effect of mixtures on the optimized cycle layout. The first part is focused on the descritpion of the effect on the S-CO_2 power cycle and the components, i.e. the $\boldsymbol{P}_c$, the $\boldsymbol{P}_{tu}$ and the $\boldsymbol{P}_{net}$. Especially, the effect on the compressor inlet temperature will be examined. The second part shows the effect of the mixtures on the optimized cycle layout. The effect of the mixtures will be shown for the binary mixtures and for hypothetical multicomponent mixtures.

8.1 Description of the Effect of Mixtures

The effect of the binary mixtures on the compressor and the turbine is shown in Figure 8.1 and Figure 8.2. [A.10] The figures are for the Re-compression cycle. In Figure 8.1 and Figure 8.2, the horizontal axis represents the percentage of CO_2 in the binary mixture.

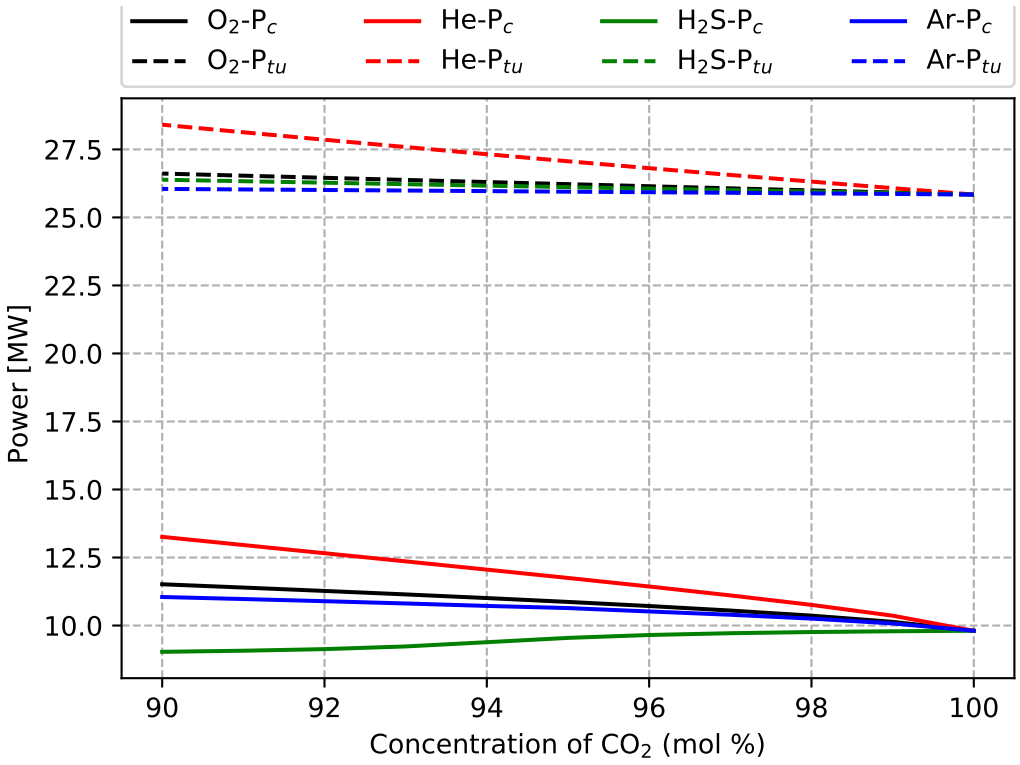

Figure 8.1: The power for the Re-compression cycle. [A.10]

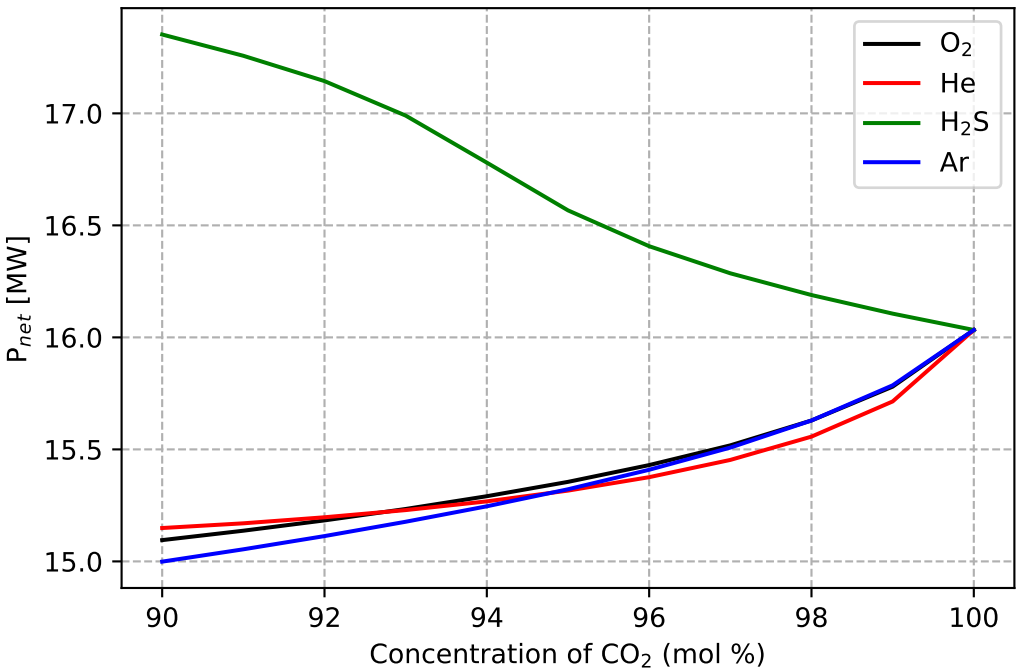

Figure 8.2: The cycle efficiency for the Re-compression cycle. [A.10]

The connection between the $\mathbf{P}_{net}$ and the $\mathbf{P}_c$ and the $\mathbf{P}_{tu}$ is clearly visible. With a decreasing purity of CO_2, the effect increases. The increase is linear for each substance with a decreasing purity of CO_2. He has a large positive effect on the $\mathbf{P}_{tu}$, however the $\mathbf{P}_{tu}$ increase cannot offset the negative effect of the $\mathbf{P}_c$ increase, so the $\mathbf{P}_{net}$ drops.

The boundary conditions for calculation are from Table 6.1 [A.7, A.8]. The optimized parameters are mass flow and **Ra**. The $\mathbf{P}_2$ is 27 MPa. The mass flow rate is 200 kg/s and the pressure ratio is 3.0.

8.2 Description of Cycle Optimization

Cycle optimization is performed to get the best possible cycle performance for the given possible boundary conditions. The parameters that are commonly optimized include mass flow rate, the heat source inlet and outlet temperatures, $\mathbf{P}_2$, **Ra** and $\mathbf{P}_c$. Taking into account the largest effect of mixtures on components of the power cycle, it is obvious that, the most important parameter for optimization is the $\mathbf{T}_1$ and the **Ra**. These parameters define the operating point of compressor and the effect on the $\mathbf{P}_c$. The effect of mixtures the $\mathbf{P}_c$ for different the **Ra** is shown in Figure 8.3 [A.8].

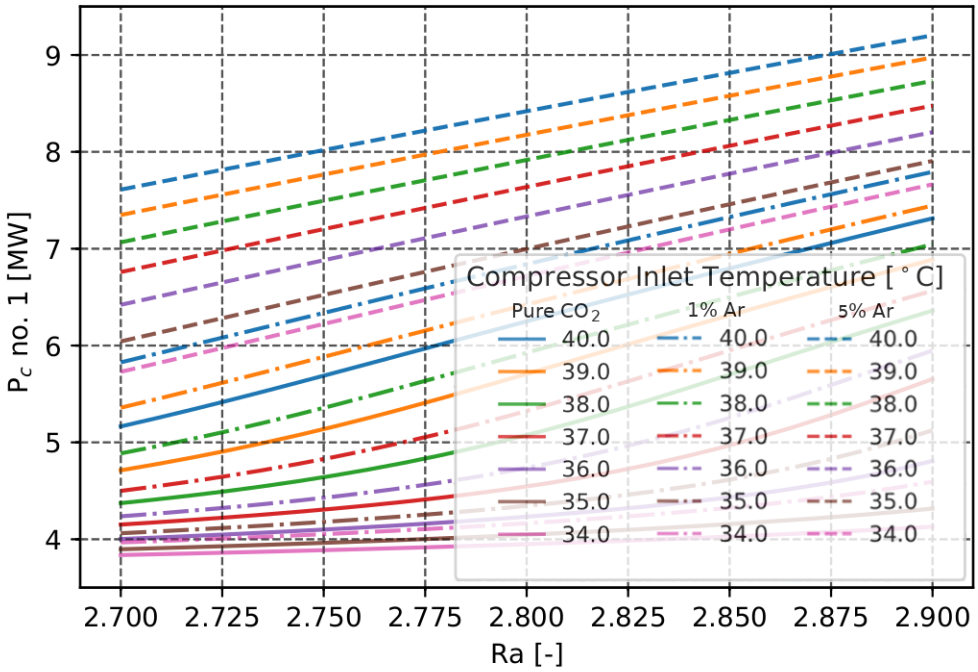

Figure 8.3: The $\mathbf{P}_c$ for the compressor no.1. [A.8]

The results are for the Re-compression cycle. The optimum **Ra** for these operating conditions is 2.8 (case with pure CO_2). However, it is obvious that for the same parameters

but with 1 % Ar, there is an increase of the $\mathbf{P}_c$. This increase is more pronounced with the addition of the second substance. In the case with 5% Ar, this increase can be twice as high than for the pure CO_2. However, it is possible to change the **Ra** and eliminate this effect. The higher the **Ra**, the higher the effect of mixtures on the $\mathbf{P}_c$. At the same time, the change of the **Ra** affects the $\mathbf{P}_{tu}$ and the $\mathbf{P}_{net}$.

The effect on the $\mathbf{P}_{net}$ is shown in Figure 8.4. The $\mathbf{P}_{net}$ decreases for each case, but for higher $\mathbf{P}_2$ the decrease is lower than for the lower $\mathbf{P}_2$. [A.8] The $\mathbf{P}_c$ affects the $\mathbf{P}_{net}$, therefore during the optimization the change of the **Ra** has an effect on both parameters. However, the **Ra** is not the only parameter which has an effect on the $\mathbf{P}_c$. Another important parameter is the compressor inlet temperature $\mathbf{T}_1$.

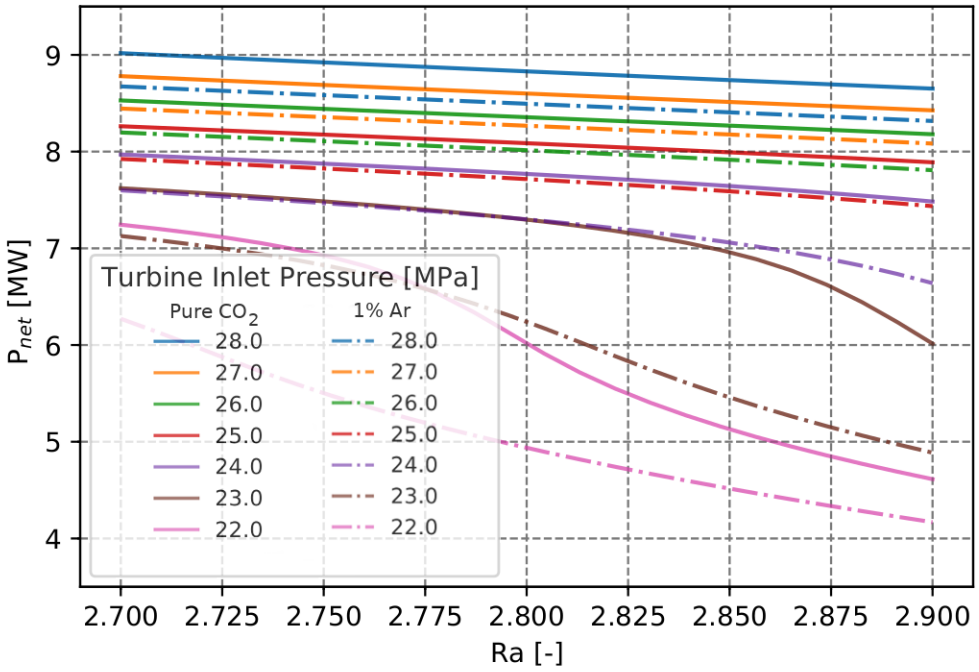

Figure 8.4: The $\mathbf{P}_{net}$ of the Re-compression cycle. [A.8]

8.2.1 Effect of Compressor Inlet Temperature

Compressor inlet temperature $\mathbf{T}_1$ is very important parameter for optimization. The $\mathbf{T}_1$ depends on the efficiency of heat transfer in a cooler and the temperature of cooling medium. The detailed description of this behavior is necessary. It is known that, the best combination of the operating conditions, equipment, working fluid and cycle layout determine the maximum achievable efficiency of a cycle. The parameters of cooling medium depends on the type of cooling systems and the ambient conditions. The usual cooling medium is water or air. [A.10] The temperature of water or air will be different for different seasons and locations. The results are very similar for both cooling media.

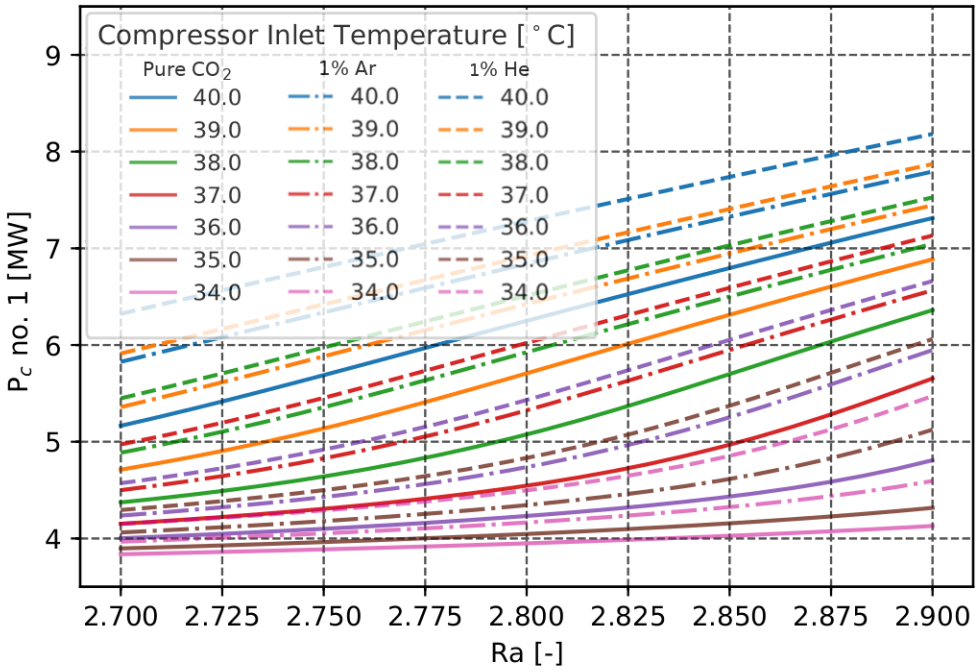

Figure 8.5: The $\mathbf{P}_c$ depends on compressor inlet temperature (compressor no.1). [A.10]

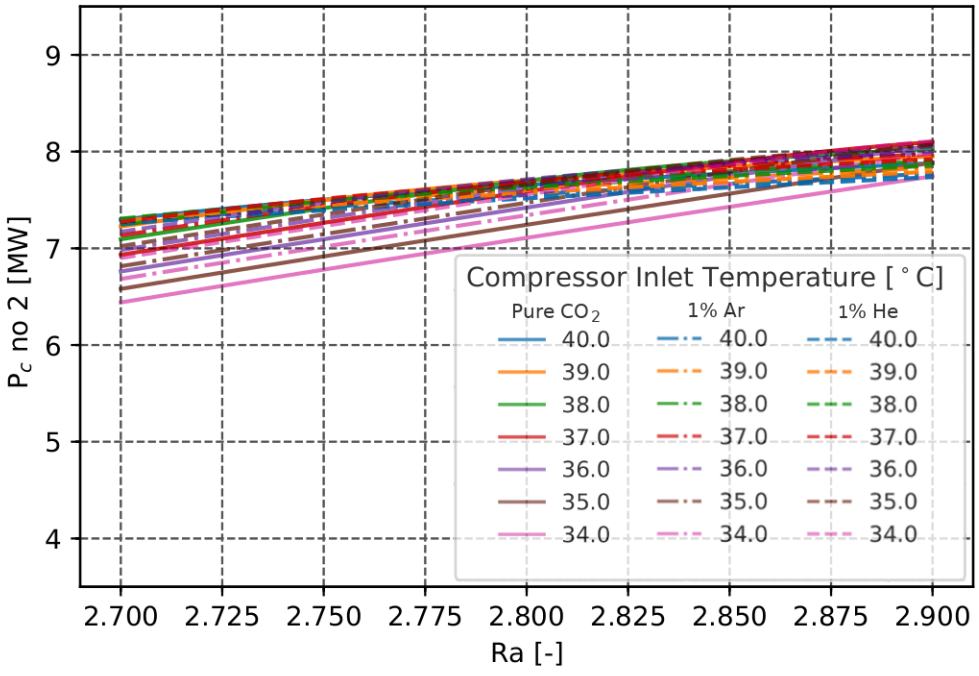

Figure 8.6: The $\mathbf{P}_c$ depends on compressor inlet temperature (compressor no.2). [A.10]

The results for the $\mathbf{P}_c$ for compressor number 1 is shown in Figure 8.5. [A.10] The results are the same as in Figure 8.3. It is possible to observe the effect of the mixtures on

the compressor operation near the critical point. This gives us the possibility to understand the influence of the change of the $\mathbf{T}_1$.

With the shift from the critical point to the supercritical region occurs, the CO_2 properties begin to stabilize. Compressors operating far from the critical point have less issues with the property change. The results for the compressor number 2 in the Re-compression cycle layout are shown in Figure 8.6. For the compressor number 2 the effect is very small. However, the $\mathbf{P}_c$ still increases for each substance. This is true for all cycle layouts and each investigated substance. [A.10]

The effect of compressor inlet temperature on cycle efficiency, $\mathbf{P}_{tu}$ and $\mathbf{P}_{net}$, is explained on the Re-compression cycle layout and on the Pre-compression cycle layout. The reference cycles have constant boundary conditions. The mass flow rate is 200 kg/s, the $\mathbf{P}_2$ is 20 MPa, **Ra** is 2.6 and the turbine inlet temperature is 550 °C. The Pre-compression cycle layout has different mass flow rate which is 130 kg/s. The mass flow rate was optimized for power from the heat source, 38 MW. [A.10] The power of the heat source is constant for each case and both cycle layouts. The compressor inlet temperature/cooler outlet temperature is in the range from 30 to 38 °C. Both cycles were optimized for the compressor inlet temperature of 34 °C. The optimization was performed for pure CO_2. The cycle efficiency for the Re-compression cycle is 42.19 % and $\mathbf{P}_{net}$ is 16.03 MW for pure CO_2. The $\mathbf{P}_c$ is 9.8 MW [A.10].

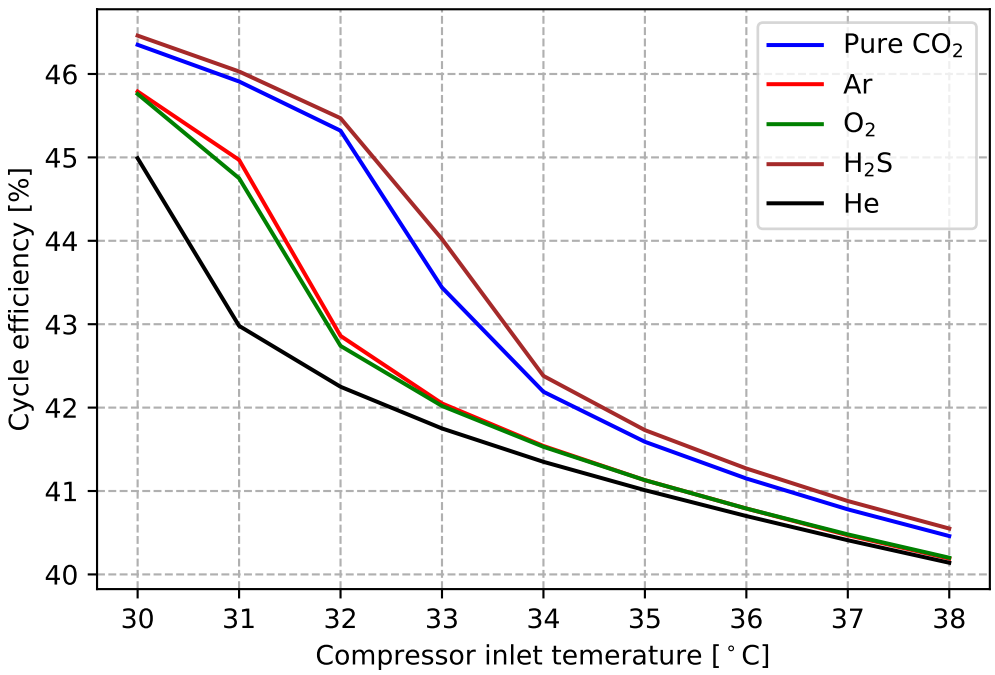

Figure 8.7: The effect on the cycle efficiency for the Re-compression cycle.

Changing the compressor inlet temperature has an effect on the cycle efficiency. This effect is shown in Figure 8.7. According to Figure 8.7, the cycle efficiency decreases with the

increase of the compressor inlet temperature. The cycle efficiency is higher for compressor inlet temperature near the critical point. This is due to change of CO_2 properties, which have an effect on compression and the $\mathbf{P}_c$, as previously described.

Figure 8.8 shown the effect on the $\mathbf{P}_c$ and the net power. [A.10] The $\mathbf{P}_c$ is the sum of all cycle compressors. The dependence between the $\mathbf{P}_c$ and the $\mathbf{P}_{net}$ is clearly visible. The simple dependence which can define the expected cycle power for different seasons and different mixtures, respectively impurities, which may occur during cycle operation, because, the effect of mixtures and the different compressor inlet temperature on the $\mathbf{P}_{tu}$ for this case is negligible. [A.10]

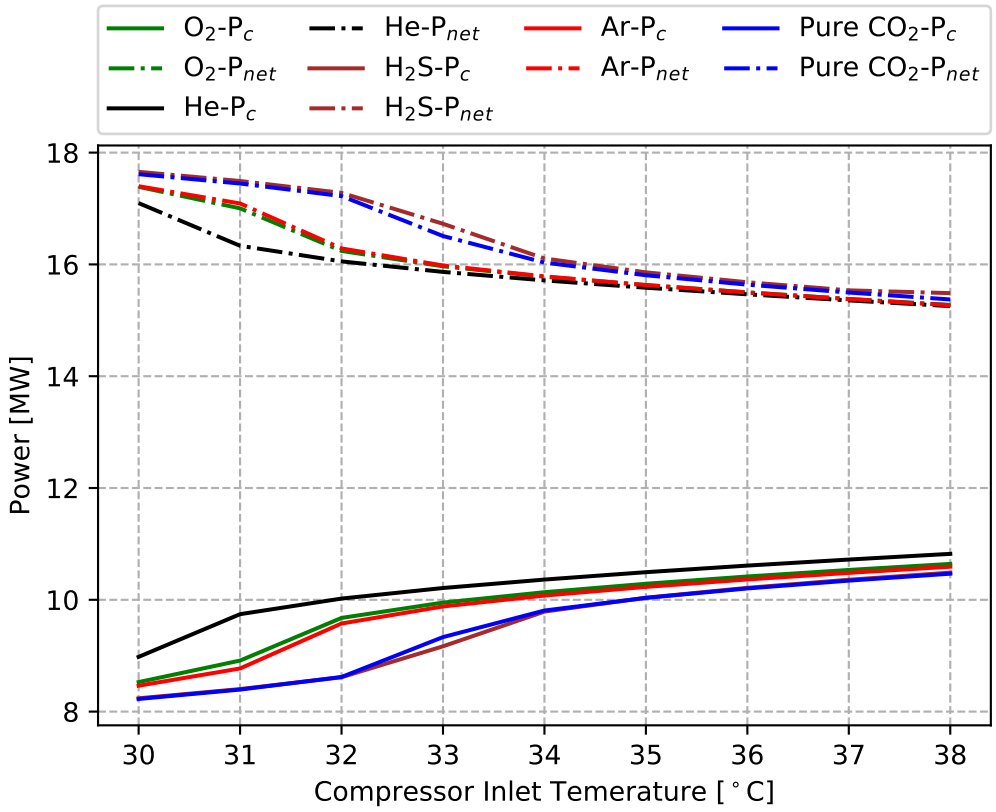

Figure 8.8: The $\mathbf{P}_c$ and $\mathbf{P}_{net}$ for the Re-compression cycle. [A.10]

The effect of mixtures on the turbine is shown in Table 8.1. [A.10] The effect on $\mathbf{P}_{tu}$ is not investigated, because input conditions for the turbine are constants. However, increase of the $\mathbf{P}_{tu}$ for different mixtures is clearly visible in Figure 8.9. [A.10]

The detailed results of the calculation are shown in Table 8.1. The results from Table 8.1 corresponds with the results shown in figures. It is clearly visible, that with increasing of the compressor inlet temperature the $\mathbf{P}_c$ increases. The $\mathbf{P}_{net}$ decreases concurrently with decreasing of the compressor inlet temperature $\mathbf{T}_1$.

According to Figure 8.8, it is seen that $\mathbf{P}_c$ decreases close to the critical point for all

cases (pure CO_2 and mixture with 99 % of CO_2), with the exception of H_2S which causes $\mathbf{P}_c$ to increase. Close to the critical point, the $\mathbf{P}_c$ may increase by up to 2 or 2.5 MW. This is a very important information for design of power cycles. [A.10]

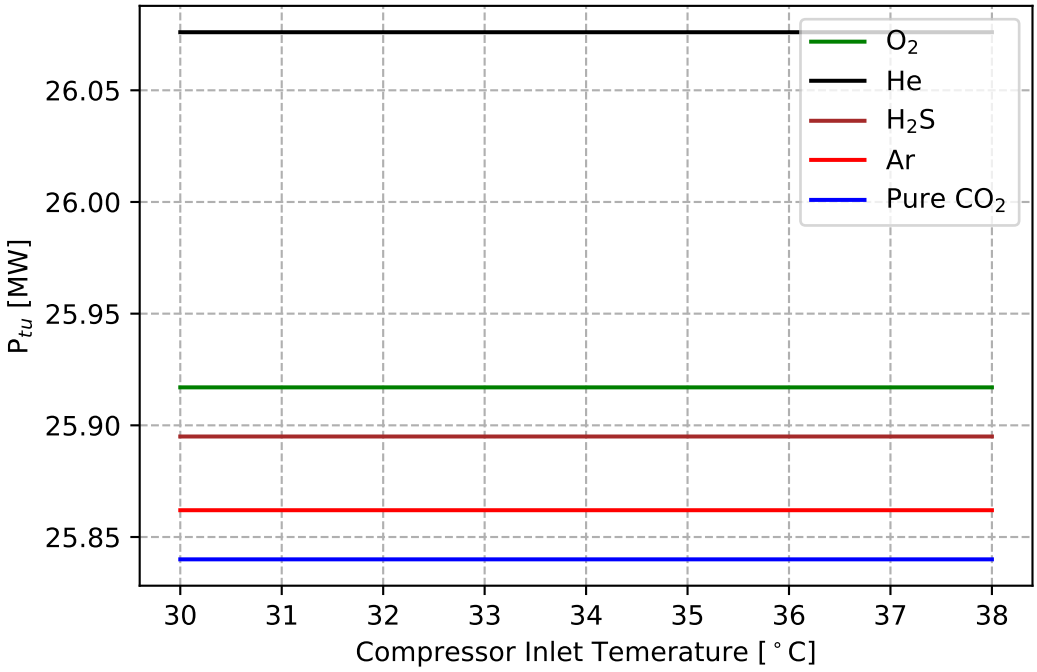

Figure 8.9: The effect on the $\mathbf{P}_{tu}$ for the Re-compression cycle. [A.10]

As can be seen from the data, the $\mathbf{P}_{tu}$ increases for all species. However, it is important to consider the net work output as those species which increase $\mathbf{P}_{tu}$ also increase compressor work input. Given this consideration, as the effects of power requirements are more detrimental to the $\mathbf{P}_{net}$, the inclusion of such species should only be considered as a means of expanding the permissible temperature limits of the S-CO_2 power cycle or as an undesirable effect of species impurity.

The same results are observed for other cycle layouts. The results for the Pre-compression cycle are shown are Figure 8.10, 8.11 and Figure 8.12. The detailed results from calculation are shown in Table 8.2. The cycle efficiency for the pre-compression is 41.67 % and $\mathbf{P}_{net}$ is 15.835 MW for pure CO_2. The $\mathbf{P}_c$ is 14.895 MW and the $\mathbf{P}_{tu}$ is 30.73 MW. [A.10]

Table 8.1: The $\mathbf{P}_c$, $\mathbf{P}_{tu}$ and $\mathbf{P}_{net}$ depending on compressor inlet temperature for the Re-compression cycle. [A.10]

Tempreratute $\mathbf{C}_1$		[°C]	**30.0**	**31.0**	**32.0**	**33.0**	**34.0**	**35.0**	**36.0**	**37.0**	**38.0**
1 % O_2	$\mathbf{P}_c$	[MW]	8.528	8.913	9.676	9.95	10.136	10.287	10.417	10.534	10.642
	$\mathbf{P}_{tu}$		25.917								
	$\mathbf{P}_{net}$		17.388	17.003	16.241	15.966	15.78	15.63	15.5	15.383	15.275
1 % He	$\mathbf{P}_c$	[MW]	8.979	9.743	10.022	10.211	10.362	10.494	10.612	10.72	10.822
	$\mathbf{P}_{tu}$		26.076								
	$\mathbf{P}_{net}$		17.097	16.333	16.054	15.866	15.714	15.583	15.465	15.356	15.254
1 % H_2S	$\mathbf{P}_c$	[MW]	8.238	8.403	8.615	9.168	9.789	10.037	10.214	10.359	10.486
	$\mathbf{P}_{tu}$		25.895								
	$\mathbf{P}_{net}$		17.656	17.492	17.28	16.727	16.106	15.858	15.681	15.536	15.486
1 % Ar	$\mathbf{P}_c$	[MW]	8.226	8.394	8.619	9.333	9.808	10.034	10.203	10.343	10.467
	$\mathbf{P}_{tu}$		25.84								
	$\mathbf{P}_{net}$		17.614	17.447	17.222	16.508	16.033	15.806	15.638	15.497	15.373
Pure CO_2	$\mathbf{P}_c$	[MW]	8.463	8.772	9.576	9.881	10.076	10.231	10.364	10.482	10.592
	$\mathbf{P}_{tu}$		25.862								
	$\mathbf{P}_{net}$		17.399	17.09	16.286	15.981	15.786	15.631	15.498	15.38	15.27

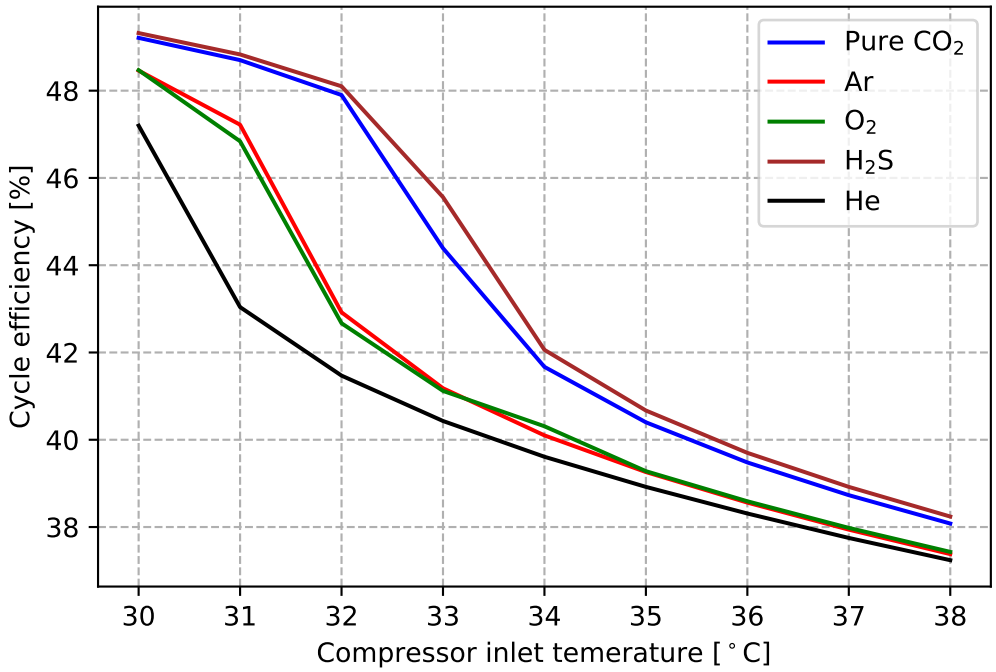

Figure 8.10: The effect on the cycle efficiency for the Pre-compression cycle.

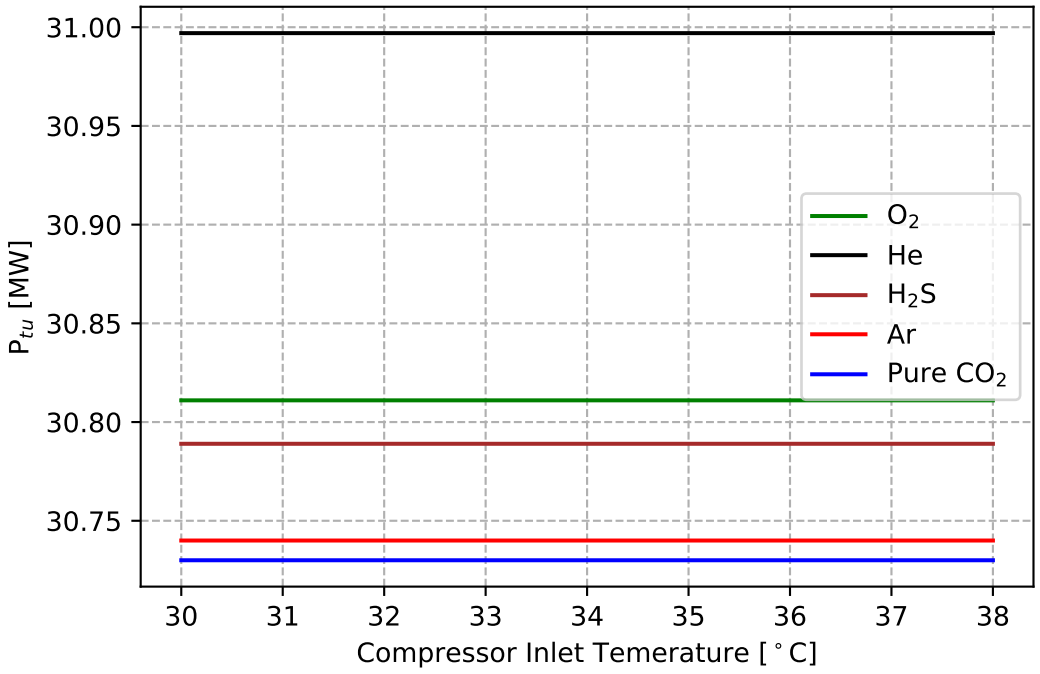

Figure 8.11: The effect on the $\mathbf{P}_{tu}$ for the Pre-compression cycle. [A.10]

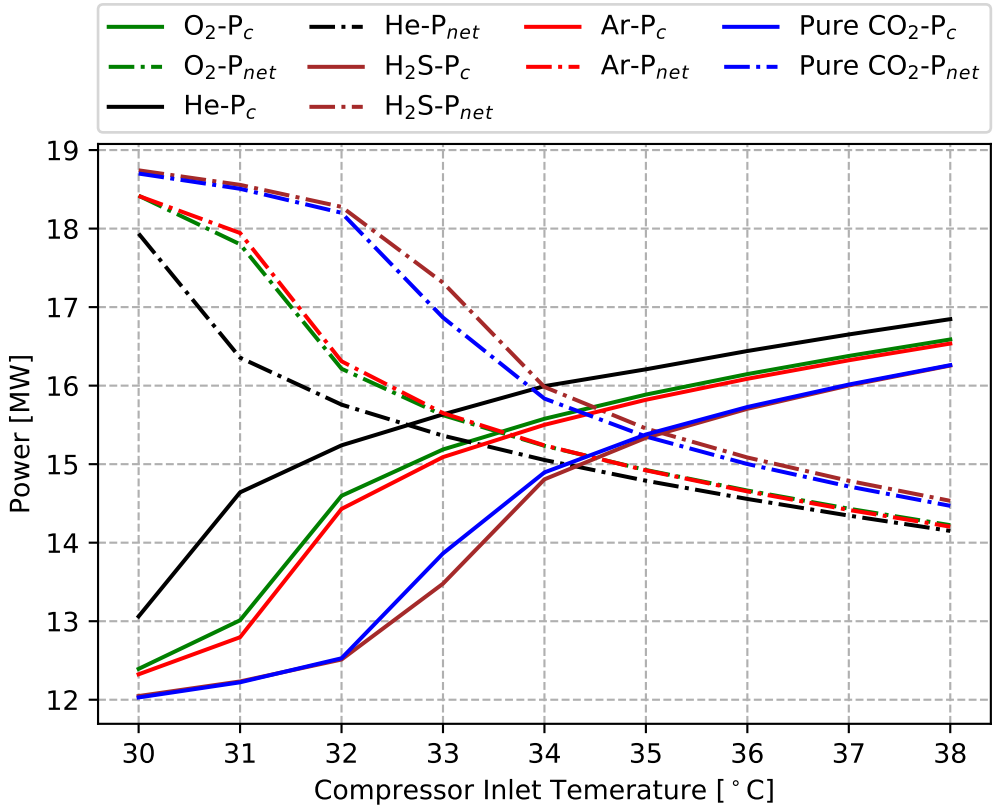

Figure 8.12: The $\mathbf{P}_c$ and $\mathbf{P}_{net}$ for the Pre-compression cycle. [A.10]

From Figure 8.12, it can be seen that between 30 °C and 33 °C there is a critical increase in the power requirements of the compressor, for temperature increases above 33 °C, this requirement becomes nearly linear. It can be argued for the Re-compression cycle that the drop in $\mathbf{P}_{net}$ is directly proportional to the increase in $\mathbf{P}_c$.

Each cycle layout has a different decrease of the $\mathbf{P}_{net}$ depending on the boundary conditions. The results for the Split expansion cycle are very similar as for the Re-compression cycle. Because, the cycle layout for both cycles is the same, only the Split expansion cycle has another turbine. Nevertheless, the effect on $\mathbf{P}_{tu}$ is very small. The design and optimization of cycle layout is important for each cycle layout, and must be done [A.7, A.8, A.10].

8.2.2 Description of the Boundary Conditions for Optimization

Optimization is a very important and necessary step in achieving acceptable operating parameters. For this reason, two cases were fully optimized for different cycle parameters. The optimized parameter is the $\mathbf{P}_{net}$ of the cycle. The cases differ in input parameters of cycle. The case no. 1 has the turbine inlet temperature 550 °C. The heat source is considered with minimum inlet temperature into heater about 600 °C. The case no. 2 has the turbine inlet temperature 400 °C and the heat source has the minimum temperature about 450 °C. It

Table 8.2: The $\mathbf{P}_c$, $\mathbf{P}_{tu}$ and $\mathbf{P}_{net}$ depending on compressor inlet temperature for the Pre-compression cycle. [A.10]

Tempreratute $\mathbf{C}_1$		[°C]	**30.0**	**31.0**	**32.0**	**33.0**	**34.0**	**35.0**	**36.0**	**37.0**	**38.0**
1 % O_2	$\mathbf{P}_c$	[MW]	12.393	13.012	14.597	15.187	15.578	15.886	16.147	16.378	16.588
	$\mathbf{P}_{tu}$		30.811								
	$\mathbf{P}_{net}$		18.419	17.8	16.215	15.624	15.234	14.926	14.664	14.433	14.223
1 % He	$\mathbf{P}_c$	[MW]	13.061	14.641	15.24	15.634	15.994	16.208	16.441	16.652	16.847
	$\mathbf{P}_{tu}$		30.997								
	$\mathbf{P}_{net}$		17.936	16.356	15.758	15.363	15.053	14.789	14.557	14.345	14.15
1 % H_2S	$\mathbf{P}_c$	[MW]	12.047	12.233	12.512	13.478	14.807	15.336	15.705	16.002	16.256
	$\mathbf{P}_{tu}$		30.789								
	$\mathbf{P}_{net}$		18.742	18.557	18.277	17.311	15.983	15.454	15.085	14.788	14.533
1 % Ar	$\mathbf{P}_c$	[MW]	12.029	12.222	12.528	13.863	14.895	15.378	15.728	16.014	16.261
	$\mathbf{P}_{tu}$		30.73								
	$\mathbf{P}_{net}$		18.701	18.507	18.201	16.867	15.835	15.352	15.002	14.716	14.469
Pure CO_2	$\mathbf{P}_c$	[MW]	12.324	12.796	14.43	15.09	15.501	15.82	16.087	16.323	16.536
	$\mathbf{P}_{tu}$		30.74								
	$\mathbf{P}_{net}$		18.416	17.944	16.31	15.65	15.239	14.921	14.653	14.417	14.204

is considered lower temperature source for example for waste heat recovery. The parameters for case no. 1 are shown in Table 8.3 [A.8].

Table 8.3: Input parameters for optimization and for turbine inlet temperature 550 °C. [A.8]

Pressure Ratio	**Ra**	2.8	[-]
Pressure	$\mathbf{P_2}$	24	[MPa]
Compressor inlet temperature	$\mathbf{T_1}$	34	°C
Turbine inlet temperature	$\mathbf{T_4}$	550	
Turbine efficiency	$\boldsymbol{\eta_{tu}}$	0.79	[-]
Compressor efficiency	$\boldsymbol{\eta_c}$	0.68	
Recuperator effectiveness	$\boldsymbol{\eta_{reg}}$	0.9	
Mass flow	$\boldsymbol{\dot{m}}$	200	[kg/s]

The parameters for the case no. 2 are shown in Table 8.4. [A.8] The compressor pressure ratio and the turbine inlet pressure were selected, for both cases independently.

Table 8.4: Input parameters for optimization and for turbine inlet temperature 400 °C. [A.8]

Pressure Ratio	**Ra**	2.6	[-]
Pressure	$\mathbf{P_2}$	24	MPa
Compressor inlet temperature	$\mathbf{T_1}$	34	°C
Turbine inlet temperature	$\mathbf{T_4}$	400	
Turbine efficiency	$\boldsymbol{\eta_{tu}}$	0.79	[-]
Compressor efficiency	$\boldsymbol{\eta_c}$	0.68	
Recuperator effectiveness	$\boldsymbol{\eta_{reg}}$	0.9	
Mass flow	$\boldsymbol{\dot{m}}$	200	[kg/s]

8.3 Results of Optimization

The calculation was performed for three cycle layouts, the Re-compression cycle, the Pre-compression cycle and the Split expansion cycle. The comparison of results from calculation are shown for binary mixtures (Chapter 3.2) and for multicomponent mixtures (Table 3.2).

8.3.1 Binary Mixtures

The results for case no.1 and for the Re-compression cycle are shown in Table 8.5. The results are for 95 % pure CO_2. The dramatic decrease of net power and the cycle efficiency is obvious. This corresponds to the previous results. However, the results are for very low purity of CO_2. The 5 % fraction of the second substance has a dramatic effect on the cycle, because each reduction of purity by 1 %, has approximately the same effect. This means that the effect on the cycle is directly proportional to the reduction of CO_2 purity. For this reason, it is possible to observe very small effect on the S-CO_2 power cycle for 99 % pure CO_2. The results for case no.1 and 99 % pure CO_2 are shown in Table 8.7. The results for case no.2 and 99 % pure CO_2 are shown in Table 8.6.

Table 8.5: The results for the case no. 1 and 0.05 mole fraction of second substance. [A.8]

		Pure CO_2	**He**	**Ar**	**H_2S**
$\boldsymbol{\eta}$	[%]	32.45	25.25	27.69	32.65
$\mathbf{P}_{tu}$	[MW]	23.56	24.67	23.65	23.8
$\mathbf{P}_c$ no.1		3.94	8.7	6.71	3.99
$\mathbf{P}_c$ no.2		7.1	7.31	7.48	7.0
$\mathbf{P}_c$ total		11.05	16.02	14.2	11.0
$\mathbf{P}_{net}$		12.5	8.65	9.45	12.8

Table 8.6: The results for the case no. 2 and 0.01 mole fraction of second substance. [A.8]

		Pure CO_2	**He**	**Ar**	**H_2S**
$\boldsymbol{\eta}$	[%]	25.76	24.84	25.27	25.8
$\mathbf{P}_{tu}$	[MW]	17.31	17.49	17.34	17.35
$\mathbf{P}_c$ no.1		3.74	3.923	3.81	3.76
$\mathbf{P}_c$ no.2		5.38	5.91	5.67	5.35
$\mathbf{P}_c$ total		9.12	9.83	9.48	9.11
$\mathbf{P}_{net}$		8.18	7.65	7.86	8.23

The results are for the binary mixtures. It is obvious, that He has the negative effect and the positive effect have H_2S, Xe and SO_2. The decrease of the cycle efficiency is in the range of about 1 % and $\mathbf{P}_{net}$ is in the range about 1 MW for both cases. The $\mathbf{P}_{tu}$ is quite similar for both mixtures as for pure CO_2. The $\mathbf{P}_c$ increases, which can be especially seen on the compressor no. 1. Each cycles layout show the same dependence of the effect of the binary mixtures as the cycles in Table 8.7. [A.8]

Table 8.7: The results for Binary mixture - 0.01 mole fraction of second substance. [A.8]

Re-compression c.		**Pure CO_2**	**He**	**Ar**	**CO**	**N_2**	**O_2**	**CH_4**	**H_2S**	**H_2**
$\boldsymbol{\eta}$	[%]	32.45	**31.39**	31.98	31.8	31.83	31.9	32.06	**32.49**	31.72
$\mathbf{P}_{tu}$	[MW]	23.56	23.77	23.58	23.65	23.65	23.63	23.72	23.61	23.79
$\mathbf{P}_c$ no.1	[MW]	3.94	4.49	4.16	4.27	4.26	4.2	4.16	3.96	4.34
$\mathbf{P}_c$ no.2	[MW]	7.1	7.55	7.34	7.4	7.37	7.37	7.31	7.08	7.45
$\mathbf{P}_c$	[MW]	11.05	12.05	11.5	11.67	11.63	11.58	11.47	11.05	11.8
$\mathbf{P}_{net}$	[MW]	12.5	11.72	12.07	11.98	12.01	12.04	12.24	12.56	11.99

Pre-compression c.		**Pure CO_2**	**He**	**Ar**	**CO**	**N_2**	**O_2**	**CH_4**	**H_2S**	**H_2**
$\boldsymbol{\eta}$	[%]	29.45	**28.12**	28.85	28.66	28.69	28.78	29.02	**29.48**	28.57
$\mathbf{P}_{tu}$	[MW]	42.72	43.09	42.73	42.88	42.87	42.84	43.03	42.8	43.13
$\mathbf{P}_c$ no.1	[MW]	6.32	7.12	6.65	6.8	6.78	6.71	6.64	6.33	6.9
$\mathbf{P}_c$ no.2	[MW]	19.8	20.85	20.22	20.4	20.38	20.31	20.24	19.82	20.59
$\mathbf{P}_c$	[MW]	26.12	27.97	26.88	27.2	27.16	27.02	26.89	26.15	27.5
$\mathbf{P}_{net}$	[MW]	16.6	15.12	15.85	15.67	15.71	15.81	16.13	16.64	15.63

Split expansion c.		**Pure CO_2**	**He**	**Ar**	**CO**	**N_2**	**O_2**	**CH_4**	**H_2S**	**H_2**
$\boldsymbol{\eta}$	[%]	29.03	**28.1**	28.62	28.46	28.48	28.55	28.7	**29.06**	28.4
$\mathbf{P}_{tu}$ no.1	[MW]	7.45	7.52	7.46	7.48	7.48	7.48	7.51	7.47	7.53
$\mathbf{P}_{tu}$ no.2	[MW]	14.98	15.25	15.06	15.13	15.12	15.11	15.14	15.01	15.22
$\mathbf{P}_{tu}$	[MW]	22.44	22.78	22.52	22.62	22.61	22.58	22.65	22.48	22.76
$\mathbf{P}_c$ no.1	[MW]	3.97	4.53	4.19	4.31	4.29	4.24	4.19	3.99	4.38
$\mathbf{P}_c$ no.2	[MW]	7.27	7.69	7.49	7.55	7.52	7.52	7.46	7.25	7.6
$\mathbf{P}_c$	[MW]	11.25	12.23	11.69	11.85	11.82	11.76	11.66	11.24	11.98
$\mathbf{P}_{net}$	[MW]	11.18	10.55	10.83	10.76	10.78	10.81	10.98	11.23	10.77

8.3.2 Multicomponent Mixtures

The results from the previously section are for the binary mixtures. Effect of the binary mixture is very interesting, but the real cycle will never use binary mixture. It will have multicomponent mixtures. Hence, the effect of multicomponent mixtures is more important for calculation of the power cycle. Due to the large amount of multicomponent mixtures, the research is focused on some typical mixtures, which may exist in the industrial applications. The considered multicompnet mixtures are shown in Table 3.2. [A.7]

The first multicomponent mixture is Air. The mixture is considered due to the possible occurrence in the system as an impurity. The second (M-I) and third (M-II) multicomponent mixture is a mixture which is derived from the recommended composition of mixtures for the transport of CO_2. [35] This composition corresponds to the composition which is usually used for transport in liquid phase (M-I) and in gas phase (M-II). Because purity of CO_2 for transport in gas phase is lower than for transport in liquid phase, mixture M-II is suitable for description of how much the effect of a mixture will be increased with increasing the amount of substances. [A.7]

The last multicomponent mixtures are mixtures which are modification of the previous mixtures. The first mixture consists of He and H_2S. He has the biggest negative effect on the cycle efficiency and H_2S has the biggest positive effect. The idea is, that H_2S may eliminate the negative effect of He. Another mixture with H_2S is mixture of Air-H and the last mixture is M-IH. [A.7] The mixture Air-H used H_2S for elimination of the negative effect of the substances. The mixture H-IM show the effect without H_2S compared with mixture H-I. Table 8.8 shows the results for the multicomponent mixtures.

The optimization was performed for multicomponent mixture and for input parameters from Table 8.3. The Re-compression, the Split expansion and the Pre-compression cycles were considered for the comparison [A.7].

The highest decrease of the $\mathbf{P}_{net}$ and the cycle efficiency is for mixture M-II. In the case with mixtures M-I a minimum effect on the S-CO_2 power cycle is observed. These results are similar for each investigated S-CO_2 power cycle. It is evident that the effect on the S-CO_2 power cycle will be insignificant if the purity of CO_2 is about 99 %. The mixture with lower than 99 % of CO_2 has a higher effect on the S-CO_2 power cycle as can be seen in the case of M-II. With the increase of the amount of each substance the effect of the substance increases. The minimum effect is observed in the case with CO_2 purity above 99.5 % [A.7].

The mixture M-IH has slightly negative effect, which is similar to M-I without H_2S. The effect of each substance is insignificant. The decrease of the $\mathbf{P}_{net}$ and the cycle efficiency for mixture Air is about 0.5 % and 0.5 MW. However, if other substance which has the positive effect as H_2S would be used, the decrease would be smaller. This effect is shown for Mixture Air and Air-H. The mixture Air with H_2S has smaller negative effect than the mixture Air. The mixture M-H has similar result. From the previous results (Chapter 8.3.1), it is obvious

that $\mathbf{P}_{net}$ for the binary mixture CO_2-He is 11.72 MW for the re-compression cycle. However, the $\mathbf{P}_{net}$ for mixture M-H is 12.245 MW. The difference in the $\mathbf{P}_{net}$ is 0.525 MW. When H_2S is added to the mixtures in a proper fraction it can observed the possible positive effect on the cycle efficiency.

Table 8.8: The results for multicomponent mixture. [A.7]

Re-compression c.		**Pure CO_2**	**Air**	**M-I**	**M-II**	**M-H**	**Air-H**	**M-IH**
$\boldsymbol{\eta}$	[%]	32.45	31.84	**32.31**	**29.74**	32.09	31.91	32.31
$\mathbf{P}_{tu}$	[MW]	23.56	23.65	23.59	23.96	23.72	23.7	23.59
$\mathbf{P}_c$ no.1		3.94	4.25	4.01	5.51	4.15	4.24	4.02
$\mathbf{P}_c$ no.2		7.11	7.38	7.19	7.68	7.32	7.36	7.19
$\mathbf{P}_c$		11.06	11.62	11.2	13.19	11.47	11.6	11.2
$\mathbf{P}_{net}$		12.5	12.02	12.389	10.74	12.25	12.1	12.388
Pre-compression c.		**Pure CO_2**	**Air**	**M-I**	**M-II**	**M-H**	**Air-H**	**M-IH**
$\boldsymbol{\eta}$	[%]	29.45	28.71	**29.29**	**25.83**	29	28.77	29.28
$\mathbf{P}_{tu}$	[MW]	42.73	42.87	42.78	43.343	42.99	42.95	42.78
$\mathbf{P}_c$ no.1		6.33	6.77	6.43	8.42	6.62	6.75	6.43
$\mathbf{P}_c$ no.2		19.8	20.37	19.94	22.08	20.26	20.37	19.94
$\mathbf{P}_c$		26.13	27.13	26.37	30.51	26.88	27.13	26.37
$\mathbf{P}_{net}$		16.6	15.74	16.409	12.84	16.11	15.82	16.408
Split expansion c.		**Pure CO_2**	**Air**	**M-I**	**M-II**	**M-H**	**Air-H**	**M-IH**
$\boldsymbol{\eta}$	[%]	29.03	28.5	**28.91**	**26.62**	28.72	28.55	28.91
$\mathbf{P}_{tu}$ no.1	[MW]	7.46	7.49	7.47	7.57	7.51	7.5	7.47
$\mathbf{P}_{tu}$ no.2		14.99	15.12	15.03	15.48	15.14	15.14	15.03
$\mathbf{P}_{tu}$		22.44	22.61	22.49	23.06	22.64	22.65	22.49
$\mathbf{P}_c$ no.1		3.98	4.28	4.05	5.55	4.19	4.28	4.05
$\mathbf{P}_c$ no.2		7.28	7.52	7.35	7.79	7.48	7.51	7.35
$\mathbf{P}_c$		11.25	11.81	11.39	13.34	11.66	11.79	11.39
$\mathbf{P}_{net}$		11.19	10.79	11.096	9.71	10.98	10.86	11.095

The effects of multicomponent mixtures on the compressor and the turbine are similar as for the binary mixture. The $\mathbf{P}_{tu}$ is quite similar for both mixtures as for pure CO_2. The $\mathbf{P}_c$ increases, which can be especially seen for the compressor no. 1.

8.4 Conclusion of the Optimization of the Power Cycles

This chapter showed the effect of mixtures on the optimized cycle layout. The first part was focused on the descritpion of the effect of the mixtures on the S-CO_2 power cycle and its components, with special attention to the compressor inlet temperature. The second part showed the effect of mixtures on the optimized cycle layout. Several conclusions can be determined from the results in the chapter.

The first conclusion is for the compressor. The effect of the mixtures on the compressor has the biggest effect on the cycle design. [A.7, A.8] The pressure ratio, the compressor inlet pressure and the compressor inlet temperature have a great impact on the $\mathbf{P}_c$ and thus on the $\mathbf{P}_{net}$, see Table 8.7. This may affect the already designed cycle when changing the condition of the cooling medium. For this reason, the design of the cooling systems is very important and must be taken into account when designing the S-CO_2 power cycles [A.10]. The optimum amount of the second substance is up to 1 %. [A.8] For this amount the negative effect of binary mixture is small.

Other conclusions are similarly as in previous chapters. He has the biggest negative effect of mixtures on the cycle and the positive effect have H_2S, Xe and SO_2. [A.8] This applies to binary mixtures. In case of the multicomponent mixtures, the effect depending on the composition of the mixtures. [A.7] The optimization of the cycle for the multicomponent mixtures is necessary and the detailed research is important.

The results are published in papers: *Effect of Gaseous Admixtures on Cycles with Supercritical Carbon Dioxide*, [A.7] *Effect of Multicomponent Mixtures on Cycles with Supercritical Carbon Dioxide* [A.8] and *Effect of Mixtures on Compressor and Cooler in Supercritical Carbon Dioxide Cycles.* [A.10]

Chapter 9

Techno-Economic Evaluation

The last part of the research is the techno-economic evaluation. The information and conclusions of this chapter are important for the global understanding of the effect of mixtures on the S-CO_2 power cycle. This chapter focuses on the techno-economic evaluation of a hypothetical power plant with S-CO_2 power cycle. Two cases are considered for techno-economic evaluation. The difference between these cases is in the heat source and the associated heat exchanger (PCHE and shell and tube heat exchanger). The results of this chapter will describe the effect of mixtures from the techno-economic point of view.

9.1 Description of Calculation of the Techno-Economic Evaluation

The cost estimation is performed for three indicators, which are important for the economic viability and the rate of return of the project: the levelized cost of electricity **(LCOE)** for the energy to be generated, the internal rate of return **(IRR)** to be offered by the project and the net present value **(NPV)** expected to be realized by investors. [3, 68]

The Levelized cost of electricity is calculated according to Equation 9.1. Where, **PC** is project cost, $\mathbf{PV}_{dts}$ is **PV** depreciation tax shield, $\mathbf{PV}_{lop}$ is **PV** lifetime operating costs, $\mathbf{PV}_{sc}$ is **PV** salvage costs and **LEP** is lifetime electric production. [3]

$$LCOE = (\frac{PC - PV_{dts} + PV_{loc} - PV_{sc}}{LEP}) \tag{9.1}$$

The net present value is calculated according to Equation 9.2, where **r** is the discount rate. The **FCF** is free cash flow and the $\mathbf{FCF}_0$ is the initial project cost. This value must be deducted, because money is spent for building the system. Other $\mathbf{FCF}_n$ is the free cash

flow for the relevant year. The internal rate of return is calculated with a similar equation, but it has to equal to zero. The **IRR** is calculated according to Equation 9.3. The difference between Equation 9.2 and 9.3 is that **IRR** is used instead of **r**. [3]

$$NPV = -FCF_0 + \left[\frac{FCF_1}{(1+r)}\right] + \left[\frac{FCF_2}{(1+r)^2}\right] + ... + \left[\frac{FCF_n}{(1+r)^n}\right] \tag{9.2}$$

$$0 = -FCF_0 + \left[\frac{FCF_1}{(1+IRR)}\right] + \left[\frac{FCF_2}{(1+IRR)^2}\right] + ... + \left[\frac{FCF_n}{(1+IRR)^n}\right] \tag{9.3}$$

9.1.1 Boundary Parameters for Evaluation

The techno-economic evaluation of a hypothetical power plant with the S-CO_2 power cycle is focused on two cases. Both cases are the in-direct S-CO_2 power cycle. The first case is the re-compression cycle with He/CO_2 PCHE heat exchanger as the heater. This is a hypothetical system with helium as a working medium, for example a GFR. The second case is the same cycle layout, but the heat source is a gas turbine. This is a hypothetical system for waste heat recovery systems. The design of heater is a shell and tube heat exchanger. The T-s diagram of the re-compression cycle for case no.1 is shown in Figure 9.1, for case no.2 in Figure 9.2.

The T-s diagrams, in Figure 9.1 and Figure 9.2 are for pure CO_2. The techno-economic evaluation is focused on three different substances: He, Ar and H_2S. From the previous chapters it is know that He has the largest negative effect of the investigated substances, while H_2S, SO_2 and Xe have a positive effect. Ar is considered as the impurities which will occur every time in the working medium. [A.7, A.8, A.10]

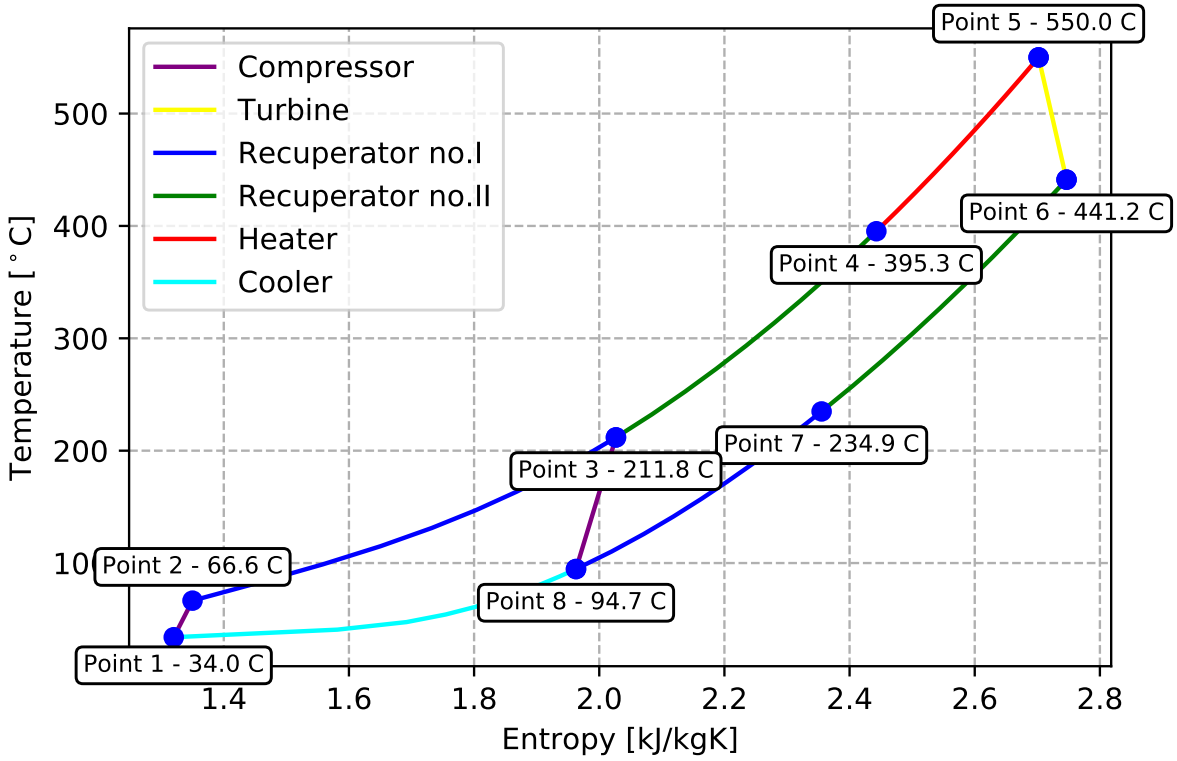

Figure 9.1: T-s diagram of the re-compression cycle with helium heater.

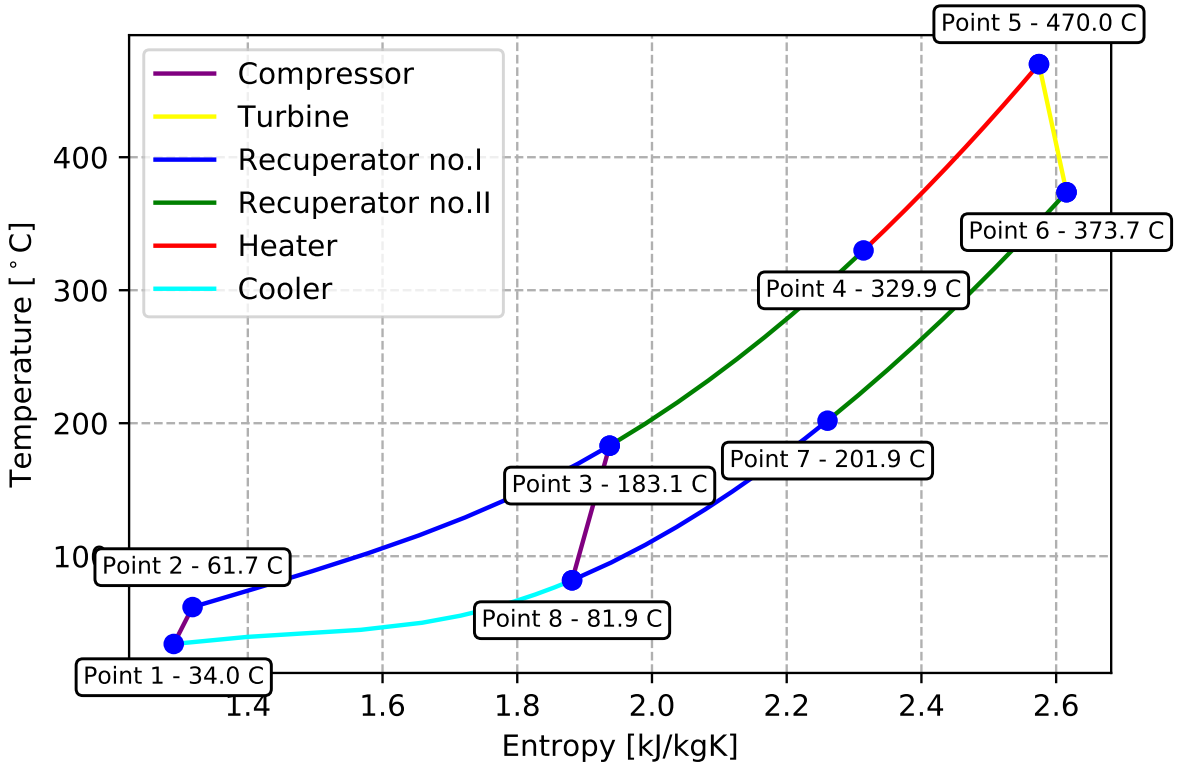

Figure 9.2: T-s diagram of the re-compression cycle with heater for WHR.

The techno-economic evaluation is calculated according to the equations defined in chapter 9.1. The important information for the analysis are the boundary conditions. The boundary conditions are shown in Table 9.1 and their values were taken from available literature. [3, 58, 69] The discount rate is 2 %, the plant utilization factor is 85 % per year and the plant lifetime is considered 20 years. The price of electricity was taken from the tariff.

Table 9.1: Boundary conditions - assumptions for cost model.

Discount Rate	2	**[%/year]**
Tax Rate	35	**[%]**
Deprecition Period	10	**[years]**
Plant Lifetime	20	**[years]**
Plant Utilization Factor	85	**[%]**
Price of Electircity	1.52	**[Kč/kWh]**
	0.07	**[$/kWh]**

Another information for analysis are the components cost, which are used to define the project capital cost. The prices are taken from the previous research, due to the small number of component manufacturers for the S-CO_2 power cycle [3, 58]. The price of the components is shown in Table 9.2.

Table 9.2: The component costs - estimate. [3]

Recuperative heat exchanger (PCHE)	2500	**[$/(kWth/K)]**
Heater (PCHE)	3000	
Cooler (PCHE)	1700	
Heater (Shell and Tube)	5000	
Turbomachinery	1000	**[$/kWe]**

The design of each heat exchanger is PCHE, except for the heater for waste heat recovery system. The different price of PCHE is determined by the choice of materials for the particular type. Different materials are considered for heater, recuperative heat exchanger and cooler. The price of shell and tube heat exchanger used for WHR systems is 5000 $/(kWth/K). The price of turbomachinery is 1000 $/kWe. Other necessary components are included in the price of turbomachinery. These components include, the generator, the gearbox, piping for connections, I&C and other components which are necessary for the turbomachinery.

9.2 Project Capital Cost

The first part of the techno-economic evaluation defines the capital cost of the system. The price of the individual components is required to determine the total cost. According to Figure 9.1 and Figure 9.2, it is obvious that the re-compression cycle has four heat exchangers and a turbomachinery (turbine and compressor) [A.7, A.8].

The calculation of the project capital cost was performed for parameters from Table 9.1 and for parameters from optimization of the re-compression cycle. The cycle efficiency, the turbine and the compressor power are shown in Table 9.3. The total price of components and the total capital cost are also shown in Table 9.3. The price of construction is set to 25 % of the total cost of all components. The data obtained from oral consultation with EGP (Energoprojekt Praha).

According to the results from Table 9.3, it is evident, that the total capital cost for the case with pure CO_2 is 21.65 M$. The capital cost for mixture with 1 % of H_2S is 21.71 M$ which is higher than the total capital cost for pure CO_2. The cost increase is 58,000 $. The total capital cost for the case with 1 % of He is 20.64 M$, which is a decrease of 1.01 M$. This is a very interesting result, since the mixture which has the negative effect on the cycle, reduces its cost. However, it is necessary to look on the specific cost as well. For this parameter a different results are observed. The cost of pure CO_2 is 1823 $/kWe, for 1 % of H_2S the cost is 1820 $/kWe (0,15 % saving) and for 1 % of He the cost is 1853 $/kWe.

The same results can be observed for the second case (WHR). The results are shown in Table 9.4. The results are for 1 % of the second substance. The total capital cost for the second case with pure CO_2 is 18.94 M$. The capital cost for mixture with 1 % of H_2S is 19.15 M$. The capital cost for 1 % of H_2S is higher than the total capital cost for pure CO_2. The cost increase is 206,000 $. The total capital cost for the case with 1 % of He is 18.38 M$, which is a decrease of 0.56 M$. The specific cost for this parameter is for of pure CO_2 1943 $/kWe, for 1 % of H_2S the cost is 1954 $/kWe and for 1 % of He the cost is 1985 $/kWe.

Table 9.3: The re-compression cycle with helium heater. (99 % purity of CO_2)

Cycle parameters					
Working medium	**Pure CO_2**	**1 % Ar**	**1 % H_2S**	**1 % He**	
$\boldsymbol{\eta}$	**32.45**	**31.98**	**32.49**	**31.39**	[%]
$\mathbf{P}_{tu}$	23.56	23.58	23.61	23.776	[MW]
$\mathbf{P}_c$ no.1	3.949	4.165	3.961	4.497	
$\mathbf{P}_c$ no.2	7.109	7.342	7.089	7.555	
$\mathbf{P}_c$	11.058	11.507	11.05	12.052	
$\mathbf{P}_{net}$	12.502	12.073	12.56	11.723	
Ra	2.8				[-]
$\mathbf{P}_2$	24.0				[MPa]
$\mathbf{P}_1$	8.571				
Mass flow	200				[kg/s]
Heat exchangers					
Recuperator no.1	519	504	522	504	[kW/K]
Recuperator no.2	616	623	615	642	
Cooler	934	886	933	817	
Heater	340	358	336	374	
Cost of HEX					
Recuperator no.1	1,298	1,26	1,305	1,26	[T$]
Recuperator no.2	1,54	1,558	1,538	1,605	
Cooler	1,588	1,506	1,586	1,389	
Heater	1,02	1,074	1,008	1,122	
Total Cost of HEX	**5,445**	**5,398**	**5,437**	**5,374**	
Net electric power	**11877**	**11469**	**11932**	**11138**	[kWe]
Turbomachinery	11,877	11,469	11,932	11,138	[T$]
Construction	4,331	4,216	4,342	4,128	
Total capital cost	**21,653**	**21,084**	**21,711**	**20,642**	[T$]
$/kWe Net	**1823**	**1838**	**1820**	**1853**	[$/kWe]

Table 9.5 show the results for the second case with 99 % purity of CO_2 and for 95 % purity of CO_2. The results show the effect on the capital cost of decreasing the purity of CO_2. The effect is significantly higher [A.7, A.10]. For example, the cycle with 5 % of He has the total capital cost about 15 M$, it is about 3 M$ lower than case with 1 % of He and about 4 M$ lower than the case with pure CO_2. If converted to $/kWe the specific cost for 5 % of He fraction is about 2282 $/kWe and for pure CO_2 it is about 1943 $/kWe.

The results for other mixtures are very similar. For example H_2S, has a negative impact

on the capital cost. The cycle with 5 % of H_2S has the total capital cost about 19.5 M$, it is about 0.33 M$ higher than case with 1 % of H_2S and about 0.51 M$ higher than the case with pure CO_2. If converted to $/kWe the specific cost for 5 % of H_2S fraction is about 1947 $/kWe and for pure CO_2 it is about 1943 $/kWe.

The dependence between reducing the purity of CO_2 and increase/decrease of capital costs is evident [A.10].

Table 9.4: The re-compression cycle with heater for WHR. (99 % purity of CO_2)

Cycle parameters					
Working medium	**Pure CO_2**	**1 % Ar**	**1 % H_2S**	**1 % He**	
$\boldsymbol{\eta}$	**29.39**	**29.01**	**29.43**	**28.67**	[%]
$\mathbf{P}_{tu}$	19.56	19.582	19.6	19.746	**[MW]**
$\mathbf{P}_c$ no.1	3.751	3.826	3.772	3.943	
$\mathbf{P}_c$ no.2	5.543	5.821	5.514	6.054	
$\mathbf{P}_c$	9.295	9.647	9.286	9.997	
$\mathbf{P}_{net}$	10.266	9.934	10.314	9.75	
Ra	2.6				[-]
$\mathbf{P}_2$	24.0				**[MPa]**
$\mathbf{P}_1$	9.231				
Mass flow	200				**[kg/s]**
Heat exchangers					
Recuperator no.1	680	647	690	629	**[kW/K]**
Recuperator no.2	534	582	574	593	
Cooler	808	793	807	787	
Heater	199	205	198	210	
Cost of HEX					
Recuperator no.1	1,7	1,618	1,725	1,573	**[T$]**
Recuperator no.2	1,335	1,455	1,435	1,483	
Cooler	1,374	1,348	1,372	1,338	
Heater	995	1,025	990	1,05	
Total Cost of HEX	**5,404**	**5,446**	**5,522**	**5,443**	
Net electric power	**9751.75**	**9438.25**	**9798.3**	**9261.55**	[kWe]
Turbomachinery	9,752	9,438	9,798	9,262	**[T$]**
Construction	3,789	3,721	3,83	3,676	
Total capital cost	**18,944**	**18,605**	**19,15**	**18,381**	**[T$]**
$/kWe Net	**1943**	**1971**	**1954**	**1985**	**[$/kWe]**

Table 9.5: The re-compression cycle with heater for WHR. (Purity of CO_2 99 and 95 %)

Cycle parameters							
Working medium	**Pure CO_2**	**1 % Ar**	**5 % Ar**	**1 % H_2S**	**5 % H_2S**	**1 % He**	**5 % He**	
η	**29.39**	**29.01**	**26.27**	**29.43**	**29.59**	**28.67**	**22.57**	[%]
P_{tu}	19.56	19.582	16.665	19.6	19.761	19.746	20.527	[MW]
P_c no.1	3.751	3.826	4.846	3.772	3.848	3.943	6.999	
P_c no.2	5.543	5.821	6.625	5.514	5.381	6.054	6.701	
P_c	9.295	9.647	11.472	9.286	9.23	9.997	13.7	
P_{net} no.1	10.266	9.934	8.193	10.314	10.531	9.75	6.827	
Ra	2.6							[-]
P_2	24.0							[MPa]
P_1	9.231							
Mass flow	200							[kg/s]
Heat exchangers								
Recuperator no.1	680	647	585	690	726	629	662	[kW/K]
Recuperator no.2	534	582	612	574	572	593	668	
Cooler	808	793	590	807	806	787	408	
Heater	199	205	241	198	193	210	268	
Cost of HEX								
Recuperator no.1	1,7	1,618	1,463	1,725	1,815	1,573	1,655	[T$]
Recuperator no.2	1,335	1,455	1,53	1,435	1,43	1,483	1,67	
Cooler	1,374	1,348	1,003	1,372	1,37	1,338	693	
Heater	995	1,025	1,205	990	965	1,05	1,34	
Total Cost of HEX	**5,404**	**5,446**	**5,201**	**5,522**	**5,58**	**5,443**	**5,359**	
Net electric power	**9751.75**	**9438.25**	**7783.35**	**9798.3**	**10004.45**	**9261.55**	**6485.65**	[kWe]
Turbomachinery	9,752	9,438	7,783	9,798	10,004	9,262	6,486	[T$]
Construction	3,789	3,721	3,246	3,83	3,896	3,676	2,961	
Total capital cost	**18,944**	**18,605**	**16,23**	**19,15**	**19,481**	**18,381**	**14,81**	[T$]
$/kWe Net	**1943**	**1971**	**2085**	**1954**	**1947**	**1985**	**2282**	[$/kWe]

9.3 Internal Rate of Return and Net Present Value

The second part of the techno-economic evaluation is the calculation of IRR (Internal rate of return). This value defines, if the project is economically viable. This metric is very important for the potential investor. The project have a positive rate of return if the interest rate is below the IRR. For both cases, the interest rate was selected at 2 % [3, 58, 69].

Another important indicator for techno-economic evaluation is the net present value. The NPV indicates how much a project will earn during its lifetime. If the NPV is positive, that project will generate more than is invest, which is necessary for construction and commissioning. If the NPV is negative, the project does not generated profit.

The results for the case with He heater are shown in Table 9.6. The IRR is about 8 % for each case. However, the IRR is smaller for He and AR and higher for H_2S. Each case is economically viable, but the benefit will be higher for the cases with substances which have the positive effect on the S-$CO2_2$ power cycle performance. According to Table 9.3, the total capital cost is lower for He and Ar. The NPV for pure CO_2 is about 22.75 M$, for the case with He it is only 21.1 M$ and for the case with H_2S it is about 22.88 M$. The NPV for case with Ar is 21.85 M$ All cases generate profit. The cases with substances with positive effect on the S-CO_2 power cycle, generate higher profit. However, the profit is quite similar for all cases, so the negative impact on the profit is negligible in the long term operation.

The similar results can be observed also for the second case (WHR). The results are shown in Table 9.7. For pure CO_2, the IRR is about 11 %. The H_2S has the positive impact on the IRR. The He has the negative effect, the IRR for 1 % of He is 10.72, but for 5 % of He it is only 8.9 %. The NPV for pure CO_2 is 18 M$, the NPV for 5 % of He is only 10 M$. This is a very dramatic reduction. The negative impact on the profit is negligible in the long term operation for working medium with 99 % purity of CO_2. [A.8, A.10]

9.4 Levelized Cost of Electricity

The LCOE defines the minimum cost at which electric power can be produced. Therefore, the price of electricity produced must be higher than LCOE, for profit. The results for the first case with He heater are shown in Table 9.8. The price is about 0.028 $/kWhe. It means, that the price of electricity produced can be the same for each case. However, this result is valid only for the case with 99 % purity of CO_2. In the event of the reduction of CO_2 purity, the LCOE will increase or decrease depending on the substance and the amount, as shown in Table 9.9. Nevertheless, the effect is still negligible for all cases. The negative effect of mixtures on the LCOE is for He and Ar. The substances with the positive effect of mixtures on the cycle efficiency have a positive effect on the LCOE.

The similar results are obtained for the second case, the WHR. The results are shown in Table 9.9. The price for 99 % purity of CO_2 is very similar for each case. In the case

Table 9.6: IRR and NPV for the re-compression cycle with helium heater. (99 % purity of CO_2)

Working medium	**Pure CO_2**	**1 % Ar**	**1 % H_2S**	**1 % He**	
Total capital cost	21.65	21.08	21.71	20.64	**[M$]**
Free cash flow					
FCO0	21.65	21.08	21.71	20.64	**[M$]**
Annual Revenue or Earnings for Electricity	6,19	5,98	6,22	5,81	**[T$]**
Sales Annual Operating Costs	2,653	2,562	2,665	2,488	
Annual Depreciation Expenses	2,165	2,108	2,171	2,064	
Taxable Income (1 – 10) years	1,372	1,308	1,383	1,253	
Tax Liability (1 – 10) years	480	458	484	439	
Depreciated Annual Cash Flow	892	850	899	814	
FCO1-10	3,057	2,958	3,07	2,879	
Taxable Income (11 – 20) years	3,537	3,416	3,554	3,317	
Tax Liability (11 – 20) years	1,238	1,196	1,244	1,161	
FCO11-20	2,299	2,22	2,31	2,156	
IRR	**8.25**	**8.15**	**8.27**	**8.06**	[%]
NPV	**22.75**	**21.85**	**22.88**	**21.1**	**[M$]**

Table 9.7: IRR and NPV for the re-compression cycle for WHR. (Purity of CO_2 99 and 95 %)

Working medium	**Pure CO_2**	**1 % Ar**	**5 % Ar**	**1 % H_2S**	**5 % H_2S**	**1 % He**	**5 % He**	
Total capital cost	18.94	18.6	16.23	19.15	19.48	18.38	14.81	[M$]
Free cash flow								
FCO0	18.94	18.6	16.23	19.15	19.48	18.38	14.81	[M$]
Annual Revenue	5,082	4,919	4,057	5,107	5,215	4,827	3,38	[T$]
Sales Annual Operating Costs	2,178	2,108	1,739	2,189	2,235	2,069	1,449	
Annual Depreciation Expenses	1,894	1,86	1,623	1,915	1,948	1,838	1,481	
Taxable Income (1 – 10) years	1,01	951	695	1,003	1,032	920	451	
Tax Liability (1 – 10) years	354	333	243	351	361	322	158	
Depreciated Annual Cash Flow	657	618	452	652	671	598	293	
FCO1-10	2,551	2,478	2,075	2,567	2,617	2,436	1,774	
Taxable Income (11 – 20) years	2,904	2,811	2,318	2,918	2,979	2,758	1,932	
Tax Liability (11 – 20) years	1,017	984	811	1,021	1,043	965	676	
FCO11-20	1,888	1,827	1,507	1,897	1,937	1,793	1,256	
IRR	**10.99**	**10.8**	**10.09**	**10.92**	**10.96**	**10.72**	**8.98**	[%]
NPV	**17.88**	**17.12**	**13.51**	**17.89**	**18.31**	**16.72**	**10.38**	[M$]

with 95 % CO_2 purity, the cost increases. However, this increase is negligible. [A.7, A.10] The negative effect on the cost is significantly smaller. The price is about 0.03 $/kWhe for 99 % purity of CO_2. For 95 % purity of CO_2, the price is higher, it is 0.035 $/kWhe for He are 0.032 $/kWhe for Ar. The price for H_2S decreases. It is 0.3036 $/kWhe for 99 % CO_2 purity and 0.3025 $/kWhe for 95 % CO_2 purity.

9.5 Conclusion of Techno-Economic Evaluation

As can be see, the techno-economic evaluation is important part in the development and design of the new power systems. The cost estimation was performed for three indicators, which are important for economic viability and the rate of return of the project. The indicatores are following: the levelized cost of electricity **(LCOE)**, the internal rate of return **(IRR)** and the net present value **(NPV)**. Each indicator show different results for the realization of the project and for potential investors.

The main conclusions of the effect of mixtures on the techno-economic evaluation from this chapter are following. The substances with the positive effect of mixtures on the cycle efficiency have the negative effect on the total capital cost. The substances with the positive effect of mixtures on the cycle efficiency have the negative effect on the IRR and the NPV. However, the substances with the positive effect of mixtures on the cycle efficiency have a positive effect on the LCOE. The overall cost estimation must be taken into account when designing the S-CO_2 power cycle. [A.7, A.8, A.10]

The information about technical-economic evaluation are presented in papers: *Effect of Gaseous Admixtures on Cycles with Supercritical Carbon Dioxide*, [A.7] *Effect of Multicomponent Mixtures on Cycles with Supercritical Carbon Dioxide* [A.8] and *Effect of Mixtures on Compressor and Cooler in Supercritical Carbon Dioxide Cycles*. [A.10]

Table 9.8: Levelized cost of electricity for the re-compression cycle with helium heater. (99 % purity of CO_2)

Working medium	**Pure CO_2**	**1 % Ar**	**1 % H_2S**	**1 % He**	
Total capital cost	21.65	21.08	21.71	20.64	**[M$]**
Total Tax Shield	7,578	7,379	7,599	7,225	**[T$]**
PV of Depreciation Shield	6,788	6,609	6,806	6,471	
Operation Price	0.03	0.03	0.03	0.03	**[$]**
Operation Cost	2,653	2,562	2,665	2,488	**[T$]**
Total Lifetime Plant Operationg Cost	53,061	51,24	53,307	49,759	
PV Plant Lifetime Operating Cost	45,102	43,554	45,311	42,295	
PV Plant Lifetime Total Cost	73,543	71,248	73,828	69,409	**[T$]**
Total Lifetime El. Production	1768707948	1708015602	1776913440	1658641176	**[kWhe]**
LCOE	**0.02832**	**0.02855**	**0.02826**	**0.02879**	**[$/kWhe]**

Table 9.9: Levelized cost of electricity for the re-compression cycle (WHR). (Purity of CO_2 99 and 95 %)

Working medium	**Pure CO_2**	**1 % Ar**	**5 % Ar**	**1 % H_2S**	**5 % H_2S**	**1 % He**	**5 % He**	
Total capital cost	18.94	18.6	16.23	19.15	19.48	18.38	14.81	**[M$]**
Total Tax Shield	6,63	6,512	5,68	6,703	6,818	6,433	5,182	**[T$]**
PV of Depreciation Shield	5,939	5,832	5,088	6,004	6,107	5,762	4,641	
Operation Price	0.03	0.03	0.03	0.03	0.03	0.03	0.03	**[$]**
Operation Cost	2,178	2,108	1,737	2,189	2,235	2,069	1,449	**[T$]**
Total Lifetime Plant O. C.	43,567	42,166	34,773	43,775	44,696	41,377	28,975	
PV Plant Lifetime O. C.	37,032	35,841	29,557	37,209	37,992	35,17	24,629	
PV Plant Lifetime Total C.	61,915	60,279	50,875	62,362	63,579	59,313	44,076	**[T$]**
Total Lifetime El. Product.	1452231	1405544	1159096	1459163	1489863	1379230	965843	**[MWhe]**
LCOE	**0.03018**	**0.03062**	**0.03239**	**0.03036**	**0.03025**	**0.03083**	**0.03546**	**[$/kWhe]**

Chapter 10

Summary and Conclusion

The research in this thesis was oriented on the description of the effect of the mixtures on the S-CO_2 power cycle. Namely, the binary mixtures of CO_2 with He, Ar, CO, N_2, O_2, H_2S, H_2, CH_4, Xe, Kr and SO_2. The research focused on the several areas which interconnects and give a complex overview complex overview and description of the effect of mixtures on S-CO_2 power cycle. The areas are following:

- The effect of binary mixture on the S-CO_2 power cycle, especially on the cycle efficiency and the net power.
- The effect on the components, especially on the turbine, compressor and heat exchanger.
- The optimization of the S-CO_2 power cycle, effect of the compressor inlet temperature.
- The techno-economical evaluation of the S-CO_2 power cycle for specific application and parameters.

Several conclusions can be made based on the above results. The main conclusion is that each mixture has an effect on the power cycle and the components. The mixtures have generally negative effect which increases with the amount of impurities in CO_2. Although, this is not true for all investigated substance. The research showed that at lease three substance have the opposite effect.

- The negative effect is caused by:
  - He, Ar, CO, N_2, O_2, H_2, Kr, CH_4
- The positive effect is caused by:
  - H_2S, Xe, SO_2

H_2S has the highest positive effect and He has the highest negative effect among investigated substances. However, for mixtures with CO_2 purity over 99 % the effect is negligible. This is effect of the mixtures on the cycle efficiency, respectively on the net power.

The cycle efficiency and the net power depends on the compressor and the turbine power and input and output heat. For this reason, the definition of the effect of mixtures on the components is necessary. The conclusions for the turbine and the compressor are following:

- The compressor performance:
  - The P_c dramatically increases with the increase of amount of the investigate substance in CO_2.
  - All the investigated mixtures have the negative effect on the P_c, expect H_2S, SO_2 and Xe.
  - The effect of H_2S, SO_2 and Xe is only marginally positive.
- The turbine performance:
  - All the investigated mixtures have the slightly increases the P_{tu}.
  - He has the biggest effect.

These results are very important for the design of the compressor, the turbine and selection of operating parameters. However, it should be noted that decreasing the compressor inlet temperature could reduce the effect of mixtures on the compressor power. This is an important information for the design of the cooling system and selection of the cooling medium. Also, this may affect the already designed cycle when the condition of the cooling medium changes.

The compressor power increase is the most important negative effect on the cycle efficiency and the net power. The same problem can be observed in other systems with CO_2, for example the compression stage for transport of CO_2 to the storage or heat pumps with CO_2. The decrease of the cycle efficiency appears to be linear, for concentration of CO_2 from 100 % to 99 %. The decrease of the cycle efficiency from 99 % to lower mol % can be approximated by exponential function. The increase of cycle efficiency is observed for H_2S, SO_2 and Xe and appears to be linear for all concentration of CO_2. Conclusion is that the optimum amount of the second substance is up to 1 %. For this amount the negative effect of binary mixture is small.

The heat exchangers are important components in the S-CO_2 power cycle. The S-CO_2 power cycle has three different type of heat exchanger. The mixtures have different effect on each HEX type. The conclusions for the heat exchangers are following:

- The recuperative heat exchanger:
  - The pinch point can be completely removed by the use of mixtures.
  - The substances with a positive effect on the cycle has a positive effect on the ΔT (increase of ΔT) and the substances which has a negative effect on the cycle has a negative effect on the ΔT (decrease of ΔT).
- The cooler:
  - The substances with a positive effect on the cycle has a negative effect on the ΔT (decrease of ΔT) and the substances which has a negative effect on the cycle has a positive effect on the ΔT (increase of ΔT).

The effect on heater is similar as for cooler. However, the effect may vary depending on the composition of the working medium and it is not possible to clearly say what will be the effect of the mixture on the heater.

From the techno-economic evaluation of a hypothetical power plant with S-CO_2 power cycle several conclusions can be made based on the presented results. The conclusions for the techno-economic evaluation are following:

- The mixtures with negative effect on the cycle, reduces effectively the project capital cost.
- The mixtures with negative effect have a negative effect on the specific cost as they lower the net power which leads to a higher specific cost.
- The mixtures with negative effect have a negative effect on the IRR and NPV. However, the negative effect on the profit is negligible in the long term operation for working medium with 99 % pure CO_2.
- The mixtures with negative effect have a negative effect on the LCOE. However, the effect is negligible.

From the results, it is obvious, that mixtures have a very important effect the S-CO_2 power cycle, operating parameters and components. However, with good optimization and design of the cycle which uses mixtures, marginal negative effect on the cycle efficiency and the net power output can be achieved. This is an important information for the design of the cycle layout and components. Regardless of the CO_2 purity, the same cycle layouts can be used, however in order to achieve good performance with the impurities the cycle operating conditions and components design must be re-optimized.

Future research will be focused on the detail description of effect of another potential mixtures on the S-CO_2 cycle, for the close S-CO_2 power cycle and the Direct-Fired S-CO_2 power cycle or other application S-CO_2 power cycle for fossil fuel power plant, for specific application. Because, these system is currently very popular, for increase of total efficiency of power plant, as waste heat recovery systems. But, the effect of the mixtures will be higher. The mixture will be product of combustion or impurities from the primary loop.

At the same time, research about impact on materials of components and chemical effect is necessary. The each substance has some effect on the materials, for example H_2S, is very interesting substance for increase the cycle efficiency and the net power. On the other hand, effect on materials of the turbine and the compressor is enormous, especially on blades. Research of the new materials is therefore necessary.

References

[1] Wright S.A., Radel R.F., Conboy T.M., Rochau G.E., *Modeling and Experimental Results for Condensing Supercritical CO_2 Power Cycles.*, 2011: SANDIA REPORT, SAND2010-8840.

[2] Allam R.J., Fetvedt J.E., Forrest B.A., Freed D.A., *The Oxy-Fuel, Supercritical CO_2 Allam Cycle: New Cycle Developments to Produce Even Lower-Cost Electricity From Fossil Fuels Without Atmospheric Emissions.*, 2014: ASME Turbo Expo 2014: Turbine Technical Conference and Exposition, Volume 3B: Oil and Gas Applications; ISBN: 978-0-7918-4566-0, doi:10.1115/GT2014-26952.

[3] Brun K., Friedman P., Dennis R., *Fundamentals and Applications of Supercritical Carbon Dioxide (S-CO_2) Based Power Cycles.*, 2016: Elsevier, ISBN: 978-0-08-100804-1.

[4] Angelino G., *Carbon Dioxide Condensation Cycles for Power Production.*, 1968: ASME Paper No. 68-GT-23.

[5] Dostal V., Driscoll M.J., Hejzlar P., *Supercritical Carbon Dioxide Cycle for Next Generation Nuclear Reactors.*, 2004: MIT-ANP-TR-100.

[6] Kacludis A., Lyons S., Nadav D., Zdankiewicz E., *Waste Heat to Power (WH2P) Applications Using a Supercritical CO_2 - Based Power Cycle.*, 2012: Echogen Power Systems LLC: Presented at Power-Gen International 2012.

[7] Zhiwen Ma, Craig S. Turchi, *Advanced Supercritical Carbon Dioxide Power Cycle Configurations for Use in Concentrating Solar Power Systems.*, 2011: NREL/CP-5500-50787.

[8] Brian D. Iverson, Thomas M. Conboy, James J. Pasch, Alan M. Kruizenga, *Supercritical CO_2 Brayton cycles for solar-thermal energy.*, 2013: Elsevier Ltd. 1-s2.0-S0306261913005278-main.

[9] Kimzey G., *Development of a Brayton Bottoming Cycle Using Supercritical Carbon Dioxide as the Working Fluid.*, Electric Power Research Institute Report, Palo Alto (CA), 2012.

[10] Echogen Power Systems Inc., Echogen Power Systems LLC., T.J.Held, *Accession Number 2011-A26971.*, 2010: patent.

[11] Shelton W.W., Weiland N., White C., Plunkett J., Gray D.,*Oxy-coal-fired circulating fluid bed combustion with a commercial utility-size supercritical CO_2 power cycle.*, 2016, The 5th International Symposium Supercritical CO_2 Power Cycles, San Antonio, TX.

[12] Shelton W.W., Weiland N., White C., Gray D.,*Performance baseline for direct-fired S-CO_2 Cycles.*, 2016, The 5th International Symposium Supercritical CO_2 Power Cycles, San Antonio, TX.

[13] Letcher T., *Storing Energy With Special Reference to Renewable Energy Sources.*, 2016, Elsevier, ISBN: 978-0-12-803440-8.

[14] Fourspring P.M., Nehrbauer J.P., *Heat exchanger testing for closed Brayton cycles using CO_2 as the working fluid.*, 2011: NNL, NY.

[15] Hoopes K., Sánchez D., Crespi F., *A New Method for Modelling Off-Design Performance of S-CO_2 Heat Exchangers without Specifying Detailed Geometry.*, 2016, The 5th International Symposium Supercritical CO_2 Power Cycles, San Antonio, TX.

[16] Moisseytsev A., Sienicki J.J., *Investigation of Alternative Layouts for the Supercritical Carbon Dioxide Brayton Cycle for a Sodium-Cooled Fast Reactor.*, Nuclear Engineering and Design 239 (2009) 1362–1371, doi:10.1016/j.nucengdes.2009.03.017.

[17] Oh H.K., Son Ch.H., *New Correlation to Predict the Heat Transfer Coefficient In-Tube Cooling of Supercritical CO_2 in Horizontal Macro-Tubes.*, Experimental Thermal and Fluid Science 34 (2010) 1230-1241, doi:10.1016/j.expthermflusci.2010.05.002.

[18] Carlson M.D., Kruizenga A., Anderson H.M., Corradini M.L., *Measurements of Heat Transfer and Pressure Drop Characteristics of Supercritical Carbon Dioxide Flowing in Zig-Zag Printed Circuit Heat Exchanger Channels.*, 2011 The International Symposium Supercritical CO_2 Power Cycles Boulder, Colorado.

[19] Ngo T.L., Kato Y., Nikitin K., Ishizukam T., *Heat transfer and pressure drop correlations of microchannel heat exchangers with S-shaped and zigzag fins for carbon dioxide cycles.*, 2007: Tokyo Institute of Technology, Japan.

[20] Nikitin K., Kato Y., Ngo L., *Printed circuit heat exchanger thermal–hydraulic performance in supercritical CO_2 experimental loop.*, International Journal of Refrigeration 29 (2006) 807–814, doi:10.1016/j.ijrefrig.2005.11.005.

[21] Mohagheghi M., Zawati H., Pinol T., Gou J., Xu Ch., Kapat J., *Use of 1-D Finite Enthalpy Method for a High-Temperature Recuperator Made of Polymer Derived Ceramic Composite for a Supercritical Carbon Dioxide Power System.*, 2016, The 5th International Symposium Supercritical CO_2 Power Cycles, San Antonio, TX.

[22] John J. D., Sanford A. K., Gregory F.N., Douglas T.R., *Modeling Off-Design of a Supercritical Carbon Dioxide Baryton Cycle.*, 2011: Solar Energy Laboratory - University of Wisconsin-Madison.

[23] Steven A. W., Ross F. R., Milton E. V., Gary E. R., Paul S. P., *Operation and Analysis of a Supercritical CO_2 Brayton Cycle.*, 2010: Sandia National Laboratories.

[24] Edward J. P., Steven A. W., Milton E. V., Darryn D. F., *Supercritical CO_2 Direct Cycle Gas Fast Reactor (SC-GFR) Concept.*, 2011: Sandia National Laboratories.

[25] Hasuike H., Yamamoto T., Utamura M., *Demonstration Test Plant of Closed Cycle Gas Turbine with Supercritical CO_2 as Working Fluid.*, 2010: Tokyo Institute of Technology.

[26] Rene Pecnik, Piero Colonna, `http://delftpe.nl/ET/scCO2`.

[27] Ludington A.R., Hejzlar P., Driscoll M.J., *Development of Tools for S-CO_2 Cycle Analysis at MIT.* Proceedings of SCO_2 Power Cycle Symposium 2009.

[28] Jeong W.S., Lee J.I., Jeong Y.H, *Potential improvements of supercritical recompression CO_2 Brayton cycle by mixing other gases for power conversion system of a SFR.*, Nuclear Engineering and Design 241 (2011) 2128–2137, doi:10.1016/j.nucengdes.2011.03.043.

[29] Jeong W.S., Jeong Y.H, *Potential improvements of supercritical recompression CO_2 Brayton cycle by mixing other gases for power conversion system of a SFR.*, Nuclear Engineering and Design 262 (2013) 12–20, http://dx.doi.org/10.1016/j.nucengdes.2013.04.006.

[30] Wetenhall B., Aghajani H., Chalmers H., Benson S.D., Ferrari M-C., Li J., Race J.M., Singh P., Davison J., *Impact of CO_2 impurity on CO_2 compression, liquefaction and transportation.*, GHGT-12, Energy Procedia 63 (2014) 2764 – 2778.

[31] Wetenhall B., Race J.M., Downie M.J., *The Effect of CO_2 Purity on the Development of Pipeline Networks for Carbon Capture and Storage Schemes.*, International Journal of Greenhouse Gas Control 30 (2014) 197–211, http://dx.doi.org/10.1016/j.ijggc.2014.09.016.

[32] Goto K., Kazama S., Furukawa A., Serizawa M., Aramaki S., Shoji K., *Effect of CO_2 purity on energy requirement of CO_2 capture processes.*, GHGT-11, Energy Procedia 37 (2013) 806 – 812.

[33] Li H., *Thermodynamic Properties of CO_2 Mixtures and Their Applications in Advanced Power Cycles with CO_2 Capture Processes.*, Energy Processes, Department of Chemical Engineering and Technology, Royal Institute of Technology Stockholm, Sweden 2008, ISBN 978-91-7415-091-9.

[34] Span R., Wagner W., *A New Equation of State for Carbon Dioxide Covering the Fluid Region from the Triple Point Temperature to 1100 K at Pressures up to 800 MPa.*, J. Phys. Chem. Ref. Data, 25:1509–1596, 1996. doi:10.1063/1.555991.

[35] Maroto-Valer M. M.,*Developments and innovation in carbon dioxide (CO_2) capture and storage technology Volume 1: Carbon dioxide (CO_2) capture, transport and industrial applications.*, Woodhead Publishing Limited, 2010, ISBN 978-1-84569-533-0.

[36] Hume S., *Performance Evaluation of a Supercritical CO_2 Power Cycle Coal Gasification Plant.*, 2016 The 5th International Symposium - Supercritical CO_2 Power Cycles.

[37] Moore R., Conboy T., *Metal corrosion in a supercritical carbon dioxide - liquid sodium power cycle.*, Sandia National Laboratories, 2012, Milestone Report: M3AR12SN08010601.

[38] Kim J.H., Cho J.M., Lee I.H., Lee J.S., Kim M.S., *Circulation concentration of CO_2/propane mixtures and the effect of their charge on the cooling performance in an air-conditioning system.*, 2017: International Journal of Refrigeration 30 (2007) 43-49. doi:10.1016/j.ijrefrig.2006.06.008.

[39] Sarkar J., Bhattacharyya S., *Assessment of blends of CO_2 with butane and isobutane as working fluids for heat pump applications.*, 2009: International Journal of Thermal Sciences 48 (2009) 1460–1465, doi:10.1016/j.ijthermalsci.2008.12.002.

[40] Heinrich J., *Vlastnosti Tekutín.*, 1980: SNTL: Státní nakladatelství technické literatury Praha.

[41] Turns S.R., *An Introduction to Combustion Concepts and applications.*, 2012: McGraw-Hill Education, ISBN 978-0-07-338019-3.

[42] Cengel Y.A., Boles M.A., *Thermodynamics an Engineering Approach.*, 2015, McGraw-Hill Education, ISBN 978-0-07-339817-4.

[43] Scalabrin G., Marchi P., Finezzo F., Span R., *A Reference Multiparameter Thermal Conductivity Equation for Carbon Dioxide with an Optimized Functional Form.*, J. Phys. Chem. Ref. Data, 35(4):1549–1575, 2006. doi:10.1063/1.2213631.

[44] Span R., Eckermann T., Herrig S., Hielscher S., Jager A., Thol M., *TREND. Thermodynamic Reference and Engineering Data 2.0.* Lehrstuhl fuer Thermodynamik, 2015: Ruhr-Universitaet Bochum.

[45] Lemmon E.W,, Jacobsen R.T., Penoncello S.G., Friend D.G., *Thermodynamic Properties of Air and Mixtures of Nitrogen, Argon, and Oxygen from 60 to 2000 K at Pressures to 2000 MPa.*, J. Phys. Chem. Ref. Data, 29(3):331–385, 2000. doi:10.1063/1.1285884.

[46] Lemmon E.W,, Jacobsen R.T., *A Generalized Model for the Thermodynamic Properties of Mixtures.*, Int. J. Thermophys., 20(3):825–835, 1999. doi:10.1023/A:1022627001338.

[47] Lemmon E.W,, Jacobsen R.T., *Viscosity and Thermal Conductivity Equations for Nitrogen, Oxygen, Argon, and Air.*, Int. J. Thermophys., 25(1):21–69, 2004. doi:10.1023/B:IJOT.0000022327.04529.f3.

[48] Lemmon E.W., Huber M.L., McLinden M.O., *NIST Standard Reference Database 23: Reference Fluid Thermodynamic and Transport Properties-REFPROP.*, 2013: Version 9.1.

[49] Bell I.H., Wronski J., Quoilin S., Lemort V., *Pure and Pseudo-pure Fluid Thermophysical Property Evaluation and the Open-Source Thermophysical Property Library CoolProp.*, Industrial & Engineering Chemistry Research, volume = 53, 2014, doi 10.1021/ie4033999.

[50] Horlock J.H., *Advance gas turbine cycles.*, 2003 Elsevier Science, ISBN 0-08-044273-0.

[51] Echogen Power Systems Inc., T.J.Held, *Accession Number 2012-G29327.*, 2012: patent.

[52] Echogen Power Systems Inc., T.J.Held, M.L.Vermeersch, T.Xie, *Accession Number 2012-G34842.*, 2012: patent.

[53] Echogen Power Systems Inc., T.J.Held, M.L.Vermeersch, T.Xie, *Accession Number 2012-G34847.*, 2012: patent.

[54] Boccaccini L.V., *Objectives and status of EUROfusion DEMO blanket studies.*, Fusion Engineering and Design, 109–111 (2016) 1199–1206.

[55] You J.H., *Conceptual design studies for the European DEMO divertor: Rationale and first results.*, Fusion Engineering and Design 109–111 (2016) 1598–1603.

[56] Federici G., *Overview of EU DEMO design and R&D activities.*, Fusion Engineering and Design 89 (2014) 882–889.

[57] Bachmann C., *Issues, and strategies for DEMO in-vessel component integration.*, Fusion Engineering and Design 112 (2016) 527–534.

[58] Wright S.A., Davidson C.S., Scammell W. O., *Thermo-Economic Analysis of Four S-CO_2 Waste Heat Recovery Power Systems.*, 2016: The 5th International Symposium-Supercritical CO_2 Power Cycle.

[59] Echogen Power Systems Inc., T.J.Held, M.L.Vermeersch, J.D.Miller, T.Xie, *Accession Number 2011-M37773.*, 2011: patent.

[60] Echogen Power Systems Inc., T.J.Held, S.Hostler, J.D.Miller, B.F.Hume, *Accession Number 2011-C92782.*, 2011: patent.

[61] Echogen Power Systems Inc., T.J.Held, M.L.Vermeersch, T.Xie, J.D.Miller, *Accession Number 2012-G34848.*, 2012: patent.

[62] Kröger, D.G., *Air-cooled heat exchangers and cooling towers V1.*, Tulsa, Okl.:Penwell Corp., c2004, 2v. ISBN 0-87814-896-5.

[63] Kröger, D.G., *Air-cooled heat exchangers and cooling towers V2.*, Tulsa, Okl.:Penwell Corp., c2004, 2v. ISBN 1-59370-019-9.

[64] Bergman T.L., Lavine A.S., Incropera F.P., Dewitt D.P., *Fundamentals of Heat and Mass Tranfer.*, 2011, John Wiley and Sons, Inc. ISBN 13 978-0470-50197-9.

[65] Van Eldik M., Harris P.M., Kaiser W.H., Rousseau P.G., *Theoretical And Experimental Analysis Of Supercritical Carbon Dioxide Cooling.*, 15th International Refrigeration and Air Conditioning Conference at Purdue, July 14-17, 2014.

[66] Gnielinski V., *New equations for heat and mass transfer in turbulent pipe and channel flow.*, Forschung im Ingenieurwesen, vol. 41, no. 1, pp. 8–16, 1975.

[67] Gnielinski, V., *A new calculation procedure for the heat transfer in the transition region between laminar and turbulent pipe flow.*, Forschung im Ingenieurwesen, vol. 61, no. 9, pp. 240-248, 1995.

[68] Driscoll M.J., *Supercritical CO_2 Plant Cost Assessment.*, Center for Advanced Nuclear Energy Systems, MIT Nuclear Engineering Department, 2014, Report No: MIT-GFR-019.

[69] Huck P., Freund S., Lehar M., Peter M., *Performance comparison of supercritical C_2 versus steam bottoming cycles for gas turbine combined cycle applications.*, 2016: The 5th International Symposium-Supercritical CO_2 Power Cycle.

Author References

[A.1] Manikantachari K.R.V., Vesely L., Martin S., Bobren-Diaz J.O., Vasu S., *A Study on Design Optimization of Direct-Fired sCO_2 Combustors.*, 2018 AIAA Aerospace Sciences Meeting, AIAA SciTech Forum, (AIAA 2018-2127) https://doi.org/10.2514/6.2018-2127.

[A.2] Vesely L., Dostal V., Bartos O., Novotny V.,*Pinch Point Analysis of Heat Exchangers for Supercritical Carbon Dioxide with Gaseous Admixtures in CCS Systems.*, 2016: Energy Procedia, Volume 86, Pages 489-499, ISSN: 1876-6102.

[A.3] Vesely L., Dostal V., *Calculation of the heat exchanger for S-CO_2 with Pinch Point.*, ERIN, The 8th International Conference for Young Researchers and PhD Students, April 23rd-25th, 2014, Blansko - Češkovice, Czech Republic

[A.4] Vesely L., Dostal V., Hajek P.,*Design of Experimental Loop with Supercritical Carbon Dioxide.*, 2014: 22nd International Conference on Nuclear Engineering, Volume 3: Next Generation Reactors and Advanced Reactors; Nuclear Safety and Security, Paper No. ICONE22-30798, pp. V003T05A023; ISBN: 978-0-7918-4593-6, doi:10.1115/ICONE22-30798.

[A.5] Vesely L., Dostal V., *Synergy of S-CO_2 Power Cycle and CCS Systems.*, 2016: The 5th International Symposium - Supercritical CO_2 Power Cycles, March 29–31, 2016, in San Antonio, Texas.

[A.6] Vesely L., Dostal V., *Research on the Effect of the Pinch Point Shift in Cycles with Supercritical Carbon Dioxide.*, 2014, The 4th International Symposium - Supercritical CO_2 Power Cycle, September 9-10, 2014, in Pittburgh, Pennsylvania.

[A.7] Vesely L., Dostal V., *Effect of Multicomponent Mixtures on Cycles with Supercritical Carbon Dioxide.*, 2017, ASME Turbo Expo 2017, Turbomachinery Technical Conference and Exposition, Volume 9: Oil and Gas Applications; Supercritical CO_2 Power Cycles; Wind Energy, Paper No. GT2017-64044, pp. V009T38A016; ISBN: 978-0-7918-5096-1, doi:10.1115/GT2017-64044.

[A.8] Vesely L., Dostal V., Stepanek J., *Effect of Gaseous Admixtures on Cycles with Supercritical Carbon Dioxide.*, 2016, ASME Turbo Expo 2016, Turbomachinery Technical Con-

ference and Exposition, Volume 9: Oil and Gas Applications; Supercritical CO_2 Power Cycles; Wind Energy, Paper No. GT2016-57644, pp. V009T36A016; ISBN: 978-0-7918-4987-3, doi:10.1115/GT2016-57644.

[A.9] Vesely L., Dostal V., Entler S., *Comparison of S-CO_2 Power Cycles for Nuclear Energy.*, Acta Polytechnica CTU Proceedings, Vol. 4, pages 107–112, 2016, Šimáně 2016 - Czech-Slovak Student Conference on Nuclear Engineering, ISSN 2336-5382 (Online), Published by the Czech Technical University in Prague, doi:10.14311/AP.2016.4.0107.

[A.10] Vesely L., Manikantachari K.R.V., Vasu S., Kapat J., Dostal V., *Effect of Mixtures on Compressor and Cooler in Supercritical Carbon Dioxide Cycles.*, 2018, Proceedings of ASME Turbo Expo 2018: Turbomachinery Technical Conference and Exposition GT2018, GT2018-75568, Accepted for publishing.

Appendix A

Author Publications

List of publications that are published in Journals and Conferences or published as research reports. At the same time, the publications which will be published, are listed. (Publications in review proceeding or publications waiting to be published in a magazine or conference).

A.1 Publications Connected with Issues of Doctoral Thesis

A.1.1 Journals

Vesely L., Dostal V., *Effect of Multicomponent Mixtures on Cycles with Supercritical Carbon Dioxide.*, 2017, ASME Turbo Expo 2017, Turbomachinery Technical Conference and Exposition, Volume 9: Oil and Gas Applications; Supercritical CO_2 Power Cycles; Wind Energy, Paper No. GT2017-64044, pp. V009T38A016; ISBN: 978-0-7918-5096-1, doi:10.1115/GT2017-64044.

Vesely L., Dostal V., Entler S., *Comparison of S-CO_2 Power Cycles for Nuclear Energy.*, Acta Polytechnica CTU Proceedings, Vol. 4, 2016, Šimáně 2016 - Czech-Slovak Student Conference on Nuclear Engineering, ISSN 2336-5382 (Online), Published by the Czech Technical University in Prague.

Vesely L., Dostal V., Stepanek J., *Effect of Gaseous Admixtures on Cycles with Supercritical Carbon Dioxide.*, 2016, ASME Turbo Expo 2016, Turbomachinery Technical Conference and Exposition, Volume 9: Oil and Gas Applications; Supercritical CO_2 Power Cycles; Wind Energy, Paper No. GT2016-57644, pp. V009T36A016; ISBN: 978-0-7918-4987-3, doi:10.1115/GT2016-57644.

Vesely L., Dostal V., Bartos O., Novotny V.,*Pinch Point Analysis of Heat Exchangers for Supercritical Carbon Dioxide with Gaseous Admixtures in CCS Systems.*, 2016: Energy Procedia, Volume 86, Pages 489-499, ISSN: 1876-6102.

Vesely L., Dostal V., Hajek P.,*Design of Experimental Loop with Supercritical Carbon Dioxide.*, 2014: 22nd International Conference on Nuclear Engineering, Volume 3: Next Generation Reactors and Advanced Reactors; Nuclear Safety and Security, Paper No. ICONE22-30798, pp. V003T05A023; ISBN: 978-0-7918-4593-6, doi:10.1115/ICONE22-30798.

A.1.2 Conference Papers

Manikantachari K.R.V., Vesely L., Martin S., Bobren-Diaz J.O., Vasu S., *A Study on Design Optimization of Direct-Fired sCO_2 Combustors.*, 2018 AIAA Aerospace Sciences Meeting, AIAA SciTech Forum, (AIAA 2018-2127) https://doi.org/10.2514/6.2018-2127.

Vesely L., Dostal V., *Synergy of S-CO_2 Power Cycle and CCS Systems.*, 2016: The 5th International Symposium - Supercritical CO_2 Power Cycles.

Vesely L., Dostal V., *Research on the Effect of the Pinch Point Shift in Cycles with Supercritical Carbon Dioxide.*, 2014, The 4th International Symposium - Supercritical CO_2 Power Cycle.

Vesely L., Dostal V., *Calculation of the heat exchanger for S-CO_2 with Pinch Point.*, 2014, ERIN, The 8th International Conference for Young Researchers and PhD Students.

A.1.3 Other Publications

Vesely L., Dostal V., *Design of experimental loop with supercritical carbon dioxide.*, Master's thesis, 2013, CTU in Prague, Faculty of Mechanical Engineering, Department of Energy Engineering.

Vesely L., Dostal V.,*Component analysis of freezing in cycle with supercritical CO_2.*, Bachelor thesis, 2011, CTU in Prague, Faculty of Mechanical Engineering, Department of Energy Engineering.

A.2 Publications not Related with Issues of Doctoral Thesis

A.2.1 Journals

Vesely L., Dostal V., Entler S., *Study of the cooling systems with S-CO_2 for the DEMO fusion power reactor.*, Fusion Engineering and Design, Volume 124, November 2017, Pages 244-247, ISSN: 0920-3796, https://doi.org/10.1016/j.fusengdes.2017.03.019.

Zacha P., Vesely L., Stepanek J., *Design of the divertor targets shielding frame of the HELCZA high heat flux experimental complex.*, Fusion Engineering and Design, Volume 124, November 2017, Pages 360-363, ISSN: 0920-3796, https://doi.org/10.1016/j.fusengdes.2017.05.029.

Roussanaly S., Skaugen G., Aasen A., Jakobsen J., Vesely L., *Techno-economic evaluation of CO_2 transport from a lignite-fired IGCC plant in the Czech Republic.*, International Journal of Greenhouse Gas Control, Volume 65, October 2017, Pages 235-250, ISSN: 1750-5836.

Burian. O., Dostal V., Vesely L.,*Study of identification of two-phase flow parameters by pressure fluctuation analysis.*, Acta Polytechnica CTU Proceedings, Vol. 4, 2016, Šimáně 2016-Czech-Slovak Student Conference on Nuclear Engineering, ISSN 2336-5382 (Online), Published by the Czech Technical University in Prague.

Vesely L., Dostal V.,*Accident at Fukushima Dai-Ichi nuclear power plant.*, 2014, 22nd International Conference on Nuclear Engineering, Volume 5: Innovative Nuclear Power Plant Design and New Technology Application; Student Paper Competition, ISBN: 978-0-7918-4595-0.

A.2.2 Conference Papers

Vesely L., Skaugen G., Vitvarova M., Roussanaly S., Novotny V., *Case study of transport options for CO_2 from IGCC coal power plant in the Czech republic for storage.*, 2016, Proceedings of the 4th International Conference on Chemical Technology, ISBN: 978-80-86238-94-4.

A.2.3 Research Reports

Vitvarová M., Hrdlička F., Roussanaly S., Pilař L., Novotný V., Veselý L. et all., *Technicko-ekonomické zhodnocení a budoucí potenciál integrace technologií CCS v podmínkách ČR.*, studie NF-CZ08-OV- 1-003- 2015/FR-TI/379/TA02020205

(výzkumná zpráva za aktivitu WP4 projektu NF-CZ08-OV-1-003-2015, Praha, ČVUT v Praze/UJV Rež/SINTEF ER, prosinec 2016.

Veselý L., Skaugen G., Roussanaly S., Bartoš O. et all., *Technicko-ekonomická analýza možnosti transportu separovaného CO_2 do uložišť na území ČR a v Severním moři.*, (výzkumná zpráva za aktivitu WP5 projektu NF-CZ08-OV-1-003-2015, Praha, ČVUT v Praze/ SINTEF ER, Listopad 2016.

Veselý L., Skaugen G., Roussanaly S., Bartoš O. et all., *CO_2 transport to storage sites in Czech Republic and North Sea and full chain evaluation.*, (WP5 report of project No. NF-CZ08-OV-1-003-2015), Prague, CTU in Prague/SINTEF ER, November 2016.

Vitvarová M., Novotný V., Veselý, L., Kolovratnik M., Hrdina Z., Roussanaly S., Bestad D., et all., *Technicko-ekonomická analýza integrace technologie CCS na báze pre-combustion do uhelného zdroje IGCC v podmínkách ČR.*, (výzkumná zpráva za aktivitu WP3 projektu NF-CZ08-OV-1-003-2015, Praha, ČVUT v Praze/UJV Rež/SINTEF ER, říjen 2016.

Vitvarová M., Novotný V., Veselý, L., Kolovratnik M., Hrdina Z., Roussanaly S., Bestad D., et all., *Techno-Economic Assessment of pre-combustion CCS technology integration into IGCC power plant in Czech Republic.*, (WP3 report of project No. NF-CZ08-OV-1-003-2015), Prague, CTU in Prague/UJV Rez/SINTEF ER, October 2016.

Pilař L., Vlček Z., Hrdina Z., Dlouhý T., Kolovratník M., Veselý L.. et all., *Analýza procesních operací.*, (výzkumná zpráva za aktivitu WP2 projektu NF-CZ08-OV-1-003-2015, Praha, ČVUT v Praze/UJV Řež/SINTEF ER, březen 2016.

Vitvarova, M.; Dlouhy, T.; Novotny, V.; Chanova, P.; Havlik, J.; Vesely, L. *Technicko-ekonomické posouzení nasazení systému záchytu CO_2 v elektrárně.*, (výzkumná zpráva ÚJV-14545), projekt TA02020205, Husinec-Řež, UJV Rež, prosinec 2015.

Dlouhý T., Slouka P., Pilař L., Vitvarová M. Veselý L.. et all., *Stanovení vstupních podmínek a analýza možností využití CO2 v podmínkách ČR.*, (výzkumná zpráva za aktivitu WP1 projektu NF-CZ08-OV-1-003-2015, Praha, ČVUT v Praze/UJV, duben 2015.

Dostal, V.; Petr, V.; Kolovratnik, M.; Dlouhy, T.; Skoda, R.; Vesely, L.; Stepanek, J.; Romsy, T. et al. *Development of Supercritical Carbon Dioxide Cycle for Waste Heat Recovery.*, 2015.

A.3 Publications in Review Process

Vesely L., Manikantachari K.R.V., Vasu S., Kapat J., Dostal V., *Effect of Mixtures on Compressor and Cooler in Supercritical Carbon Dioxide Cycles.*, 2018, Proceedings of

ASME Turbo Expo 2018: Turbomachinery Technical Conference and Exposition GT2018, GT2018-75568, Accepted for publishing.

Appendix B

Code

The code for calculation of the compressor is following.

```
    def (T_in, P_out, Ra, Eta, m, medium):
        P_in        - Inlet pressure            [Pa]
        S_in        - Inlet entropy             [J/kg/K]
        d_H_ideal   - Ideal enthalpy increase   [J/kg]
        d_H         - Real enthalpy increase    [J/kg]
        W_k         - Compressor power          [W]
        T_out       - Outlet temperature        [K]
        S_out       - Outlet entropy            [J/kg/K]
        H_out       - Real output enthalpy          [J/kg]
        T_in        - Inlet temperature         [K]
        P_out       - Outlet pressure           [Pa]
        Eta         - Compressor efficiency     [-]
        m           - Mass flow                 [kg/s]
        medium      - Working medium            [-]

        P_in = P_out/Ra
        H_in = PropsSI('H', 'T', T_in, 'P', P_in, medium)
        S_in = PropsSI('S', 'T', T_in, 'P', P_in, medium)
        H_out_ideal = PropsSI('H', 'S', S_in, 'P', P_out, medium)
        d_H_ideal = (H_out_ideal - H_in)/Eta
        H_out = H_in + self.d_H_ideal
        d_H = (H_out - self.H_in)
        W_k = m * d_H
        T_out = PropsSI('T', 'P', P_out, 'H', H_out, medium)
```

```
25          S_out = PropsSI('S', 'H', H_out, 'P', P_out, medium)
```

The code for calculation of the turbine is following.

```
1       def (T_in, P_out, Ra, Eta, m, medium):
            d_H_ideal   - Ideal enthalpy drop   [J/kg]
3           d_H         - Real enthalpy drop    [J/kg]
            W_tu        - Turbine power         [W]
5           Eta         - Turbine efficiency    [-]

7           H_in = PropsSI('H', 'T', T_in, 'P', P_in, medium)
            S_in = PropsSI('S', 'T', T_in, 'P', P_in, medium)
9           H_out_ideal = PropsSI('H', 'S', S_in, 'P', P_out, medium)
            d_H_ideal = (H_in - H_out_ideal) * Eta
11          H_out = self.H_in - d_H_ideal
            d_H = (H_in - H_out)
13          W_tu = m * d_H
            T_out = PropsSI('T', 'P', P_out, 'H', H_out, medium)
15          S_out = PropsSI('S', 'H', H_out, 'P', P_out, medium)
```